# Synthesis, characterization and effects of addition of titania particles on properties of epoxy-amine matrix




A dissertation submitted to the Department of Chemistry,
Quaid-i-Azam University, Islamabad,
in partial fulfilment of the requirements for degree of
Master of philosophy
In
Organic Chemistry
BY

**Maria Zubair**
Department of chemistry
Quaid-i-Azam University
Islamabad

**2017**

## DECLARATION

This is to certify that this dissertation entitled **"Synthesis Characterization and Effects of Addition of Titinia Particles on the Properties Epoxy-Amine Matrix"** Submitted by ***Ms. Maria Zubair,*** is accepted in its present form by the Department of Chemistry, Quaid-i-Azam University, Islamabad, as satisfying the dissertation requirements for the degree of ***Master of Philosophy in Organic Chemistry***


**External Examiner:**

**Dr. Shaukat Saeed**
Professor
Department of Metallurgy and Materials Engineering
Pakistan Institute of Engineering & Applied Sciences (PIEAS), P.O. Box 45650 Nilore, Islamabad

**Supervisor:**

**Prof. Dr. Mrs. Humaira Masood Siddiqi**
Department of Chemistry
Quaid-i-Azam University
Islamabad

**Head of Section:**

**Prof. Dr. Aamer Saeed Bhatti**
Department of Chemistry
Quaid-i-Azam University
Islamabad

**Chairman:**

**Prof. Dr. M. Siddiq**
Department of Chemistry
Quaid-i-Azam University
Islamabad.

In the Name of Allāh, the Most Gracious, the Most Merciful

This dissertation is

Dedicated

To

**My loving parents**

For their never-ending support and guidance

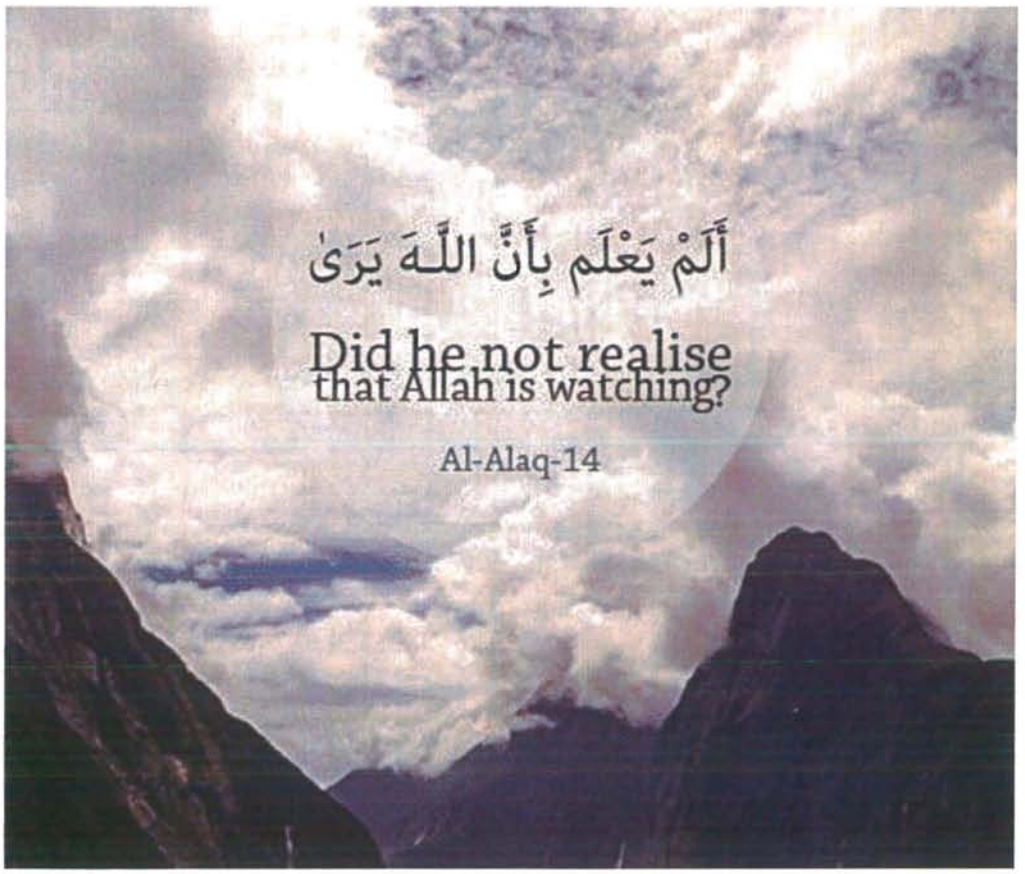
أَلَمْ يَعْلَم بِأَنَّ اللَّـهَ يَرَىٰ
Did he not realise
that Allah is watching?
Al-Alaq-14

The Prophet ﷺ said: 'The people whom I hate the most and who are the farthest from me on the Day of Judgment are those who talk uselessly, and those who put down others, and those who show off when they talk.'
(Tirmidhi)

# Acknowledgments

First and foremost, from the depth of my heart I owe my profound thanks and deepest sense of gratitude to Almighty **ALLAH** for the blessings He had bestowed upon me to accomplish this work.

Secondly, my humblest gratitude to **Holy Prophet Muhammad (peace be upon him)** whose way of life has been a continuous guidance for me.

I wish to express my profound sense of appreciation to my supervisor **Prof. Dr. Mrs. Humaira M. Siddiqi (Department of chemistry Quaid-i-Azam University Islamabad)**, for his guidance, sincere advice, motivation and ongoing support throughout my M.Phil.

I am thankful to the chairman of chemistry department **Prof. Dr. Muhammad Siddiq** and head of organic section **Prof. Dr. Amir Saeed** for providing me necessary research facilities in order to accomplish my research work.

I am highly indebted to Dr. Fida for his timely help whenever I needed. I cannot pay him back the amount of support, kindness and help he has bestowed upon me. I am also thankful to Noor-ul-Ameen for his help throughout my research work.

I would like to thanks my lab fellows (Asma Iqbal, Sadaf Ikram, Saba Ashraf Inshad Khan, Shafaq Waqar, Sahar Shumail, Salma Bilquees and Faria Anwar).

I woud like to express my hearties thanks to my friends Rabia Jamil and Tayyaba Habib for her moral support.

I have no words to acknowledge the efforts, guidance, support and prayers from my parents.

I am thankful to everybody who have contributed, even a smile, to my success.

*Maria Zubair*

## Contents

# Table of Contents

# Table of Contents

# List of Schemes

# List of Figures

# List of Figures

# List of Figures

# List of Tables

# Abbreviations

| | |
|---|---|
| *A* | Arrhenius Constant |
| **b.p** | Boiling point |
| **CTNP** | Calcined titania nanoparticles |
| **DDM** | 4,4′-Diaminodiphenylmethane |
| **DGEBA** | Diglycidylether of bisphenol A |
| **DMT** | Dynamic thermal analysis |
| **DSC** | Differential scanning calorimetry |
| $E_a$ | Activation energy |
| $E_k$ | Kissinger activation energy |
| $E_o$ | Ozawa activation energy |
| **FMT** | Functionalized mesoporous titania |
| **FMTEC** | Functionalized mesoporous titania epoxy composites |
| **FTIR** | Fourier transform infrared spectroscopy |
| **FTNP** | Functionalized titania nanoparticles |
| **IDT** | Initial decomposition temperature |
| **MACM** | 2,2′-Dimethyl-4,4′-diaminodicyclohexylmethane |
| **MT** | Mesoporous titania |
| **MTEC** | Mesoporous titania epoxy composite |
| **ODA** | 4,4′- Oxydianiline |
| **PFA** | Perfluoroheptanoic acid |
| **SDS** | Sodium dodecyl sulphonate |
| **SEM** | Scanning electron microscopy |
| **TENC** | Titania epoxy nanocomposites |

# Abbreviations

| | |
|---|---|
| **TGA** | Thermogravimetric analysis |
| **UTNP** | Uncalcined titania nanoparticles |
| **XRD** | X-ray diffraction analysis |

# Abstract

The present study aimed at synthesis, characterization and effect of addition of titania particles [$TiO_2$ nanoparticles (TNP) and mesoporous titania (MT)] on the properties of epoxy-amine matrix. For this purpose, titania particles were synthesized and subjected to different processes, *i.e.* thermal and surface treatment. The treated titania particles were characterized by FTIR, TGA, SEM and XRD. These particles were embedded in epoxy matrix to form titania epoxy composite (TENC, MTEC) and surface functionalized titania epoxy composites (FTENC, FMTEC) with 5 and 7.5 wt. % titania particles (TNP, MT). The prepared composites were characterized by FTIR, DSC, TGA, and XRD. It was found that initial decomposition temperature (IDT), % char yield and glass transition temperatures were greater for TENC and MTEC as compared to neat system due to presence of crystalline titania particles. FTENC and FMTEC on the other hand possess greater contact angle. The increased in contact angle was due to incorporation of fluoro moiety in epoxy amine matrix in the form of perfluoroheptanoic acid on the surface of titania particles.

Epoxy resins have been extensively used in different industrial applications and their properties can be enhanced using different inorganic particulates which demand careful knowledge of cure kinetics. For this purpose curing kinetics of epoxy titania systems were carried out. The curing kinetic parameters *i.e.* activation energy and Arrhenius constant were calculated by Kissinger and Ozawa methods using dynamic DSC. Kinetic parameters were lower for TENC as compared to FTENC and neat system due to catalytic effect of $TiO_2$ on curing of epoxy resins. Kinetic parameters for FTENC were almost similar to neat system which shows that surface modification of titania particles retards its catalytic activity.

# Chapter 1 Introduction

## 1.1 Introduction to nanotechnology:

The term "nanotechnology" was used first time in 1974 by a researcher at the university of Tokyo, to engineer materials at nanometer level. Earlier in 1970's at united state, electron beam lithography was used to synthesize nanostructure 40 to 70 nm in size.

Nanotechnology is defined as the science that involves synthesis, characterization and application of materials and devices having smallest functional organization in nanometer scale, i.e. from a few to several hundred nanometer[1,2]. A nanometer is one billionth of a meter or three order magnitude smaller than micron. DNA molecule is about 2.5 nm, human hair is about 80000 nm and a virus is 100 nm in size[3].

Nanotechnology is a multidisciplinary field. Nanotechnology associates different areas of science like physics, chemistry, biology, mathematics and engineering etc[4]. The building blocks of nanotechnology are nanowires, nanorods, nanoparticles and nanotubes[5]. The nanomaterials are getting more attention due to enhanced properties as compared to bulk materials. This is due to high surface to volume ratio as compared to bulk materials. As the size of nanoparticles decreases, the surface to volume ratio increases and binding energy and coordination number increase. The properties of bulk materials are size independent while in the case of nanomaterials, size dependent properties are observed. When size of any material approaches nanoscale many atoms become part of crystallite surface as compared to bulk materials. The properties like optical, magnetic, conductivity and other preliminaries properties change when particle size reaches up to nano scale[6].

### 1.1.1 Application of nanotechnology:

Nanomaterials make versatile and novel applications in different fields as given below:

**a) Medical field:**

The biocompatible nano sized particles are used in medical field. For application to medical science, nanoparticles are synthesized to interact with cell at molecular level with high degree of specificity. Nanoparticles of ferric oxide and ZnO are used for diagnosis and destruction of cancerous cell[2,7,8]. Nanotechnology have revolutionary impact on diagnosis of neurodegenerative diseases.

Titanium dioxide nanoparticles have antibacterial activity[9,10,11]. Zinc oxide nanoparticles play role in bio-labelling[12]. Nanotechnology also plays important role in the field of tissue engineering, gene therapy, bio imaging, cardiac therapy and orthopedic field[13,14,15].

**b) Food sector:**

Due to promising results and applications in the field of food packaging and food safety, nanotechnology is becoming important in food sector. The incorporation of nanomaterials in food packaging improves the barrier properties. Bio nanocomposites for food packaging not only protect food but are environment friendly as the incorporation of nanoparticles increases the biodegradability of packaging material[16,17,18]. Food spoilages can be detected using nano sensors that are designed to florescence in different color on contact with pathogens[19].

c) **Cosmetics**:

Nanotechnology is used in many cosmetic products like moisturizers, sun screen and make up[20]. Nanoparticles are used as UV filter and the use of polymer nanocapsules help in active delivery of ingredients into the deeper layers of skin[21]. Gold nanoparticles are used as anti-aging[22].

**d) Optical application**:

Nanoparticles like $TiO_2$ are used for optical application due to unique optical properties including high refractive index, high transparency, and photonic rays etc[23].

**d) Energy:**

The storage of energy is the most promising projects of nanotechnology. Nanotechnology provides insulators like carbon and silicon nanostructure which are so smaller and lighter than conventional insulator[24]. Commercially available solar cells have much lower efficiency, which can be enhanced by using $TiO_2$ and ZnO nanoparticles[25,26].

## 1.2 Polymer composites:

Polymer composites represent the class of materials with improved polymer properties like mechanical strength, thermal stability, barrier properties and heat resistance[27,28].

# Chapter 1 Introduction

Polymer composites primarily consist of polymer matrix as a continuous phase and filler as a discontinuous phase. The matrix material can be of three types; metallic, ceramic and polymeric. Among these polymeric matrix is mostly used. The toughness and mechanical properties of polymer matrix is very low and this limitation can be overcome by incorporating nanoparticles in polymer matrix[29]. The solid phase may be amorphous, semi crystalline, or purely crystalline[30]. So the mechanical and thermal properties of polymer composites differ remarkably from that of neat polymer. Incorporation of inorganic filler in polymer matrix improves its thermal, mechanical, electrical, optical and catalytic activity. Polymer matrices like thermoplastic and thermosets have been reinforced with filler from the past few years[31]. Because the processing of polymer matrix composites requires no drastic condition like high pressure and temperature. The properties of composites depend upon the size of nanoparticles. By slightly changing the size of nanoparticles the composite properties will be changed[27,32].

The combination of polymers and inorganic nanoparticles, also called organic-inorganic hybrids display improved thermal, mechanical, electrical, optical and catalytic properties as compared to the neat polymer. Thus nanocomposite have been extensively studied in the past few years[33,34].

## 1.3 Epoxy resins:

Epoxy resin are one of the most important class of thermosetting polymers due to the properties like heat, chemical and moisture resistance, toughness, mechanical and adhesion[35]. The epoxies have application in the field of aerospace, engineering, electronics and transportation[36,37].

Epoxy resins are the molecule containing more than one epoxy groups capable of being transformed to useful thermoset form. The simplest epoxy is three membered ring, i.e. oxirane or 1,2-epoxy. Primarily, they are oligomeric compounds with epoxy groups, which can be synthesized by chemical reaction of bisphenol-A and epichlorohydrin which constituting more than 90% of world production[38]. For commercial epoxy, the degree of polymerization i.e. n value, ranges from 0 to 25. The epoxy resins that have lower n value are cured using epoxy ring while the one having higher values are cured using hydroxyl group[39].

### 1.3.1 Properties of epoxy resins:

The promising properties of epoxy resins are as follows:

**1) Low shrinkage**

During curing of epoxy resin there is slight rearrangement in structure and no volatile by products are evolved due to which the epoxy resins show low shrinkage after curing[40].

**2) High electrical insulation**

Epoxy resins are very good insulating materials having dielectric strength of about 100-220 kV/cm. Generally, polymeric insulators perform better than ceramics due to these reasons epoxy resins are used as electrical insulator[41].

**3) Good chemical resistance**

This property of epoxy resins depends on curing agent. Cured epoxy resins possess high chemical resistance and cannot be solubilized in any solvent[42].

**4) Low viscosity**

Viscosity of epoxy resins is dependent on molecular mass. With an increase in molecular mass, the viscosity of epoxy resins increases[43].

**5) High mechanical strength**

Epoxy resins have high mechanical strength, this property of cured epoxies makes their use possible in industries[44].

### 1.3.2 Epoxy resin as insulating material:

Polymeric insulating materials due to their good dielectric properties and light weight have been widely used in distribution and transmission lines. When polymeric insulating material like epoxy resin is used as outdoor insulator then due to climate stresses such as ultraviolet rays in sunlight, moisture, humidity, temperature, acid rain and other contaminants it shows degradation which reduces its performance. This reduction is due to physical and chemical changes that take place on the surface of polymer[45].

Epoxy resins are used as adhesives, in electronics and for transportation and to small extent in road surfacing because compared to polyester, epoxies have better mechanical properties and are chemical and heat resistance[46].

When insulators made of epoxy resin are used for outdoor, the presence of contaminants on the surface of insulator become serious problem. Different materials have different contamination performance but generally polymeric insulators perform better than ceramic[47].

Epoxy resin is a hydrophilic material, therefore in tropical area, humidity, ultraviolet radiation and rain fall play role in degradation of the insulator[48].

Contamination layer will be formed on the surface and it results in surface tracking and current leakage, especially when insulator surface wet caused by fog, dew or rain. Leakage current initiates a process of heat conduction which occurs on the surface and finally flashovers or insulation breakdown would occur[49].

The increase in hydrophobic character of epoxy resin by incorporation of silicon rubber and silica increases the contact angle and surface degradation of epoxy resin[50]. To increase the hydrophobic character the surface were coated with low-surface energy compounds[51] and by deposition of nanoparticles[52,53] or by increasing the surface roughness[54]. Additionally nanosilca with different size increase the hydrophobic character[55].

### 1.3.3 Classification of epoxy resins:

Epoxy resins are mainly divided into two categories:

1. Glycidyl epoxy resins.
2. Non-glycidyl epoxy resins.

The primary difference between these two types is position of epoxy group. In glycidyl epoxy resins the epoxy group is present at terminal position while in non glycidyl epoxy resins epoxy group is present inside the molecules as shown in figure 1.1.

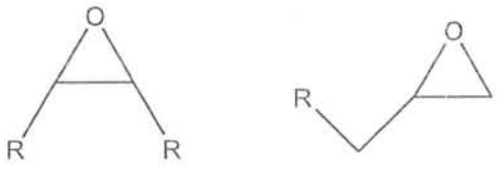


Non-glycidyl-epoxy Glycidyl-epoxy

**R= alkyl or aryl group**

**Figure 1.1** Structure of glycidyl and non glycidyl resins

**1.3.3.1 Glycidyl epoxy resins:**

As mentions above glycidyl epoxy resins have epoxy functionality at the terminal position. The glycidyl epoxy resins impart flexibility and reduce viscosity of resins, due to which its process ability increases. But due to presence of glycidyl epoxy groups, heat resistance of cured epoxy resins also decrease. Diglycidyl ether of bisphenol-A (DGEBA) is one of the most important resin. It is synthesized by condensation of epichlorohydrin and bisphenol A. It has low viscosity and high strength after curing[56]. The structural formula of diglycidyl ether of bisphenol-A is shown in figure 1.2.

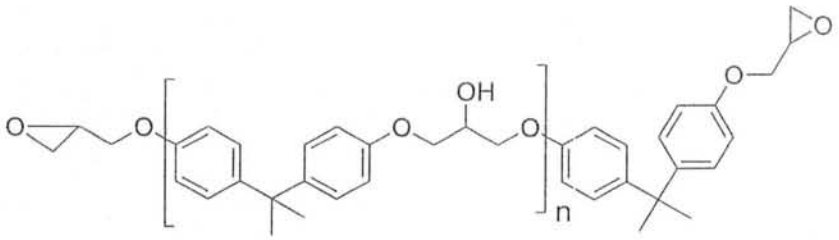


**Figure 1.2** Diglycidyl-ether of bisphenol-A

**1.3.3.2 Non-glycidyl epoxy resins:**

Non-glycidyl epoxy resins have epoxy group inside the molecule and are prepared by peroxidation of olefin double bond. Cycloaliphatic epoxy resins that are non-glycidyl resin have application in adhesive and coating materials[57].

### 1.3.4 Characterization of epoxy resins:

For the characterization of epoxy resins following methods are used;

1. **Determination of Epoxy equivalent:**

Epoxy resin are characterized by two or more epoxy groups. To cure an epoxy group with suitable hardener accurate estimation of epoxy group is necessary. Equivalent weight of epoxy is determined by standard titration using hydrogen bromide solution in acetic acid[49].

2. **Spectroscopic analysis**:

Epoxy resins are characterized by FTIR and NMR spectroscopic analysis. In FT-IR peaks at 890 to 910 $cm^{-1}$ and in $^{1}$HNMR, the signal at 2.8-3.2 ppm is due to epoxy group[39].

### 1.3.5 Applications of epoxy resins:

Application of epoxy resin are following

a) **In electronics:**

In the electronics industry epoxy resins are used in molding integrated circuits, transistors and printed circuit board[58].

b) **In paint industry:**

These system provide a tough protective coating with excellent hardness. Some epoxy coatings are formulated as emulsion in water and can be cleaned up without solvents[59].

c) **As matrix for composites:**

Epoxy resins can be used as a matrix for making high strength composites. such application are used exclusively for aerospace application[60].

d) **Liquid crystalline epoxy:**

Liquid crystalline epoxies have application in electro optics, acoustics, and in information technology[61].

## 1.4 Curing agents:

Such active compound or functionality which converts epoxy resins into hard and rigid material is called hardener and curing agent. Epoxy resins can be cured using different curing agents depending on condition of curing reaction and final product application. The reaction proceeds through opening of epoxy ring through nucleophilic addition reaction. No volatile by products are formed during curing reaction due to the involvement of addition reaction. To increase the curing process sometime accelerator is used. Lewis acid are used for accelerating when alcohol is the curing agent[62].

### 1.4.1 Amine based curing agent:

Amines are the mostly used curing agent. In general primary and secondary amines are more reactive hardeners whereas tertiary amines are used as accelerator for curing reactions[63].

Amines used for curing are classified into three categories: aliphatic, cycloaliphatic and aromatic. The reactivity of amines increases with its nucleophilic character: aliphatic>cycloaliphatic>aromatic.

Diethylenediamine (DETA) and triethylenetetramine (TETA) are highly reactive primary amine and are used for curing of epoxy at ambient temperature.

The curing temperatures of cyclic aromatic amines are higher than cyclic aliphatic amine and give better thermal and mechanical properties[64]. Some examples of amine based curing agents are shown in figure 1.3.

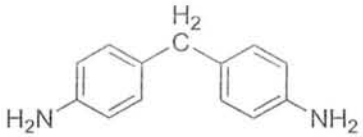

4,4'-Diaminodiphenyl methane(DDM)

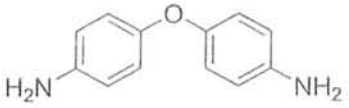

4,4'-Oxydianiline(ODA)

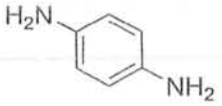

Benzene-1,4-diamine

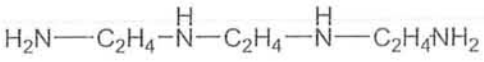

Triethylene tetramine

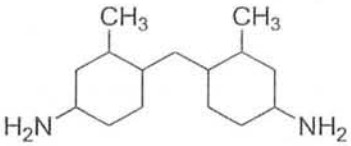

2, 2′-Dimethyl-4,4′-diaminodicyclohexylmethane (MACM)

**Figure 1.3** Diamine based curing agents[65]

### 1.4.2 Anhydride based curing agent:

Anhydride curing agents are getting more attention due to certain properties like less toxicity, absorb less water, and less poisonous. Epoxy anhydride systems have high network $T_g$ compared with amine curing agent and have very good chemical and heat resistance of the resulting network[42]. Some examples of anhydride based curing agents are shown in figure 1.4.

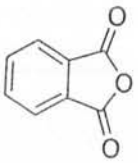

Pthalic anhydride

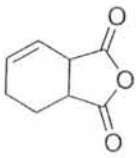

Tetrahydrophthalic anhydride

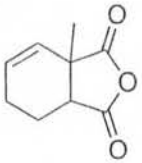

Methyltetrahydrophthalic anhydride

**Figure 1.4** Anhydride based curing agents[65]

## 1.5 Mechanism of epoxy and amine curing reaction:

Each primary amine group of amine curing agent is capable of curing two oxirane rings of epoxy resins. It is anticipated that oxirane ring of epoxy resin opens by primary amine and branch formation occurs by reaction of resulting secondary amine hydrogen with new epoxy resins.

Epoxy curing with amine as curing agent involves three step[66]:

1) First step is the nucleophilic addition of primary amine group of curing agent with the oxirane ring of epoxy resin resulting in the formation of new C-N bond and hydroxyl group.

2) Second step is the reaction of secondary amine with another oxirane ring which results in formation of another C-N bond.

3) Last step is ether bridge formation by etherification of epoxide group with hydroxyl groups that is generated in previous step. This reaction take place at elevated temperature or when curing agents are consumed[67].

The schematic representation of curing reaction is given in scheme 1.1.

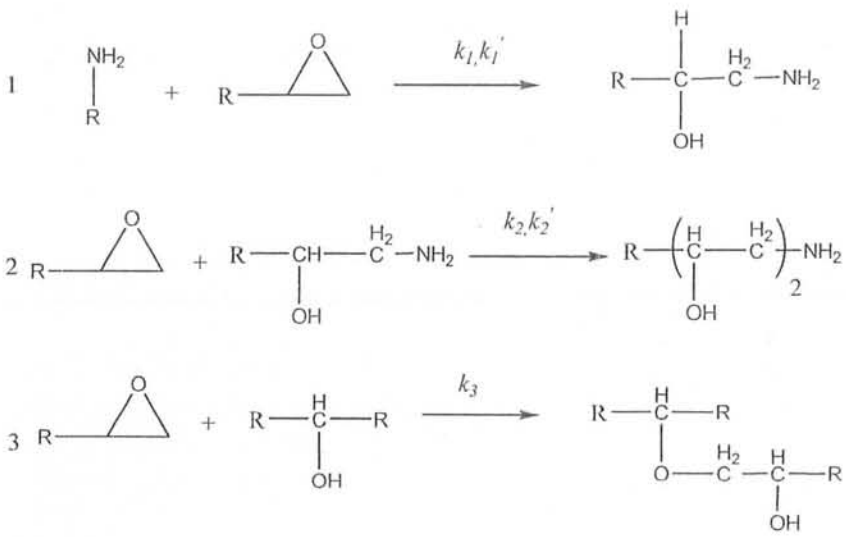

**Scheme 1.1** : Reactions involved in curing of epoxy oligomers with diamine[68]

Where, $k_1$, $k_2$, $k_1'$ $k_2'$ and $k_3$ are the rate constants. The curing reaction between epoxy and diamine take place by two competitive routes: catalytic addition and non-catalytic addition mechanism.

### 1.5.1 Catalytic addition mechanism:

In catalytic addition mechanism, the reaction proceeds through the formation of trimolecular transition state between epoxy and hydroxyl group already present or generated during the reaction with nucleophilic attack of primary amine with the rate constant of $k_1$. The resultant secondary amine attacks on another trimolecular transition state with rate constant of $k_2$ and results in the formation of tertiary amine (scheme 1.2).

The ratio ($r = k_2/k_1$) gives the difference of chemical reactivity of primary and secondary hydrogens in diamine towards epoxy. The more basic curing agent is more reactive and reactivity of diamine depends on substitution of phenyl ring, i.e. electron withdrawing groups decrease nucleophilic attack while donating groups enhance the nucleophilicity of diamine[69].

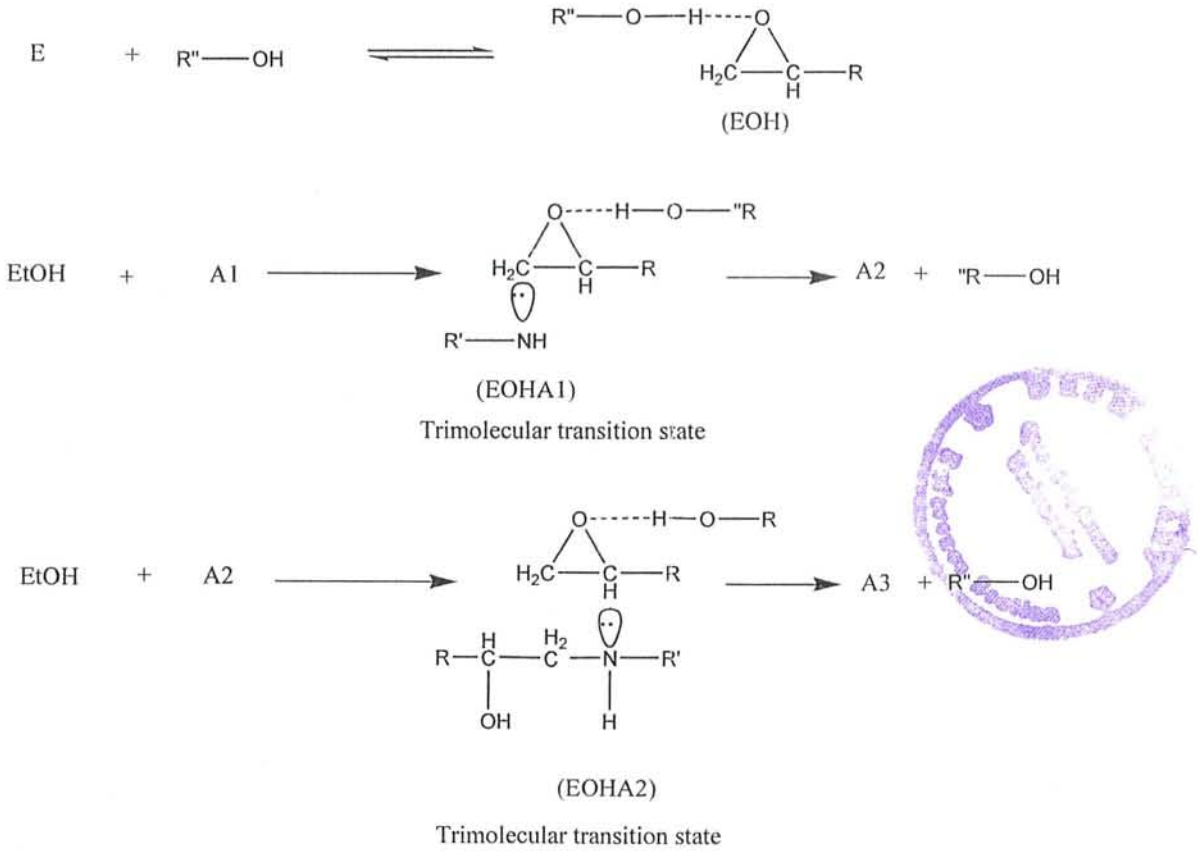


R′ and R′′ = alkyl group

**Scheme 1.2** Catalytic addition mechanism[70]

Where E is the epoxy, R-OH are the hydroxyl group already present or generated in curing reaction, A1 and A2 are the primary and secondary amine respectively. EOHA1 and EOHA2 are the trimolecular transition states.

### 1.5.2 Non-Catalytic addition mechanism:

The non-catalytic addition mechanism involves donor acceptor complex formation between amine and epoxy. As amine acts both as electrophilic and nucleophilic so push and pull transition state are formed in non-catalytic addition mechanism as shown in scheme 1.3[71].

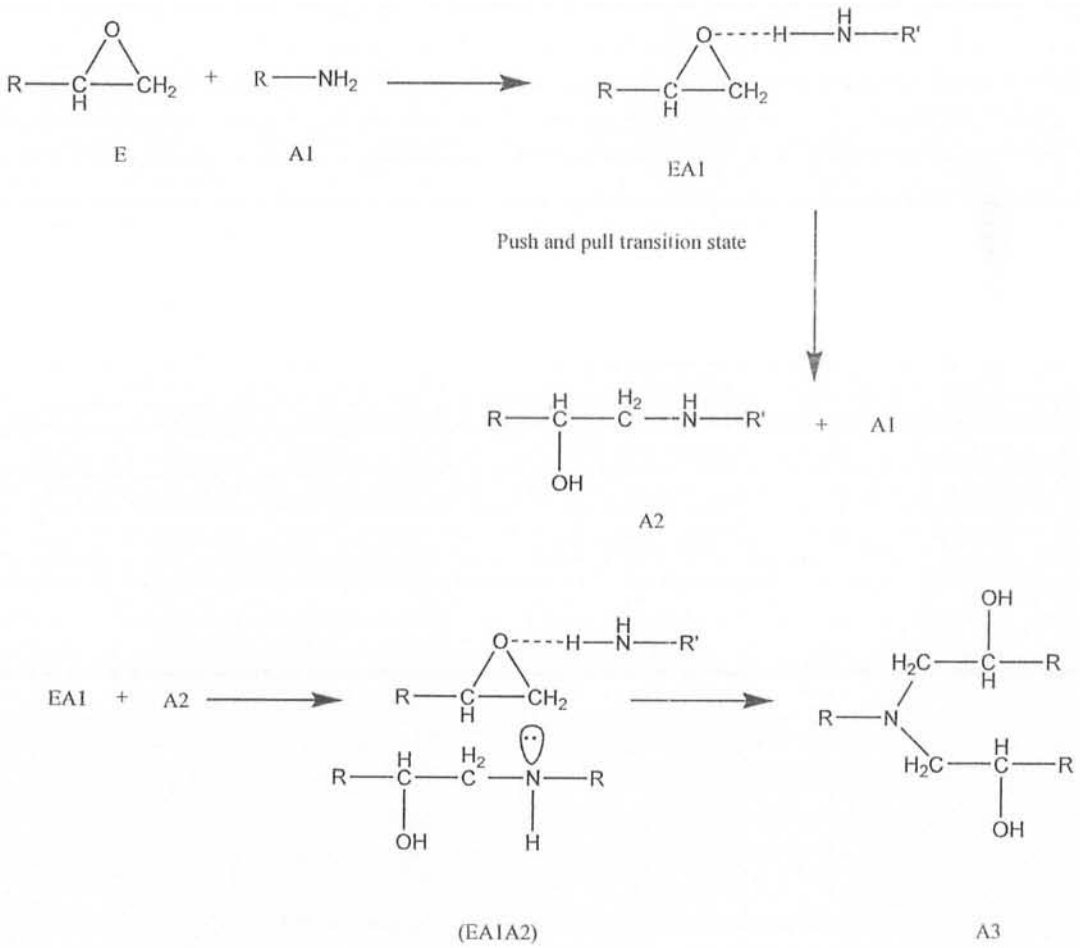


**Scheme 1.3** : Donor acceptor transition state of non-catalytic mechanism[72]

Where E is the epoxy resin, A1 and A2 are the primary and secondary amines respectively. EA1A2 and EA1A1 are the push and pull transition state.

## 1.6 Curing kinetics of epoxy amine reaction:

As properties of cured epoxy resin depend on structure of hardener and epoxy, curing condition, extent of cure, temperature and time of cure therefore it is important to set up the relationship between the properties of epoxy resin and curing condition to optimize the parameters of curing. For that purpose strong information about curing kinetics of epoxy resin is required[62].

The prime aim of curing kinetics is to understand the numerical relationship of kinetic parameters. These parameters are helpful to predict the life time of material and to understand curing reaction[73].

The kinetics of curing can be examined by different techniques i.e. ultrasonic measurements, infrared spectroscopy, dynamic mechanical thermal analysis (DMTA), nuclear magnetic resonance and differential scanning calorimetry (DSC). The DSC has been employed more regularly than other techniques[74,75].

Differential scanning calorimetry is a technique based on thermal analysis and is used to measure the difference in amount of heat flow required to increase the temperature of sample and reference as a function of temperature. DSC is extensively used technique and basic principle of this technique is that when system under consideration undergoes physical change due to chemical reaction, it will take more or less heat to keep the temperature of specimen increasing at the same rate as that of reference. This will deduce either the reaction is endothermic or exothermic. DSC provides incredible data about glass transition temperature, heat of cure and degree of cure of thermosets[76].

### 1.6.1 Methods for kinetic analysis:

The curing kinetics of epoxy/amine reaction can be estimated by using following methods

1) Isothermal DSC method
2) Non-isothermal or dynamic method

#### 1.6.1.1 Isothermal DSC method:

By using isothermal DSC method, the curing of sample is studied at fixed temperature for different time duration. The extent and rate of curing reaction can be studied using this method during curing[77].

#### 1.6.1.2 Non-isothermal DSC method:

Dynamic or non-isothermal curing can be utilized to examine the cure kinetics by heating the sample at constant heating rate over desired temperature range. This method is mostly used as the curing kinetics can be studied at variety of temperature in a brief period of time as compared to isothermal method[78].

### 1.6.2 Kinetic modeling:

Kinetic modeling for curing reaction falls into two fundamental classifications:

1) **Phenomenological models**

   This method deals with prominent features of reaction and can be used if exact mechanism of curing may not be known[79].

2) **Mechanistic models**

   Mechanistic models depict the detail of each reaction that takes part in curing reaction. As curing reaction of epoxy is very complex so it is difficult to understand this model[80].

The temperature and extent of conversion are two main variables of curing process and can be related by given equation.

$$d\alpha/dt = k(T) f(\alpha) \qquad \text{Eq (1)}$$

Where $d\alpha/dt$ is the rate of reaction, $k$ (T) is the rate constant that describes the dependency of rate on temperature, $f(\alpha)$ is a function that defines the dependency of rate of reaction on fraction conversion ($\alpha$). The $k$ (T) can also be obtained by using Arrhenius equation 2.

$$K(T) = A \exp(-E_a/RT) \qquad \text{Eq (2)}$$

Where $E_a$ is the activation energy of reaction, $A$ the pre-exponential factor which measures the probability with which particles possessing activation energy participate in the reaction.

In non-isothermal methods which are mostly used for thermosets, the temperature changes linearly with time as given in equation (3).

$$\beta = dT/dt = \text{constant} \qquad \text{Eq (3)}$$

Where $\beta$ is the heating rate. T and t are the temperature and time respectively.

By combining equation 1 and 2 another relationship can be obtained as shown in equation (4).

$$d\alpha/dt = A\ exp\ (-E/RT)\ f(\alpha) \qquad \text{Eq (4)}$$

In equation 4, (E/RT) is reduced activation energy. For describing fractional conversion, a large variety of reaction models can be used (Sestak-Berggren, Johnson-Mehl Avrami etc.)[81].

By calculating kinetic parameters, energy of activation ($E_a$), and Arrhenius constant, an appropriate kinetic model can determined. $E_a$ and $A$ are correlated, change in activation energy is compensated by change in Arrhenius constant as shown in equation (5) so it is not good to calculate all kinetic parameters from single scan thermal analysis[82].

$$\ln A = a + bE_a \qquad \text{Eq (5)}$$

Where $A$ is Arrhenius constant or pre-exponential factor

a and b are linear equation constant

$E_a$ is energy of activation

Kissinger and Ozawa methods are the most popular methods for the determination of kinetic parameters[83,84].

### 1.6.3 Kissinger and Ozawa methods:

Kissinger and Ozawa methods are mostly used for calculation of kinetic parameters because they are simple approaches to examine non-isothermal curing reaction of epoxy resin/amine system. The kinetic parameters calculated from these methods are without any presumption about conversion-dependent equation.

In Kissinger method activation energy and pre-exponential factors are assumed to be constant. The Kissinger method assumes a first order equation by looking only at one data point for each heating rate which is peak temperature ($T_p$).

$$\ln (\beta/T_p^2) = \ln AR/E_a - E_a/R\ T_p \qquad \text{Eq (6)}$$

Where $\beta$ is the heating rate

$E_a$ is the activation energy and R is general gas constant and $T_p$ is peak temperature.

By plotting ln $(\beta/T_p^2)$ versus $1/T_p$ the value of activation energy and pre-exponential factor can be calculated from the slope of linear fit and the y-intercept[85].

Ozawa method is another approximation for determination of kinetic parameters. The basic of this method is that degree of conversion at peak temperature for different heating rates is constant.

$$\ln (\beta) = \text{constant} - (-1.052E/RT_p) \qquad \text{Eq (7)}$$

All variables are same as mentioned in equation (5) $E_a$ can be determined by plotting ln ß vs. $1/T_p$[85].

## 1.7 Titanium dioxide nanoparticles:

Titanium oxide particles have outstanding chemical and physical properties, which are of interest for applications as catalysts, optics, gas sensor, photovoltaic and precursor materials for mesoporous material[86,87,88,89,90,91]. Titania particles must possess a wide variety of requirements in terms of size distribution, morphology, crystallinity and particle size. The sensing and photocatalytic activity of particles increases as the size decreases[92,93].

### 1.7.1 Historical background:

$TiO_2$ is inorganic compound produced as white powder and is mainly extracted from its ore Ilmenite from Menachem valley and was discovered in 1821 as an industrial chemical[94]. In 1972 the photocatalytic activity of titania was reported and after that titania attracted the attention of researchers[95]. Its properties like nontoxicity, inertness and thermal stability makes it more attractive to use it as photo catalytic material.

Photocatalytic reduction of nitrogen using titanium dioxide was successfully observed. By using photocatalytic activity of $TiO_2$, degradation of aromatic hydrocarbons in visible as well as in ultraviolet region has been studied[96]. In literature, anti-fogging, self-cleaning and hydrophilic properties of $TiO_2$ have also been reported. Over the past few years research efforts have been made to understand advancement in the area of $TiO_2$ and a number of articles have been published to underscore various aspects of $TiO_2$[97,98]. Due to its physiochemical properties, great accessibility, and excellent stability it is widely used for multiple purposes like in pigments, paints, sun screening and coating. The application of $TiO_2$ depends on surface morphology and crystal phase[99].

### 1.7.2 Crystalline phases of $TiO_2$

The phase and degree of crystallinity of titania also play important role. $TiO_2$ exists in three phases: anatase, brookite and rutile. Each phase has different physical properties. Anatase and rutile possess tetragonal crystal phase while brookite has octahedral structure. As a bulk material, rutile is the stable phase. However, in solution phase preparation method generally anatase phase of $TiO_2$ is preferred. Anatase phase particles are synthesized in aqueous environment using alkoxide precursor. For phase pure anatase nanoparticles with diameters in range from 6-30 nm titanium isopropxide and acetic acid are used. If stronger acid is used, a fraction of product will consist of brookite nanoparticles. For phase pure brookite amorphous titania is used as a starting material[100]. The crystal structure data and crystal structure of these phases are shown in table 1.1 and figure 1.5 respectively.

**Table 1.1** Crystal structure data of titanium dioxide[101]

| Phases | Crystal structure | Density ($g\ cm^{-3}$) | Volume/molecule $(A^0)^3$ | O-Ti-O bond angle(degrees) |
|---|---|---|---|---|
| Anatase | Tetragonal | 4.13 | 31.2160 | 81.2<br>90.0 |
| Rutile | Tetragonal | 3.79 | 34.061 | 77.7<br>92.6 |
| Brookite | Orthorhombic | 3.99 | 32.172 | 77.0<br>105 |

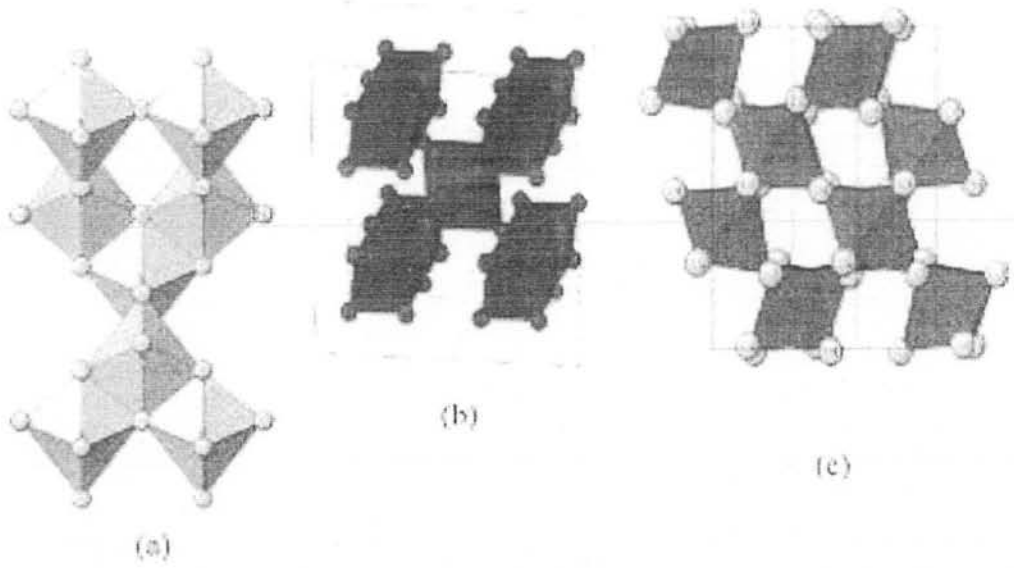


**Figure 1.5** Crystal structure of titanium dioxide (a) anatase (b) brookite (c) rutile[102]

### 1.7.3 Phase transformation:

Transformation of one phase of solid to another by heat treatment is phase transition.$TiO_2$ is synthesized either using inorganic salt such as titanium tetrachloride or using titanium isopropxide as an organic precursor. The reaction conditions such as temperature, pressure, impurities, particle size and hydrothermal condition strongly affect the phase transformation. Some factors that mostly affect phase transformation are discussed below[103].

**a) Effect of temperature**

Temperature is one of the major factor that affects the phase transformation. At temperature lower than 400 °C, amorphous titania is transformed to anatase structure, which is further transformed to rutile phase when heated between 600-1100 °C. There is an increase in particle size as the temperature is increased. For transformation of anatase phase to rutile, the reported temperature is 700 °C and it completely transforms to rutile at 900 °C. Compared to atmosphere anatase phase is more stable in vacuum than in air.

As rutile is more stable at high temperature than anatase and brookite, both these phases transform to rutile at high temperature. As the anatase phase is more stable than brookite, so brookite first transforms to anatase rather than to rutile. Transformation of brookite to rutile on the other hand can take place beyond 700 °C[104].

**b) Effect of hydrothermal treatments**

During hydrothermal treatment crystal size decides phase transformation. If crystal size is small there will be less effect of pressure. With the size less than 50 nm anatase phase is more stable but transforms to rutile when temperature is higher than 700 °C. As prepared $TiO_2$ has anatase phase or rutile or both which transforms to rutile phase which has more growth rate after attaining particular size. For equally sized $TiO_2$ anatase is more stable when size is less than 11nm, for size between 11-35 nm brookite is stable and above 35nm rutile is more stable[105].

**c) Dopants**

The presence of different cations such as $Li^+$, $K^+$, $Al^{3+}$ in crystal structure of $TiO_2$ affects the phase transformation. Silica and alumina stabilize the anatase phase of titania, while ions like chloride increase the transformation of anatase phase to rutile[106].

The interstitial spaces of titanium as well as concentration of oxygen vacancies in $TiO_2$ structure in the presence of different additives affect the phase transformation. Dopants create oxygen deficiency.

### 1.7.4 Methods for the synthesis of titania nanoparticles:

Titanium dioxide has been synthesized by using organic and inorganic precursor i.e. titanium tetrachloride and titanium isopropxide. These precursor can be converted to $TiO_2$ using following methods.

1) Sol-gel method
2) Hydrothermal method
3) Solvothermal method
4) Vapor deposition method
5) Microwave method

Among these, sol gel, hydrothermal and solvothermal methods are commonly used in laboratory.

**1) Sol- gel method**

In a typical sol-gel process, a colloidal suspension is formed from hydrolysis and condensation of the precursors, which are usually inorganic metal salts or metal alkoxide. Complete polymerization leads to transition from liquid sol to gel phase. Commonly used precursors are titanium tetrachloride and titanium alkoxide.

When titanium alkoxide is used as precursor the sol gel method completes in three steps namely hydrolysis, alcohol condensation and water condensation[107]. Figure 1.6 shows the synthesis of $TiO_2$ particles by sol-gel method.

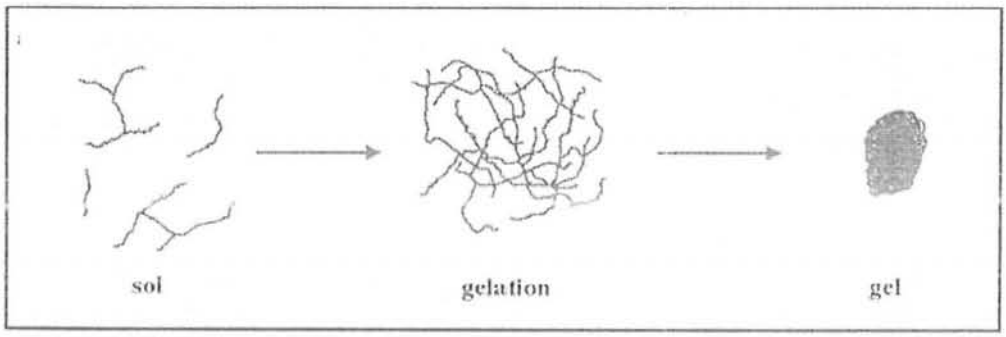


**Figure 1.6** Synthesis of titania nanoparticles[108]

$$TiOR + H_2O \xrightarrow{\text{Hydrolysis}} TiOH + HOR \qquad \text{Eq (6)}$$

$$TiOR + TiOH \xrightarrow{\text{Alcohol condensation}} Ti\text{-}O\text{-}Ti + HOR \qquad \text{Eq (7)}$$

$$TiOH + TiOH \xrightarrow{\text{water condensation}} Ti\text{-}O\text{-}Ti + H_2O \qquad \text{Eq (8)}$$

In case of inorganic metal as precursor, this method completes within two step i.e. hydrolysis and condensation[109].

$$TiCl_4 + H_2O \xrightarrow{\text{Hydrolysis}} TiOH + HCl \qquad \text{Eq (9)}$$

$$TiOH + TiOH \xrightarrow{\text{Condensation}} Ti\text{-}O\text{-}Ti + H_2O \qquad \text{Eq (10)}$$

### 2) Hydrothermal method

The hydrothermal synthesis is done in steel pressure vessels called autoclaves with or without teflon lining that are filled with aqueous solutions of organic or inorganic precursor. The temperature of system can be elevated above the boiling point of solvent, reaching the pressure of vapor saturation. The temperature and amount of solution added to autoclave largely determine the internal pressure produced[108].

$TiO_2$ synthesis using hydrothermal method is carried out by addition of precursor to distilled water, resulting solution is then poured into vessel and is treated at 80-100 °C for few hours. Figure 1.7, shows the typical autoclave used in hydrothermal synthesis.

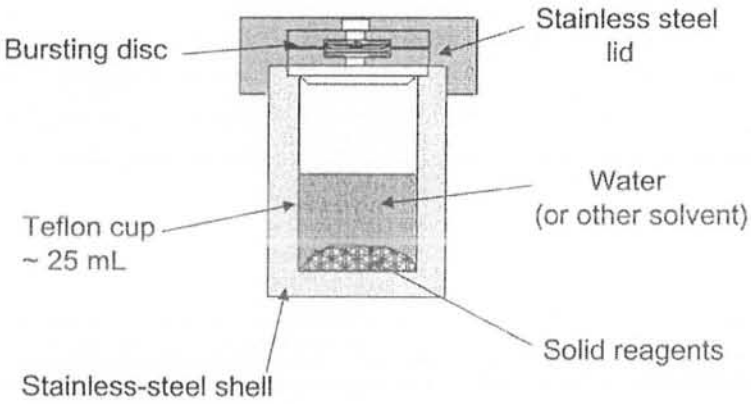


**Figure 1.7** Autoclave used in hydrothermal synthesis[110]

### 3) Solvothermal method

The solvothermal method is almost similar to the hydrothermal method except that the solvent used is non aqueous. However, the temperature can be elevated much higher than hydrothermal methods. This method has better control on size and shape distributions than hydrothermal method. This method is versatile for nanoparticles with narrow size distribution and dispersity[111].

### 1.7.5 Mesoporous titania particles:

Titania is used in many applications like electrode in dye sensitized solar cell, as catalyst in organic reactions such as oxidation of toluene or 1-butene. Titania can be used for photocatalytic degradation of pollutants[112,113,114].

The above applications of titania particles can be improved with large surface area and high porosity. Different pathways for synthesis of mesostructures have been followed using variety of templates such as alkyl phosphate anionic surfactants. One of the major issue during synthesis of $TiO_2$ based mesostructures is to attain adequate balance between hydrolysis-condensation processes. The high reactivity of titanium precursors leads to densely and poorly structured inorganic networks. The addition of stabilizing agents controls the reactivity of titanium alkoxide precursor such as alkyl phosphate templated synthesis of mesostructures. Unfortunately, significant amount of phosphate remains in calcined particles which affects the surface catalytic sites of particles[115,116].

Recently an efficient synthetic approach to mesoporous titania process i.e. evaporation-induced self-assembly (EISA) has been introduced. Up till now many reports involving mesostructured titania particles synthesis have been reported that emphasized on control of different processes occurring during synthesis and removal of template. Removal of template by thermal decomposition gives mesostructured phase composed of pure amorphous phase. Further thermal treatment transforms amorphous phase to anatase phase resulting in total collapse of pore system.

The ammonia treatment can convert the amorphous mesoporous phase into crystalline without collapse of porous structure[117].

### 1.7.6 Applications of titania nanoparticles:

The development of porous, complex form with high surface area led titania to be used in a variety of novel applications.

**1) $TiO_2$ in sunscreens**

Every sunscreen contains titanium dioxide. It is a physical blocker for UVA radiation with wavelength between 315-400 nm and UVB radiation with wavelength between 280-315 nm.$TiO_2$ is chemically stable and will not decolorize under UV light.

Titanium dioxide is coated with silica and alumina because $TiO_2$ particles when come into contact with water produce hydroxyl radicals that cause cancer. By modifying the surfaces, chances of contact decreases and it is safe to use it in sunscreen products[118].

**2) In cement and tiles**

Titanium dioxide is added to the surface of cement, tiles and paints to give it anti fouling, deodorizing and sterilizing properties. In the presence of water hydroxyl free radicals are formed and convert into organic molecule i.e. $CO_2$ and water and destroy microorganisms using photocatalytic properties[119].

**3) Catalyst**

Nanoscale titanium dioxide is used as a support material for catalyst applications, in automotive industry. Titanium dioxide is used to removes harmful exhaust gas emissions and removes nitrous oxides in power stations[120].

**4) Paints and coatings**

Titanium dioxide is used as pigment in paints, provide durability, long life and protection to painted surfaces[121].

**5) Plastics and coatings**

Titanium dioxide minimize the brittleness, fading and cracking that can occur as a result of light exposure. This can enhance the life of plastic component in vehicles, building materials and other exterior applications[122].

**6) Cosmetics**

Titanium dioxide is used for hiding disfigurement and brightening of skin. It is used for thinner coating of makeup[123].

**7) Food contact materials and ingredients**

Titanium dioxide protects food, beverages and pharmaceuticals from premature degradation, enhancing the life of product due to opacity to visible and ultraviolet light[124].

The most promising application of $TiO_2$ nanomaterial include paint, toothpaste, electrochemical, sensing and photovoltaics[125].

**8) From UV protection:**

$TiO_2$ nanomaterials are very stable, nontoxic, and cheap. The optical and biological properties make it suitable for UV protection application[126].

**9) Degradation of pollutant**

$TiO_2$ is most efficient and environmentally friendly photo catalyst and is widely used for photo degradation of various pollutants[127].

**10) In photo chromic devices**

Titania nanomaterial when sensitized with dyes or metal nanoparticles is used to build photochromic devices[125].

**11) As a sensor**

These nanomaterials have been used in sensors due to electrical and optical properties which change upon adsorption[87].

**12) In solar cell**

$TiO_2$ nanoparticles can absorb light into visible light region and convert solar energy into electrical energy for solar cell application[128].

## 1.8 Why particles surface are modified?

Metal oxide nanoparticles possess unique properties to equivalent large scale materials. The properties of polymer composites depend on type and size of nanoparticles that are incorporated. The main problem with composite material is that nanoparticles form aggregate and cannot produce monodispersed nanoparticles in polymer matrix. Surface modification can;

1. Stabilize nanoparticles against agglomeration.
2. Render them compatible with polymeric phase
3. Avoid homogeneity and compatibility problems between two phases.
4. Enable their self-organization.

### 1.8.1 Carboxylic acid as modifiers:

Carboxylic acid with coordination of carboxylic groups (COOH) to surface Ti atoms are often used as modifiers. Modification can be accomplished either *in situ* or post modification approach. *In situ* modification is the attachment of modifier molecule on the surface of $TiO_2$ particles during growth of crystals. It is difficult to control both the growth features and surface chemistry of nanoparticles by *in situ* approach. The best way to modify $TiO_2$ particles is by post modification after their formation. The post modification of nanoparticles can be done by immersing particles into organic solution to adsorb carboxylic modifiers at room temperature[129,130].

The carboxylic group can bind on surface of $TiO_2$ by simple adsorption (electrostatic attraction and hydrogen bonding) and chemical adsorption (ester linkage, bridging, and chelating) as shown in scheme 1.4.

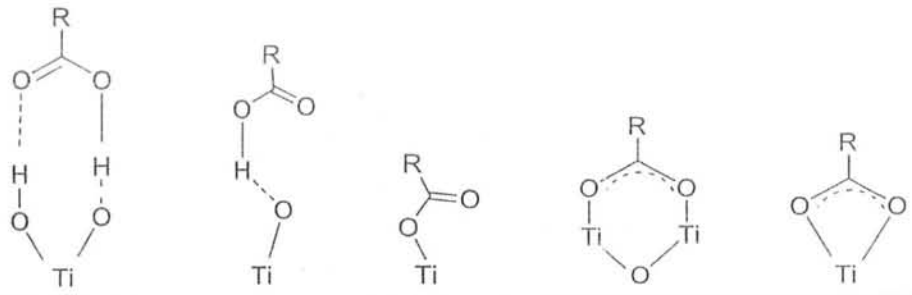


(a) (b) (c) (d) (e)

**Scheme 1.4** Possible binding modes of COOH group on $TiO_2$ surface (a), (b) hydrogen bonding (c) ester like linkage (d) Bidentate bridging linkage (e) Bidentate chelating[131]

A weak and unstable binding of modifier molecule is formed on $TiO_2$ surface by simple immersion method that is desorbed during application. In ruthenium dye molecule the physically adsorbed carboxylic acid group desorb in the presence of electrolyte because the trace water in electrolyte will break the weak interaction formed by adsorption during immersion process[132].

Solvothermal approach is a convenient way to chemically modified $TiO_2$ nanoparticles with carboxylic acid. Modification efficiency by solvothermal method is much higher than that of conventional immersion approach. The reaction processes in solvothermal method have two key interactions: the formation of double hydrogen bondings between the carboxylic acid molecule and $TiO_2$ at Ti site and by dehydration from the hydrogen bondings. The solvothermal method chemically post modifies $TiO_2$ surface and is expected to have many potential applications[131].

## 1.9 Titania epoxy composites:

Epoxy resins are widely used in industrial applications such as matrices in composite materials, adhesives, coatings, and electronic circuit board laminates, and so forth due to their excellent mechanical and thermal properties. The major problems with epoxy are low stiffness and strength[133]. Nanoparticles embedded in epoxy increase its thermomechanical properties[134].

Titania composites have generally been synthesized to investigate the effects of filler on mechanical and thermal properties of composites[135] .The basis of improvement in properties is the interaction between filler and the matrix, which is evidenced by various technique such as IR and DMTA[136]. This interaction facilitates load transfer from the matrix to the reinforcement. Since titania has photocatalytic behavior as well, so some decrease in thermal properties has also been observed[137]. Titania hybrids with epoxy showed earlier degradation temperature, which was attributed to the catalytic activity of titania[138]. Both the $TiO_2$ and $SiO_2$ filler are used simultaneously to overcome the deteriorative feature of titania[139]. Apart from mechanical and chemical resistance, titania also improves the weather resistance of the composite materials[140].

Moloney *et al.* reported that increasing the volume fraction and filler modulus increase the modulus of particulate-filled epoxy resins[141]. Nanometer-$TiO_2$-filled epoxy composites have higher scratch resistance than both pure epoxy and micron-$TiO_2$-filled epoxy composites[142].

$TiO_2$ filled polymers are well known antimicrobial materials. Addition of $TiO_2$ may act as substitute for pollution treatment. $TiO_2$ generate hydroxyl radical in the presence of UV light which can degrade the pollutant into environment friendly products[143].

Parameswaranpillai and his coworker reported the cure reaction, rheology, volume shrinkage, and thermomechanical behavior of epoxy-$TiO_2$ nanocomposites. It was found that $TiO_2$ act as catalyst and decrease the overall degree of cure[144].

Carballeria and his coworker studied the influence of adding different volume concentration of $TiO_2$ in epoxy resin. Plain strain fracture toughness, elastic modulus, tensile strength, and maximum sustained strain were measured in mechanical tensile test. The results showed that incorporation of titanium dioxide into epoxy matrix improved the stiffness, toughness, maximum strain and crack propagation as compared to neat resin[145].

Epoxy nanocomposite system with inorganic oxide fillers display some advantageous dielectric behaviors at low nano filler loadings. The permittivity and tan delta values in the nanocomposites are found to be lower than that of micro composites as well as unfilled systems[146].

Shaorong, *et al* and his coworkers synthesized new inorganic-polymeric hybrid material of epoxy/silica-titania which showed high glass transition temperature and modulus than that of unmodified systems[140].

Suspension of titania nanoparticles in benzyl alcohol was mixed with aliphatic epoxy resin. In the resulting epoxy-titania hybrid, presence of titania increased both glass transition temperature and modulus, thus confirming the reinforcing and stiffening effect of inorganic nanofillers[147].

Zakya Rubab and coworkers reported the comparative effect of thermally treated and surface modified titania nanoparticles on the mechanical properties of epoxy amine matrix. Studies showed that crystalline $TiO_2$ nanoparticles enhanced thermal stability of composites due to their rigid, crystalline nature, and high thermal diffusivity. However, surface modified titania nanoparticles provide greater mechanical strength, high modulus, improved toughness, and high $T_g$ due to better interlinking of inorganic and organic phase[148].

Epoxy-titania-silica hybrid materials with covalent bonding interaction between polymer and inorganic phases have been prepared using titania/silica mesoporous particles. The glass transition temperature and modulus of modified system increased as compared to neat system. The impact strength and tensile strength of hybrid increased by 53.5 % and 14 % when the $SiO_2$-$TiO_2$ content is up to 3wt %[149].

A systematic study was conducted by Chatterjee and his coworker to investigate matrix properties by introducing nanosized $TiO_2$ filler into an epoxy resin. The results showed that infusion of nanofillers improve the thermal, mechanical and viscoelastic properties of epoxy resin[150].

Federica and his coworkers prepared organic-inorganic hybrids with silica, zirconia, or titania. These particles were generated *in situ* with epoxy resins based on bisphenol-A diglycidyl ether and jeff amine by means of the aqueous sol-gel process. Silica and zirconia filled epoxies were characterized by a significant increase in thermal stability, which was attributed to high thermal stability of silica and zirconia phases. On contrary, the introduction of titania induced a strong decrease in thermal stability of epoxy/titania hybrids in comparison to pure epoxy resin, attributable to metal-catalyzed oxidative decomposition mechanism in the polymer/titania composite[151].

Jan sumfleth prepared multiwalled carbon nanotube-epoxy composites modified with titania nanoparticles in order to obtain multiphase nanocomposites with an enhanced dispersion of carbon nanotubes. Besides an enhanced dispersion, the hybrid structure leads to synergistic effect in terms of glass transition temperature of the nanocomposites. Although a decrease of glass transition temperature ($T_g$) is observed for nanocomposites containing only one type of filler. The combination of titania and carbon nanotubes into hybrid structures reduces the decrease in $T_g$, thus demonstrating the potential of such hybrids structure as fillers[152].

A systematic approach was considered to study the matrix properties by introducing $TiO_2$ –$SiO_2$ filler into an epoxy resin. The dependence of the activation energy on the conversion degree was interpreted by isoconversional method. Morphology studies using SEM showed that the nanoparticles were dispersed into the entire volume of resin, homogeneously. From the experimental data, the nanocomposite exhibited increase in storage modulus, glass transition temperature, and decomposition temperature from neat system[153].

## 1.10 Plan of work:

The objective of this work was to synthesize $TiO_2$ particles and modification of their surface chemistry. These particles were disperse in epoxy-amine matrix using perfluoroheptanoic acid as coupling agent. The epoxy resin used for this work was diglycidylether of bisphenol-A (DGEBA) and 2,2′-dimethyldicyclohexylmethane (MACM) was used as curing agent. The titania particles were synthesized by sol gel method using $TiCl_4$ and titanium tetrabutoxide as precursor for $TiO_2$ nanoparticles and mesoporous titania particles respectively.

This research work is divided in two parts

1) Synthesis of titania particles
2) Synthesis of titania epoxy amine and mesoporous titania epoxy amine composites.

The scheme for synthesis of titania particles is elaborated in figure 1.8.

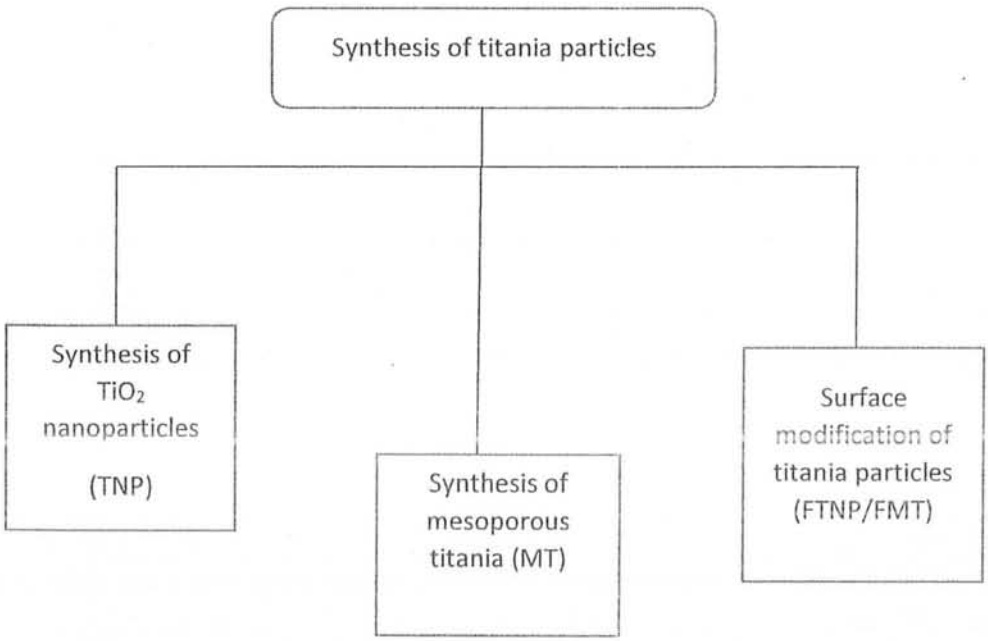


**Figure 1.8** A general scheme for synthesis of titania particles

These particles were characterized by FTIR, XRD, TGA, and SEM

Four series of $TiO_2$ epoxy amine composites and mesoporous titania epoxy amine system were synthesized. The effect of filler on the properties of epoxy amine system was studied using 5% and 7.5% of filler. The scheme for the synthesis of composites is shown in figure 1.9.

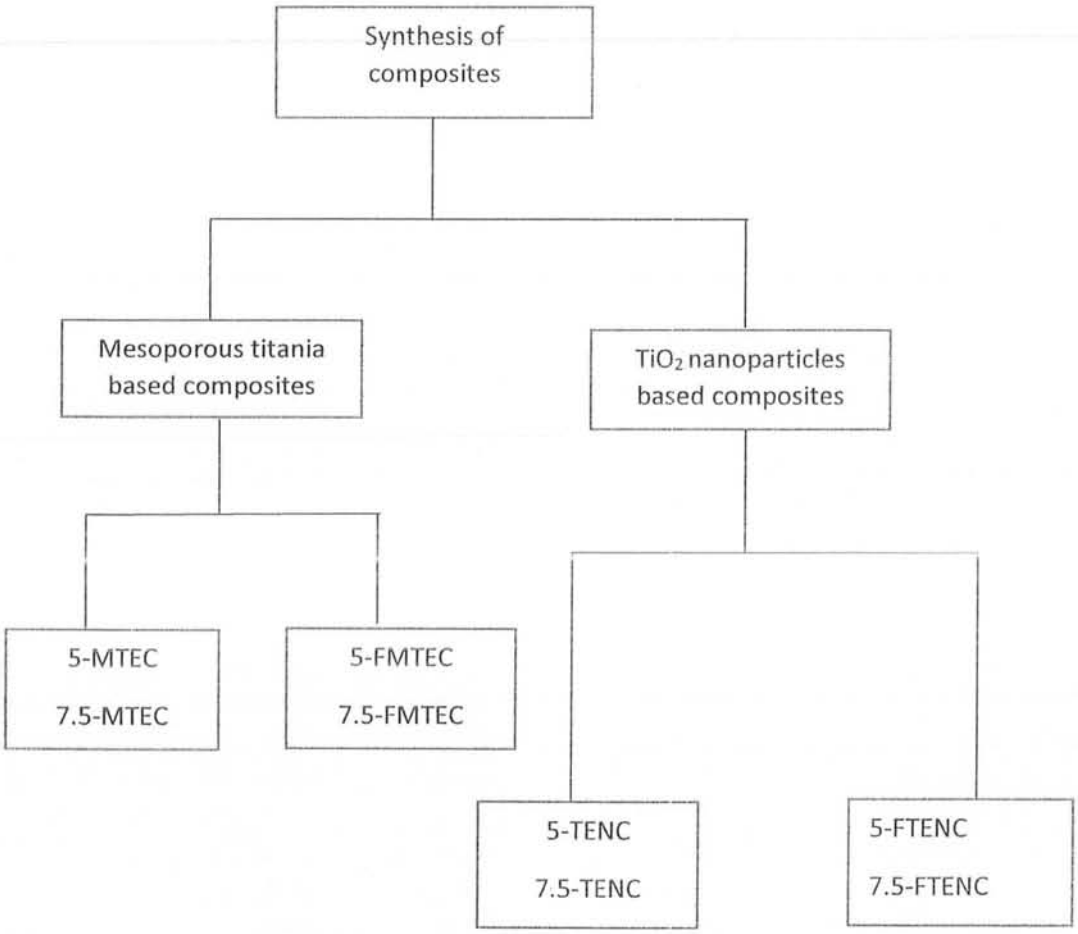


**Figure 1.9** A general scheme for synthesis of composites

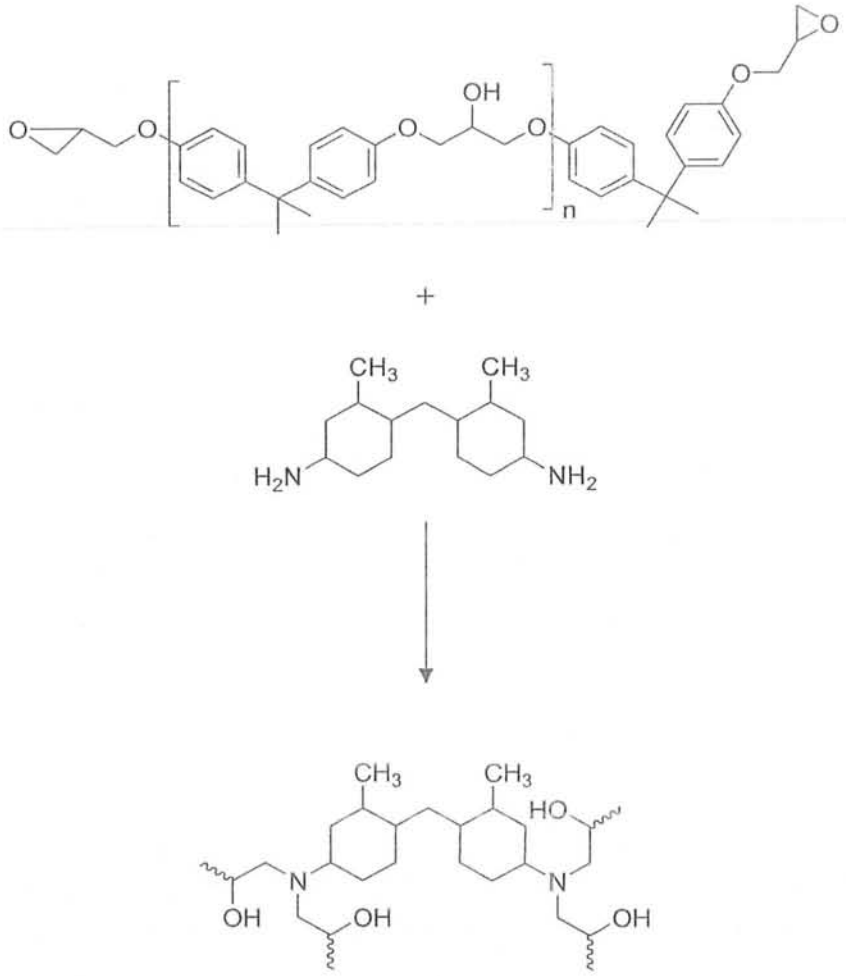


**Scheme 1.5** A general reaction between epoxy –amine

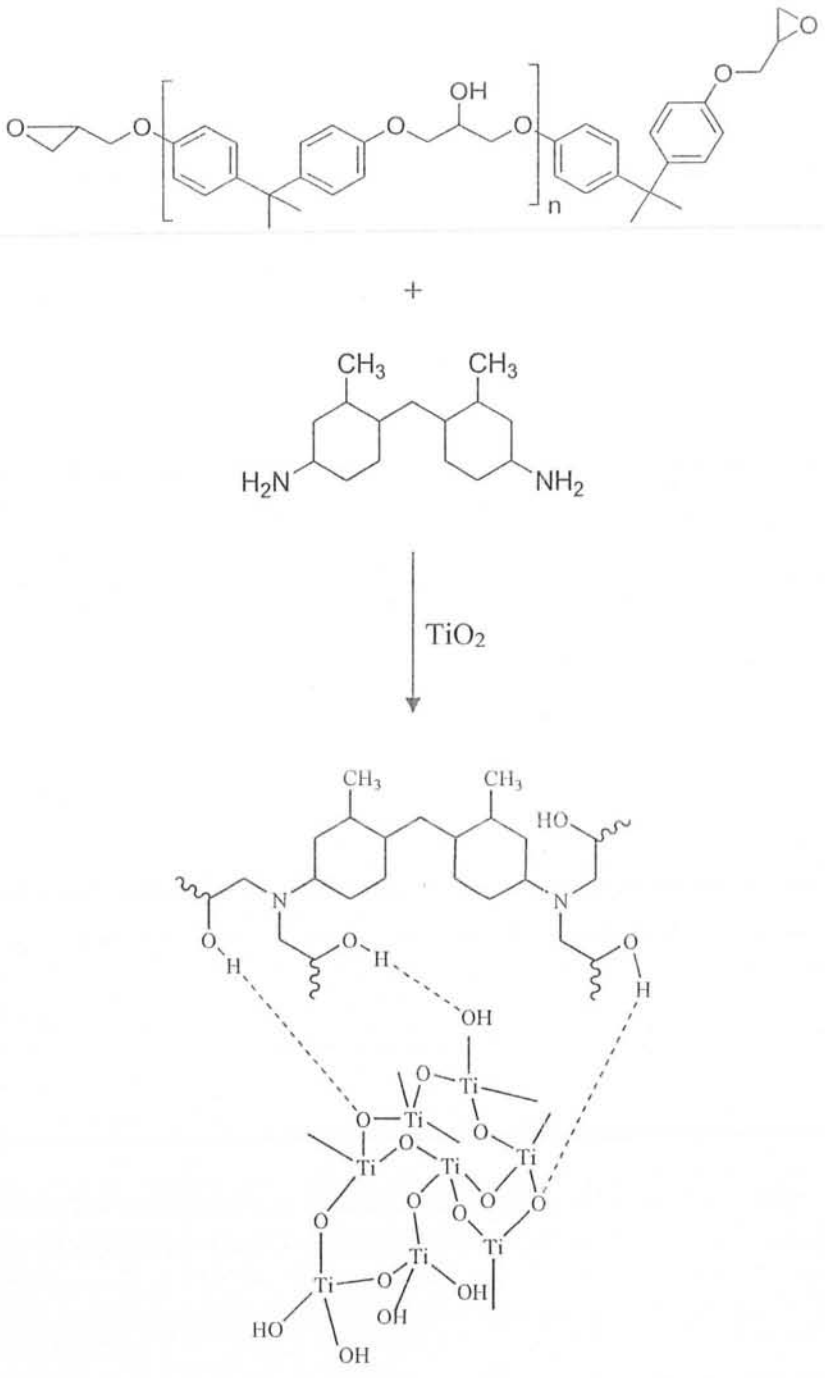


**Scheme 1.6** Hypothetical scheme showing a general interaction between titania epoxy amine system

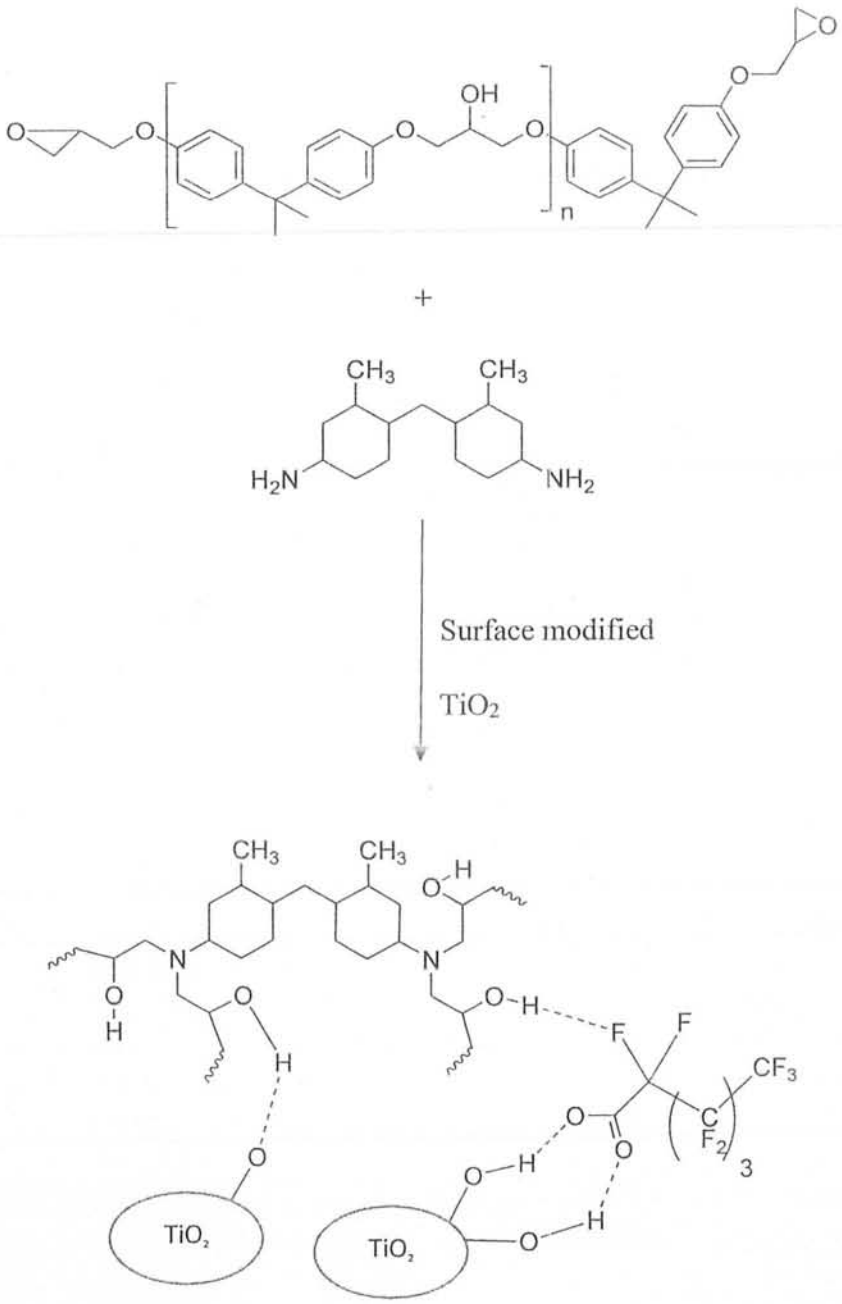


**Scheme 1.7** Scheme showing interaction between surface modified titania epoxy and amine system

# Chapter 2 Experimental

This chapter illustrates the chemicals used, the synthetic methodology for the preparation of $TiO_2$ nanoparticles, mesoporous titania, composites and characterization techniques used for their analysis.

## 2.1 Chemicals used

The precursors for the synthesis of $TiO_2$ particles and titania epoxy based nanocomposites are given as follows.

### 2.1.1 Epoxy resin

The epoxy of type, diglycidylether of bisphenol A, abbreviated as DGEBA was obtained from DOW chemicals and was used as received. It has molar mass of 355 g/mol, the equivalent weight per unifunctional group is $E_E$ =177.5 g/mol.

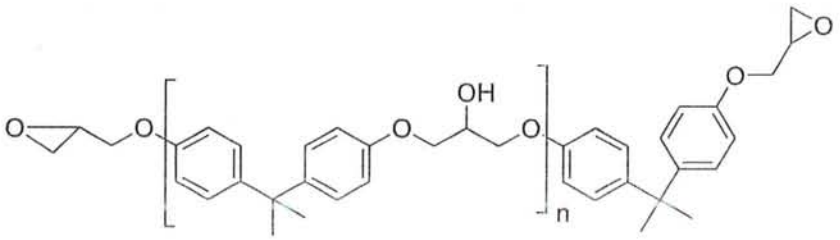


**Fig: 2.1** Diglycidylether of bisphenol A (DGEBA)

### 2.1.2 Coupling agent

Perfluoroheptanoic acid (PFHA) was obtained from Sigma Aldrich and was used as received. It has molar mass 364.06 g/mol and boiling point 175 °C.

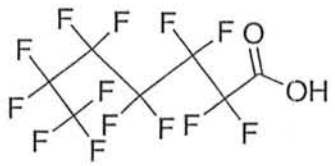


**Figure 2.2** Perfluoroheptanoic acid (PFHA)

### 2.1.3 Curing agent

2,2′-Dimethyl-4,4′-diaminodicyclohexylmethane abbreviated as (MACM) was available commercially. It has molar mass of 238.4 g/mol, the equivalent weight per $NH_2$ functionality is 59.60 g/mol.

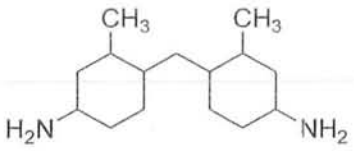


**Figure 2.3** 2,2′-Dimethyl-4,4′-diaminodicyclohexylmethane (MACM)

### 2.1.4 Precursor for the synthesis of $TiO_2$ nanoparticles

Titanium tetrachloride ($TiCl_4$) was obtained from Fluka and was used as received. It has molar mass 189.67 g/mol and boiling point 136.4 °C.

### 2.1.5 Precursor of mesoporous titania

Titanium tetrabutoxide $Ti(OBu)_4$ was obtained from Sigma Aldrich and was used as received. It has molar mass 340 g/mol and boiling point 312 °C.

### 2.1.6 Other solvent and reagent used

Ethanol was dried on CaO for 6 hours and distilled. HCl 33 % was obtained from AnalaR and was used as received. Amrnonium hydroxide ($NH_4OH$) was obtained from lab scan and used as received. It's molar mass is 35.04 g/mole and its boiling point (b.p) is 24.7°C. Sodium dodecylsulphonate (SDS) was used as surfactant.

## 2.2 Characterization techniques

The specification of all characterization techniques are given below.

### 2.2.1 Fourier transform -infrared spectroscopy (FT-IR)

Spectra of nanoparticles were recorded at 25 °C in 400-4000 $cm^{-1}$ range by using THERMOSCIENTIFIC NICOLET 6700 solid state attenuated total reflectance-fourier transform infrared spectroscopy (ATR-FTIR).

### 2.2.2 X-ray diffraction analysis

X-ray diffraction analysis was carried out at room temperature (25 °C) using Siemens d 5000 X-ray instrument using Cu Kα radiation.

### 2.2.3 Scanning electron microscopy (SEM)

To study the morphology of titania particles, scanning electron microscopic analysis of all powder and composite films was done at 25 °C using Jeol,JSM-6490A SEM analyzer manufactured by Japan.

### 2.2.4 Differential scanning calorimetry (DSC)

The curing kinetics of sample was done with METTLER TOLEDO 823e DSC instrument. 7-8 mg of samples were filled in sealed aluminum pan and cured with multiple heating rates in desired temperature range under nitrogen flow of 20 mL/min.

### 2.2.5 Thermogravimetric analysis (TGA)

Thermogravimetric analysis of composites, was carried out with NETZSCH STA 409 TGA/DSC analyzer at 25 °C. 9.5 mg of sample was heated to 950 °C in aluminum pan under nitrogen atmosphere at a heating rate of 10 °C/min.

## 2.3 Synthesis of particulate reinforcement

Titania particles were used as reinforcement. Inorganic sol gel route was used to generate $TiO_2$ from titanium tetrachloride while mesoporous titania was synthesized from titanium tetrabutoxide as precursor. Three types of particles were synthesized by varying reaction parameters and processing conditions. These three types will be called titania nanoparticles (TNP), mesoporous titania (MT) and functionalized titania (FTNP, FMT) in further discussion for the sake of convenience.

### 2.3.1 Synthesis of $TiO_2$ nanoparticles by sol-gel method (TNP):

$TiO_2$ nanoparticles were synthesized using $TiCl_4$ as precursor. 3 mL of $TiCl_4$ was added dropwise to a solution of ethanol: water (3:1). Clear solution was formed immediately which indicated hydrolysis of precursor. To control the pH, 8 mL of $NH_4OH$ was added dropwise. White precipitate of $TiO_2$ was formed following condensation and settled down at the bottom of beaker. Solvent was decanted off and the particles were washed with distilled water three times. After that the nanoparticles were separated by using centrifuge machine. The separated nanoparticles (1 g) were dried in oven at 100 °C and then calcined at 450 °C for 4 hours. The as synthesized $TiO_2$ nanoparticles were characterized by XRD, SEM and FT-IR[148].

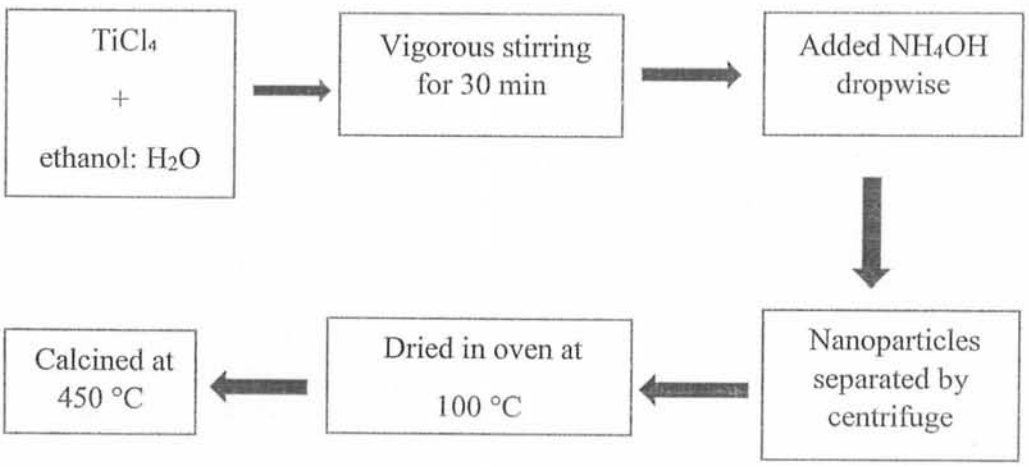


**Figure 2.4:** Synthetic methodology of $TiO_2$ nanoparticles[148]

### 2.3.2 Synthesis of mesoporous titania (MT):

Mesoporous titania particles were synthesized using sol-gel method. SDS was used as surfactant and titanium tetrabutoxide $Ti(OBu)_4$ as titania precursor. 1.12 g of sodium dodecylsulphonate (SDS) was added to 30 mL of ethanol and sonicated for 30 min. In a separate beaker 5 mL titanium tetrabutoxide $Ti(OBu)_4$ was added to 20 mL of ethanol, white suspension formed immediately. This white suspension was added to surfactant dropwise. Ammonia solution /ethanol (1:4) was then added and stirred at room temperature for two hours. Additionally the solution was aged at room temperature for 12 hours. The mesoporous particles were then separated using centrifuge machine. During centrifugation particles were washed with ethanol. The separated mesoporous particles (1.8 g) were dried in oven at 100 °C and calcined in furnace at 550 °C for 4 hours.

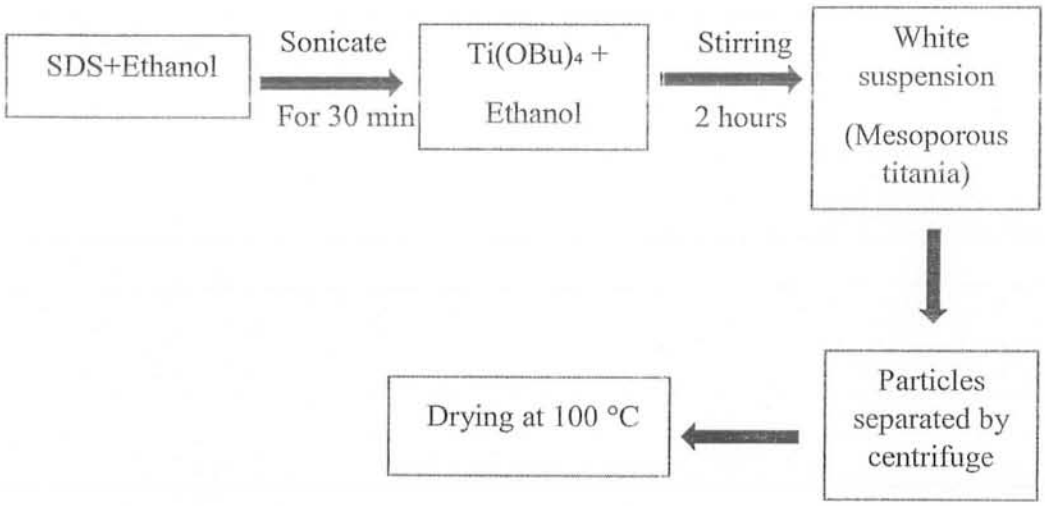


**Figure 2.5** Synthetic methodology of mesoporous titania (MT)

### 2.3.3 Functionalization of titania particles (FTNP, FMT):

The $TiO_2$ nanoparticles synthesized by above procedure were functionalized using perfluoroheptanoic acid. 0.5 g of $TiO_2$ nanoparticles in 200 mL of toluene were sonicated in two neck round bottom flask for two hours. After sonication 1.5 mL of perfluoroheptanoic acid was added to titania nanoparticles and reaction mixture was kept under refluxed at 110 °C for 24 hours. After that functionalized nanoparticles were separated by filtration and then washed with deionized water three times. Separated nanoparticles (0.3 g) were dried in oven at 50 °C. Figure 2.6 shows schematic pathway followed for functionalization of titania particles and possible interaction between perfluoroheptanoic acid (PFHA) and Ti surface.

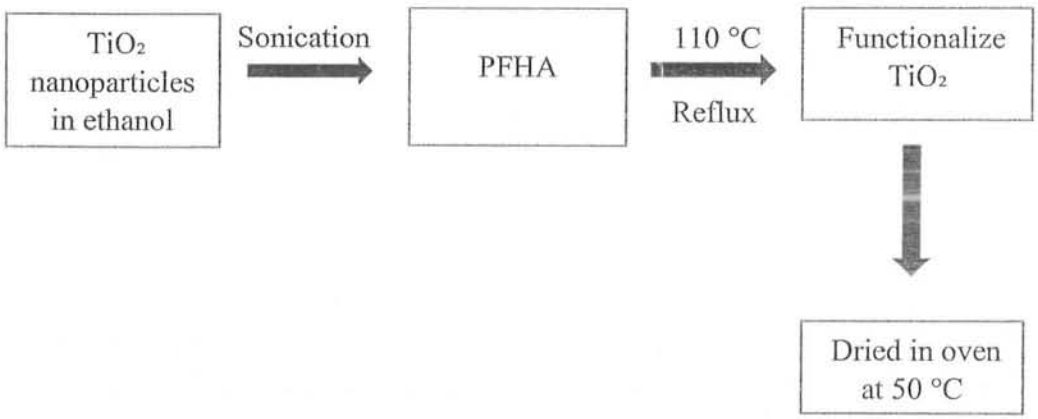


(a)

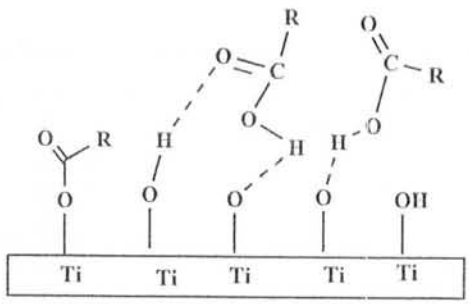


(b)

**Figure 2.6** (a) Schematic representation showing functionalization of $TiO_2$ nanoparticles (b) Possible interaction of Ti surface with perfluoroheptanoic acid.

## 2.4 Synthesis of composite materials

$TiO_2$ epoxy–amine nanocomposites were synthesized using diglycidyl ether of bisphenol A (DGEBA DER-355) as epoxy resin and curing agent used was MACM i.e. 2,2′-dimethyl-4, 4′-diaminodicyclohexylmethane. Neat epoxy - amine system were also synthesized for comparative study.

### 2.4.1 Synthesis of neat epoxy –amine film.

For the synthesis of neat epoxy –amine network, 2.25 g (6 mmol) of DGEBA was taken in 50 mL beaker and heated at 50 °C for 30 minutes under vigorous stirring to obtain transparent viscous liquid. The melted epoxy was degassed under vacuum oven to remove air bubbles. Then 0.75 g (3 mmol) of MACM was added and stirred for 15 minutes. Mixture was then poured on teflon moulds and cured in oven at 50 °C, 60 °C, 70 °C, 80 °C, and 90 °C for one hour and 100 °C for 6-8 hour. Figure 2.7 shows the schematic representation of neat epoxy –amine network.

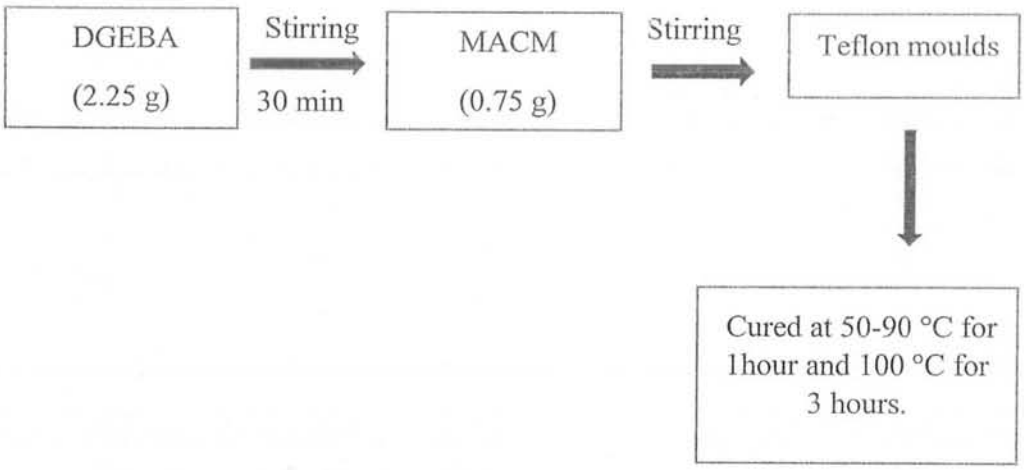


**Figure 2.7** Schematic representation of neat epoxy-amine system[148]

### 2.4.2 Synthesis of epoxy titania hybrids:

In most cases, the optimum thermal and mechanical properties of particulate epoxy composites are achieved at 3-5 wt.% loadings of inorganic nanoparticles such as nano-titania and nano-clay[154,27]. It has been learnt that an increase in nanoparticles content, generally above 5 wt.%, not only reduces toughness, but it is also accompanied by loss in $T_g$ due to increase in crosslink density of matrix chains and increase in free volume[155]. In the view of these findings three types of composite systems were synthesized with 5% and 7.5% of reinforcement to study the effect of titania on properties of epoxy amine matrix. The samples obtained were then analyzed by ATR-IR, TGA and DSC.

**Table 2.1** Composition of unmodified titania based composite (5-TENC, 7.5-TENC, 5-MTEC, 7.5-MTEC)

| Sr. No. | System | Abbreviation | EAT Composites (% wt) |
|---|---|---|---|
| 1 | Neat epoxy –amine network | Neat | ----- |
| 2 | Epoxy-amine-titania composite | TENC | 5, 7.5 |
| 3 | Epoxy-amine-mesoporous titania composite | MTEC | 5, 7.5 |

In the following section the synthesis and procedures adapted to synthesize the epoxy-amine-titania composites and epoxy-amine-mesoporous titania composites will be discussed.

### 2.4.2.1 Synthesis of $TiO_2$/MT epoxy - amine composites:

In order to synthesize $TiO_2$ /MTN epoxy – amine composites, titania particles were sonicated in acetone for two hours and then added to DGEBA and stirred for 30 minutes. After that MACM hardener was added and stirred for two hours. Then mixture was poured on teflon moulds and cured in vacuum oven at 50 °C, 60 °C, 70 °C, 80 °C, 90 °C for one hour and 100 °C for 6-8 hours. Figure 2.8 shows the schematic pathway for the synthesis of $TiO_2$/MT epoxy-amine composites.

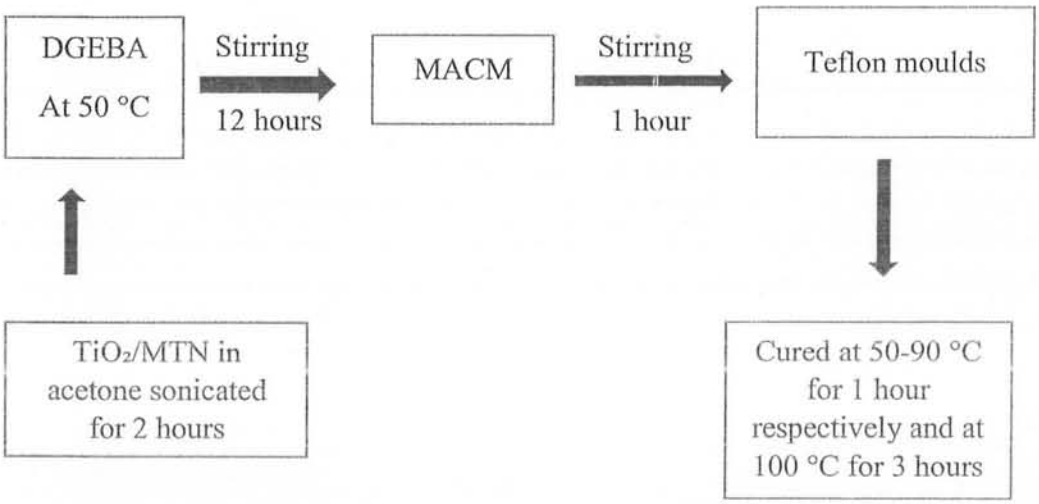


**Figure 2.8** Schematic representation for synthesis of $TiO_2$/MT epoxy amine composites

Three types of composite systems were synthesized with surface modified particles. The samples obtained were then analyzed by ATR-IR, TGA and DSC.

**Table 2.2** Composition of surface modified titania based composites (5-FTENC, 7.5F-TENC, 5-MTEC, 7.5-MTEC)

| Sr. No. | System | Abbreviation | FEAT Composites (% wt) |
|---|---|---|---|
| 1 | Neat epoxy –amine network | Neat | ----- |
| 2 | Epoxy-amine-titania composite with functionalized titania | FTENC | 5, 7.5 |
| 3 | Epoxy-amine-mesoporous titania composite with functionalized mesoporous titania | FMTEC | 5, 7.5 |

In the following section the synthesis and procedures adapted to synthesize the surface modified titania-epoxy-amine composites and epoxy-amine-mesoporous titania composite will be discussed.

### 2.4.2.2 Synthesis of F-$TiO_2$ /F-MT epoxy amine composites:

In order to synthesize F- $TiO_2$ /F-MTN epoxy – amine network, surface modified particles were sonicated for two hours and then added to DGEBA and stirred for 30 minutes. After that MACM hardener was added and stirred for two hours .Then the mixture was poured on teflon moulds and cured in vacuum oven at 50 °C, 60 °C, 70°C, 80 °C, 90 °C for one hour and 100 °C for 6-8 hours. Figure 2.9 shows the schematic representation for synthesis of F-$TiO_2$/F-MT epoxy-amine composites.

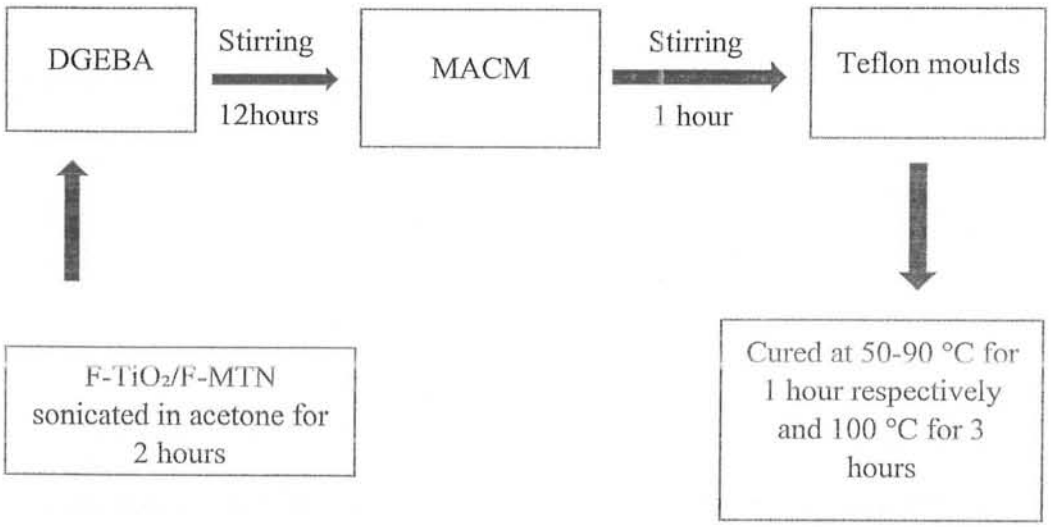


**Figure 2.9** Schematic representation for F-$TiO_2$/F-MTN epoxy amine composites

### 2.4.2.3 Procedure for measurement of contact angle:

To analyze surface wettability, the static contact angle measurements of double deionized water on neat epoxy-amine system and epoxy-titania composites were carried out. Liquid drops of 5 μL were deposited on different spots of the substrates to avoid the influence of roughness and gravity on the shape of drop. The drop contour was analyzed from the image of deposited liquid drop on the surface and contact angle was determined manually using protector. To minimize the errors due to roughness and heterogeneity, the average values of contact angles of the drops were calculated approximately 30 s after the deposition.

Five static contact angle measurements were performed on different spots all over the composites films and used to determine the average contact –angle values with an estimated error in reading of $(\theta \pm 1.0)^{\circ}$ [55]. Figure 2.10 shows image taken for contact angle measurement.

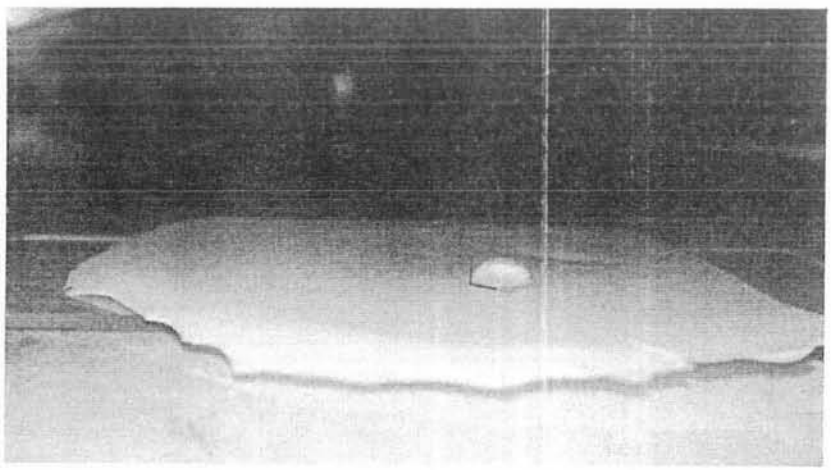

**Figure 2.10** Image for contact angle measurement

This chapter is divided into three parts, the first part discusses characterization of titania particles, the second one is contributed to kinetics of titania-epoxy composites and last one to the characterization of composites.

## 3.1 Characterization of titania particles:

The titania particles were characterized by ATR-FTIR, X-ray diffraction analysis (XRD), scanning electron microscopy (SEM) and thermogravimetric analysis (TGA).

### 3.1.1 Fourier transform infrared spectroscopy (FTIR):

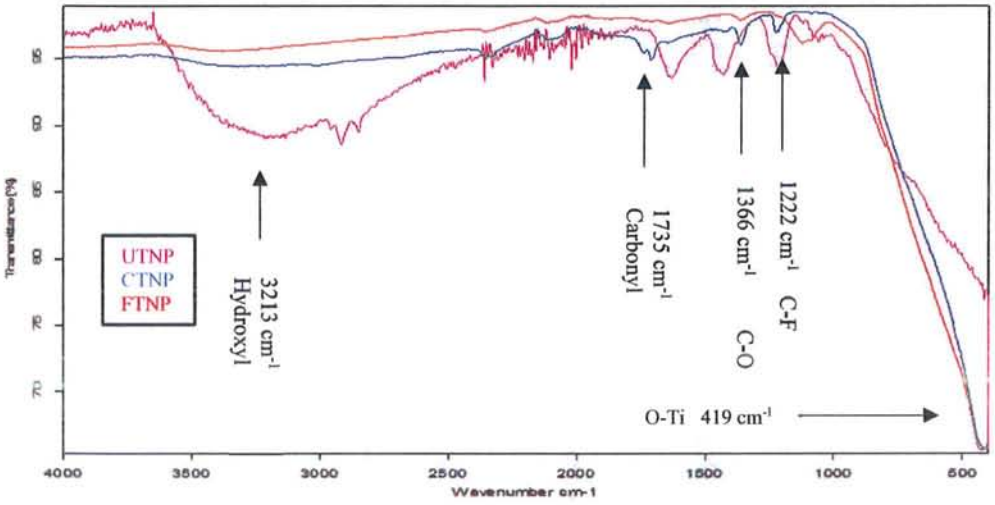


**Figure 3.1** FTIR spectra of as prepared (UTNP), thermally treated (CTNP) and surface modified titania particles (FTNP)

Figure 3.1 shows the IR spectra of as prepared (UTNP), thermally treated (CTNP) and surface modified titania particles (FTNP). Three main peaks were observed for as-prepared titania nanoparticles (UTNP) corresponding to the vibration of Ti-O bond around 419 $cm^{-1}$, the bending vibration of O-H bond around 1625 $cm^{-1}$, and to stretching vibration of O-H bond at 3213 $cm^{-1}$ (broad) attributed to the surface hydroxyl groups and adsorbed water molecule. Thermally treated titania particles (CTNP) lack O-H peaks at 1625 and 3213 $cm^{-1}$, which indicated the absence of hydroxyl groups and formation of crystalline titania particles obtained after thermal treatment.

IR spectra of surface modified $TiO_2$ particles (FTNP) showed several peaks of variable intensities corresponding to O-Ti at 419 $cm^{-1}$, carbonyl at 1735 $cm^{-1}$, C-O at 1336 $cm^{-1}$ and C-F at 1222 $cm^{-1}$ which indicated the surface functionalization of titania particles with perfluoroheptanoic acid.

Perfluoroheptanoic acid was used as capping agent. The surfactant perfluoroheptanoic acid has two functionalities; the carboxylic group and C-F. The acid can either be adsorbed physically on titania particles surface or by chemical adsorption through the formation of ester linkage, by reaction between acid group of PFHA and surface hydroxyl of titania particles[129]. The appearance of carbonyl signal at 1735 $cm^{-1}$ indicated formation of ester linkage with acid.

**Table 3.1** IR data of $TiO_2$ particles (TNP) and surface modified $TiO_2$ particles (FTNP)

| Sr# | Wavenumber $cm^{-1}$ | Functional groups |
|---|---|---|
| 1 | 419 | -O-Ti |
| 2 | 1626, 3215 | -O-H |
| 3 | 1326 | -C-O |
| 4 | 1222 | -C-F |
| 5 | 1735 | Carbonyl of ester |

### 3.1.2 X-ray diffraction analysis (XRD):

The XRD analysis was carried out to study the crystalline structure, purity and phase characteristics of $TiO_2$ particles. The XRD diffractograms of titania particles and reference are shown in figure 3.2 and 3.3. The sharp and intense peaks showed the presence of crystallinity of anatase phase of titania. Characteristics peaks corresponding to 25.5°, 38.2°, 48° and 58° was observed. Which were assigned to the crystalline anatase phase of titania. It should be noted that there is slight difference between the unmodified and modified titania particles at $2\theta$ = 25.5°. This might be due to functionalization that caused a shift in crystalline structure[156].

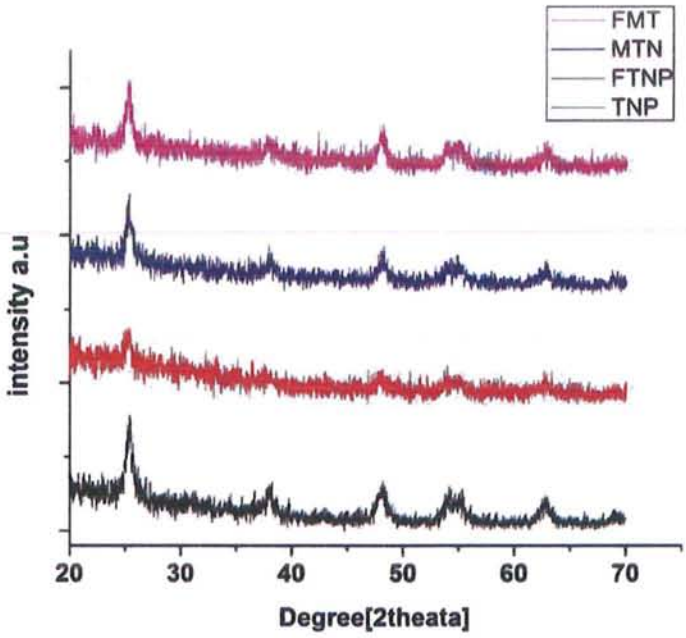


**Figure 3.2** XRD diffractograms of $TiO_2$ nano particles (TNP), surface modified $TiO_2$ nanoparticles (FTNP), mesoporous titania particles (MTN) and surface modified mesoporous titania particles (FMTN)

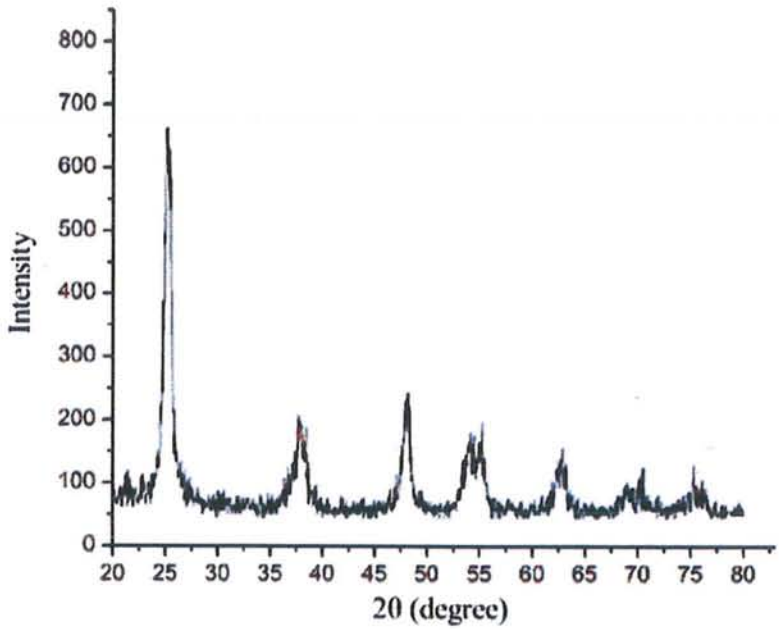


**Figure 3.3** Standard spectrum for anatase phase of titania[157]

### 3.1.3 Thermogravimetric analysis:

Thermogravimetric analysis were carried out to investigate the difference between thermal stability of surface modified and unmodified titania particles.

Thermograms for titania particles are shown in figure 3.4. The observed weight loss around 380 °C during heating was due to the loss of adsorbed water molecule or condensation of Ti-OH species, while the weight loss in the case of surface modified titania particles (FTNP, FMT) around 250 °C was attributed to the organic moieties present on the surface that are more sensitive to high temperature and decrease the initial decomposition temperature[158]. The % char yield of TNP and MT at 800 °C was 89 and 90 % respectively. While % char yield of FTNP and FMT was found to be 87.8 and 88 %. This decrease in % char yield was due to functionalization of particles.

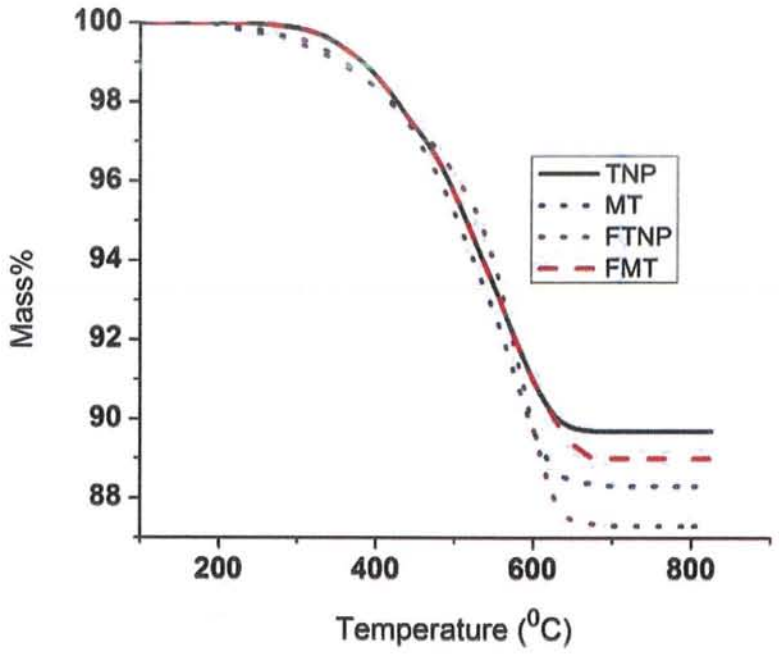


**Figure 3.4** Thermograms of surface modified and unmodified titania nanoparticles (FTNP, TNP) and mesoporous titania particles (MT, FMT)

### 3.1.4 Scanning electron microscopy of titania particles (SEM):

The surface morphology of $TiO_2$ nanoparticles and mesoporous titania were examined by SEM. The SEM images shown in figure 3.5, showed that thermally treated $TiO_2$ nanoparticles have sintered powdered morphology. However due to aggregation it is difficult to perceive individual $TiO_2$ nanoparticle[148]. The mesoporous titania particles have rounded sponge like morphology due to the addition of surfactant during its synthesis[117].

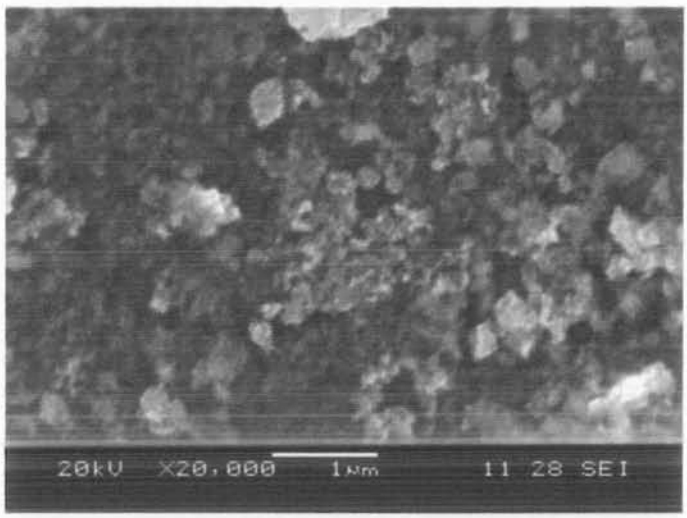


**(a)**

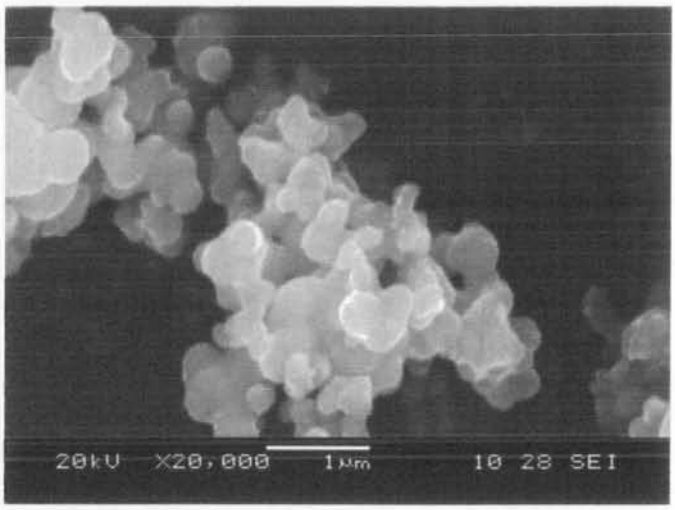


**(b)**

**Figure 3.5** SEM images of (a) $TiO_2$ nanoparticles (TNP) (b) mesoporous titania (MT)

From this part of results and discussion it is concluded that titania particles have anatase phase and surface modification of titania particles decrease its initial decomposition temperature due to presence of organic moieties that are present on the surface of particles. From SEM images it was observed that mesoporous titania have spherical morphology while titania nanoparticles have sintered powdered morphology.

## 3.2 Curing kinetics of epoxy resins and its composites:

The synthesized titania particles were used as filler for epoxy amine system and the curing kinetics of neat epoxy-amine, surface unmodified titania epoxy and surface modified titania epoxy systems with different wt. % were carried out to study the effect of titania particles on activation energy of epoxy-amine matrix.

The results of different system will be discussed as follows:

1) Neat system
2) Unmodified titania based composites (5-TENC and 7.5-TENC)
3) Surface modified titania based composites (5-FTENC and 7.5-FTENC)

### 3.2.1 Neat system:

Neat system consisted of the epoxy resin (DGEBA) and hardener (MACM). The stoichiometric amount of DGEBA and MACM was mixed for kinetic studies.

#### 3.2.1.1 Dynamic differential scanning calorimetry of neat system:

Dynamic DSC for the curing reaction of neat system was carried out at three different heating rates (figure 3.6). All thermograms showed exothermic peak which corresponded to the curing reaction of oxirane ring and diamine. The thermograms showed that the initial curing temperature ($T_i$), peak curing temperature ($T_p$) and the final curing temperature ($T_f$) increased with increase in heating rate. The reason behind this is that the sample did not have enough time to cure at low temperature when heating rate is increased.

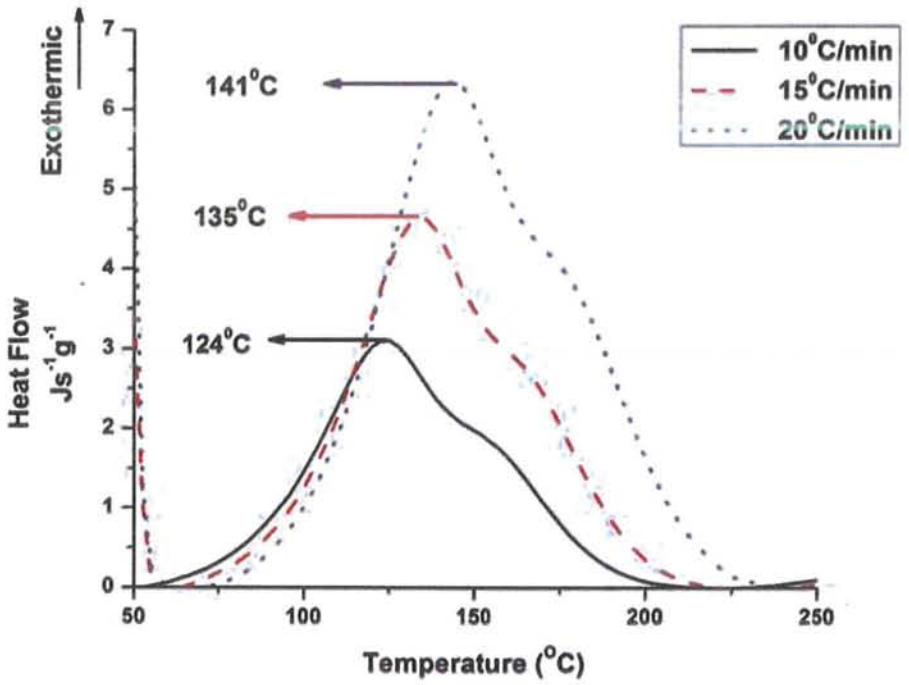


**Figure 3.6** DSC thermograms for neat system

### 3.2.1.2 Curing cycle of neat system:

The curing cycle of neat epoxy resin system was assessed by extrapolation of straight lines from graph between temperatures (°C) versus heating rates. Curing of neat system started from 68 °C, maximum reaction took place at 133 °C and ended at 213 °C as shown in figure 3.7.

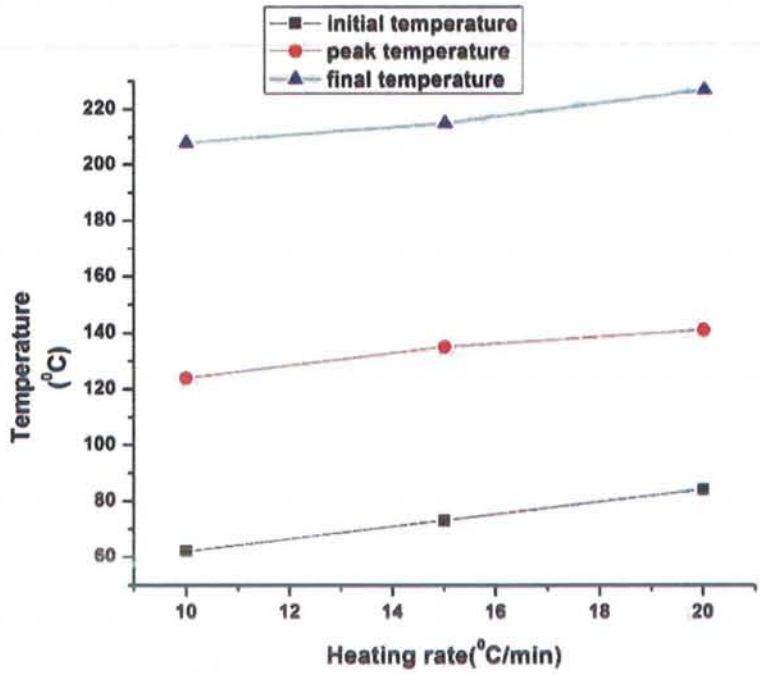


**Figure 3.7** Curing cycle of neat system

### 3.2.1.3 Curing kinetics of neat system:

Kissinger and Ozawa methods were used to find the activation energy and the pre-exponential factor. Different parameters, ln ($\beta/T_p^2$), $1/T_p^2$, and ln$\beta$ were calculated from Kissinger and Ozawa method as shown in table 3.2.

**Table 3.2** Kinetic parameters from Kissinger and Ozawa methods for neat system

| $\beta$ (°C/min) | $T_p$(°C) | $T_p$ (K) | $T_p^2$ | $1/T_p$ x$10^{-3}$ ($k^{-1}$) | -ln($\beta/Tp^2$) | ln $\beta$ |
|---|---|---|---|---|---|---|
| 5 | 124 | 397 | 157609 | 2.51 | 9.66 | 1 |
| 10 | 135 | 406 | 165649 | 2.45 | 9.30 | 1.176 |
| 15 | 141 | 414 | 173056 | 2.40 | 9 | 1.301 |

The activation energy ($E_a$) and Arrhenius constant ($A$) of neat system was found to be 49.8 KJ/mol and 1.8 $s^{-1}$ calculated from the slope of linear fit and intercept of Kissinger graph (figure 3.8).

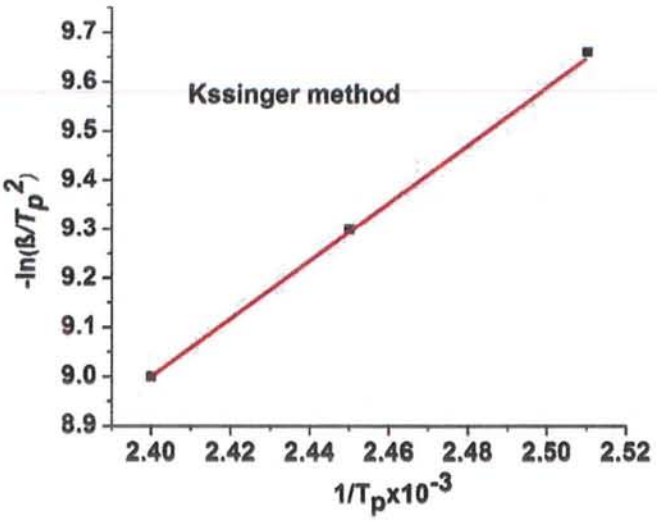


**Figure 3.8** Kissinger linear fit graph for neat system

Activation energy $E_a$ from Ozawa method was 49.9KJ/mol calculated from slope of linear fit Graph (figure 3.9).

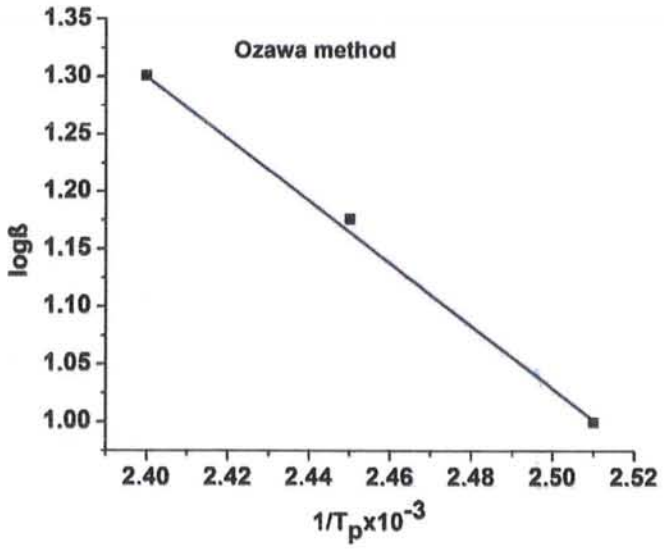


**Figure 3.9** Ozawa linear fit graph for neat system

### 3.2.2 Epoxy –titania composites:

Epoxy-titania system consisted of epoxy resin (DGEBA), hardener (MACM) and titania particles as filler. The stoichiometric amount of DGEBA, MACM and particles with 5 % and 7.5 % were mixed for kinetic studies.

#### 3.2.2.1 Dynamic differential scanning calorimetry of 5-TENC system:

Dynamic DSC for the curing reaction of 5-TENC system was carried out at three different heating rates (figure3.10). All three thermograms showed single exothermic peak which corresponded to the curing reaction of oxirane ring and diamine. The thermograms showed that the initial curing temperature ($T_i$), peak curing temperature ($T_p$) and the final curing temperature ($T_f$) increased with an increase in heating rate. The reason behind this is that the sample did not have enough time to cure at low temperature. Initial, peak and final temperatures of 5-TENC were lower than that of neat system due to catalytic effect of $TiO_2$ particles. It is reported by Parameswaranpillai and his coworker that $T_p$ of DDS/epoxy titania system is lower than its neat system due to catalytic effect of $TiO_2$[144]. So the decrease in $T_p$ of 5-TENC than neat system was assumed due to catalytic activity of $TiO_2$.

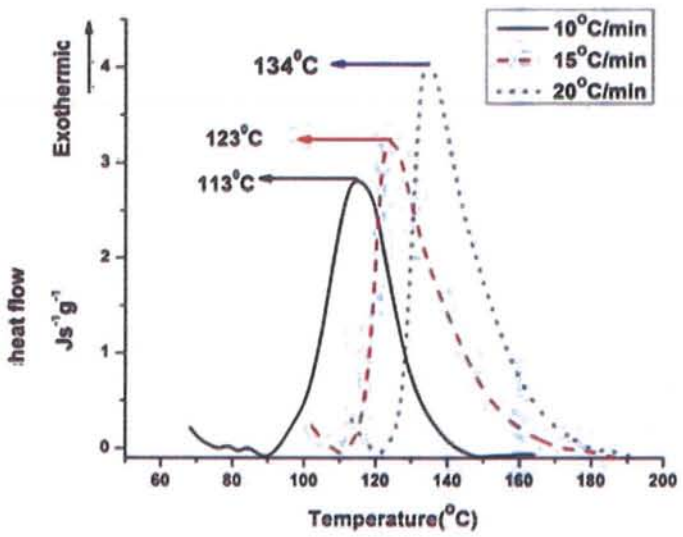


**Figure 3.10** DSC thermograms for 5-TENC system

### 3.2.2.2 Curing cycle of 5-TENC:

The curing cycle of 5-TENC was assessed by extrapolation of straight lines from graph between temperatures versus heating rates. Curing of 5-TENC system started from 86 °C, maximum reaction occurred at 102 °C and ended at 120 °C as shown in figure 3.11.

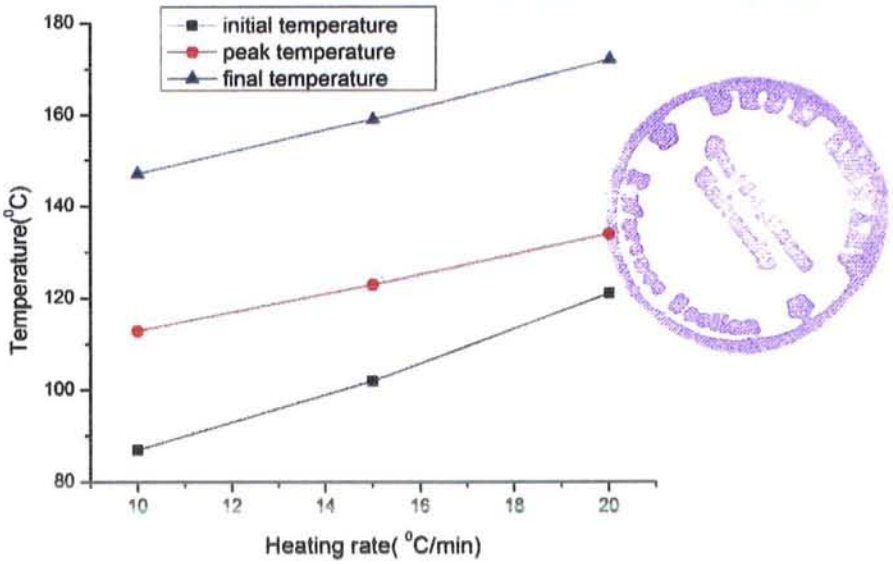


**Figure 3.11** Curing cycle of 5-TENC System

### 3.2.2.3 Curing kinetics of 5-TENC:

Kissinger and Ozawa methods were used to find the activation energy and the pre-exponential factor. Different parameters, ln ($\beta/T_p^2$), $1/T_p^2$, and ln$\beta$ were calculated from the DSC thermograms by using Kissinger and Ozawa method (table 3.3)

**Table 3.3** Kinetic parameters from Kissinger and Ozawa methods for 5-TENC

| $\beta$ (°C/min) | $T_p$(°C) | $T_p$ (K) | $T_p^2$ | $1/T_p$ x$10^{-3}$ ($k^{-1}$) | -ln($\beta/Tp^2$) | ln $\beta$ |
|---|---|---|---|---|---|---|
| 5 | 113 | 386 | 148996 | 2.59 | 9.6 | 1 |
| 10 | 123 | 396 | 156816 | 2.52 | 9.2 | 1.176 |
| 15 | 138 | 407 | 165649 | 2.45 | 9 | 1.301 |

The activation energy ($E_k$) and Arrhenius constant ($A$) of 5-TENC were found to be 37.69 KJ/mol and 1.3 $s^{-1}$ calculated from the slope of linear fit and intercept of Kissinger graph (figure 3.12).

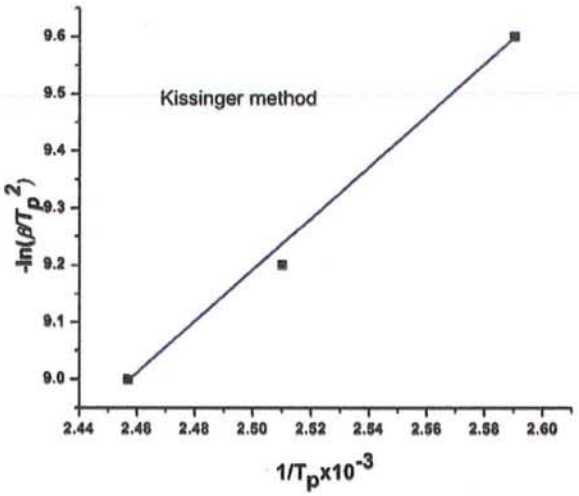


**Figure 3.12** Kissinger linear fit graph for 5-TENC

Activation energy ($E_o$) from Ozawa method was 40.01 KJ/mol calculated from slope of linear fit graph. Activation energies calculated from Kissinger and Ozawa methods for 5-TENC were less than that of neat system due to catalytic activity of $TiO_2$ nanoparticles (figure 3.13).

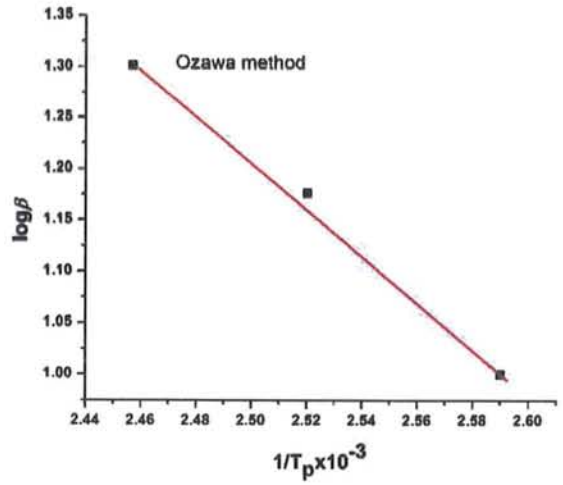


**Figure 3.13** Ozawa linear fit for 5-TENC

### 3.2.3.1 Dynamic differential scanning calorimetry of 7.5-TENC:

Dynamic DSC for the curing reaction of 7.5-TENC system was carried out at three different heating rates (figure3.14). All thermograms showed single exothermic peak which corresponded to the curing reaction of oxirane ring and diamine. The thermograms showed that the initial curing temperature ($T_i$), peak curing temperature ($T_p$) and the final curing temperature ($T_f$) increased with increase in heating rate. The reason behind this is that the sample did not have enough time to cure at low temperature. Initial, peak and final temperature of 7.5-TENC were also lower than that of neat system and 5-TENC due to catalytic effect of particles. Thus an increase in particles wt.% further decreased these temperatures[144].

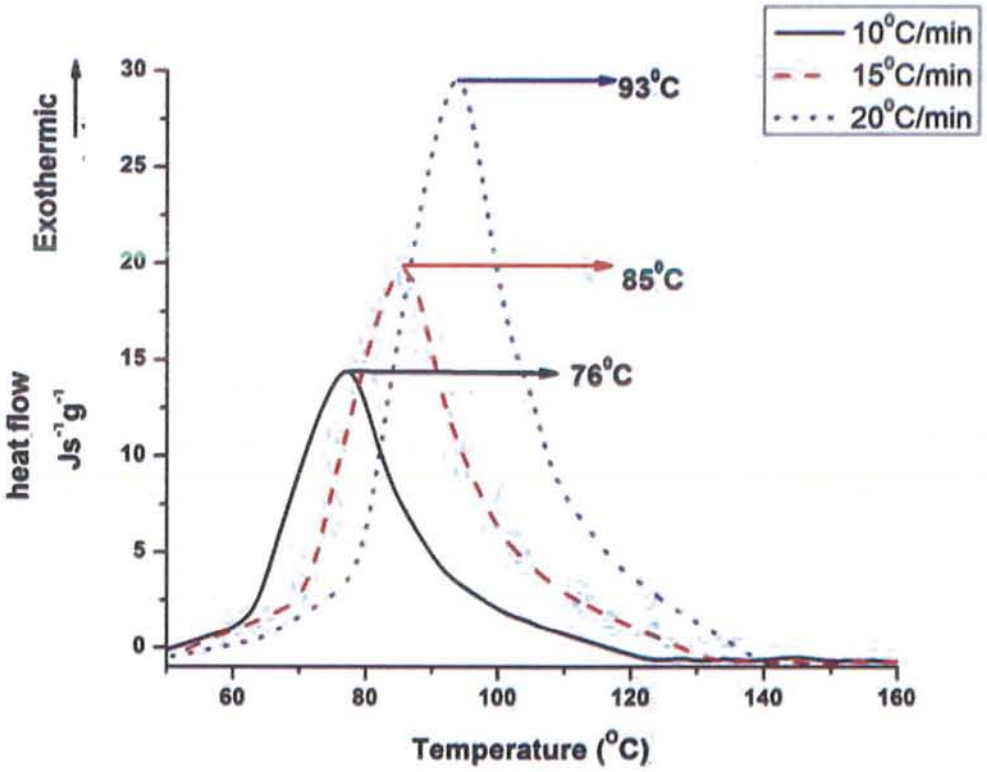


**Figure 3.14** DSC thermograms for 7.5-TENC

### 3.2.3.2 Curing cycle of 7.5-TENC:

The curing cycle of 7.5-TENC was assessed by extrapolation of straight lines from graph between temperatures versus heating rates. Curing of 7.5-TENC system started from 65°C, maximum reaction occurred at 84°C and ended at 131°C as shown in figure 3.15.

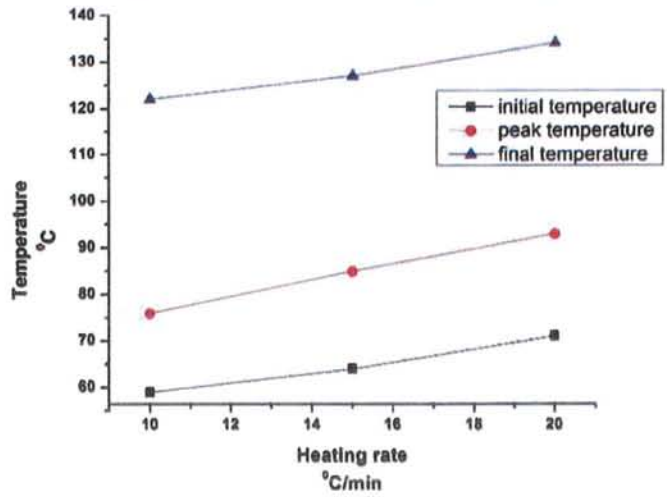


**Figure 3.15** Curing cycle of 7.5-TENC

### 3.2.3.3 Curing kinetics of 7.5-TENC:

Kissinger and Ozawa methods were used to find the activation energy and the pre-exponential factor. Different parameters, ln ($\beta/T_p^2$), $1/T_p^2$, and ln$\beta$ were calculated from Kissinger and Ozawa method as shown in table 3.4.

**Table 3.4** Kinetic parameters from Kissinger and Ozawa methods for 7.5-TENC

| $\beta$ (°C/min) | $T_p$(°C) | $T_p$ (K) | $T_p^2$ | $1/T_p$ (x$10^{-3}$ $k^{-1}$) | -ln($\beta/Tp^2$) | ln $\beta$ |
|---|---|---|---|---|---|---|
| 5 | 76 | 349 | 121801 | 2.865 | 9.4 | 1 |
| 10 | 85 | 358 | 128164 | 2.793 | 9.0 | 1.176 |
| 15 | 94 | 367 | 134689 | 2.724 | 8.8 | 1.301 |

The activation energy ($E_k$) and Arrhenius constant ($A$) of 7.5-TENC were found to be 34.91 KJ/mol and 1.03 $s^{-1}$ calculated from the slope of linear fit and intercept of Kissinger graph (figure 3.16).

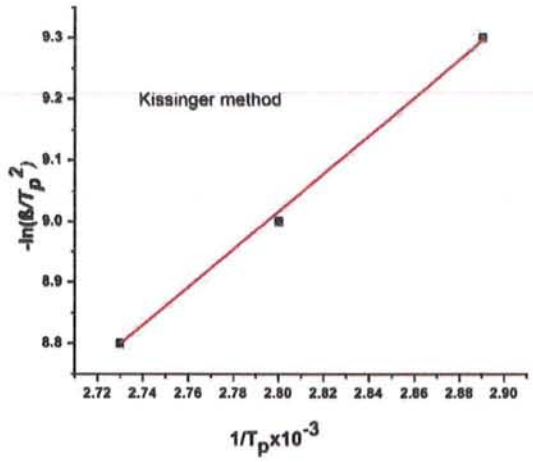


**Figure 3.16** Kissinger linear fit graph for 7.5-TENC

Activation energy ($E_o$) from Ozawa method was 34.4 KJ/mol calculated from slope of linear fit graph (figure 3.17). Activation energies ($E_k$, $E_o$) for 7.5-TENC were less than that of 5-TENC due to catalytic effect of $TiO_2$ nanoparticles an increase in wt.% of nanoparticles leads to increase in catalytic activity and decrease in activation energy.

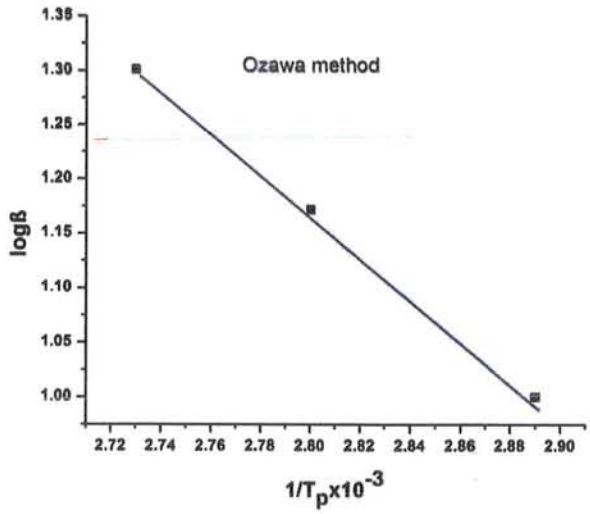


**Figure 3.17** Ozawa linear fit graph for 7.5-TENC

### 3.2.4.1 Dynamic differential scanning calorimetry of 5-FTENC:

Dynamic DSC for the curing reaction of 5-FTENC system was carried out at three different heating rates (figure 3.18). All thermograms showed single exothermic peak which corresponded to the curing reaction of oxirane ring and diamine. The thermograms showed that the initial curing temperature ($T_i$), peak curing temperature ($T_p$) and the final curing temperature ($T_f$) increased with increase in heating rate. The reason behind this is that the sample did not have enough time to cure at low temperature. Initial, peak and final temperatures of 5-FTENC were higher than 5-TENC because when the surface of $TiO_2$ was modified the surface hydroxyl groups that are responsible for catalytic activity are consumed resulting in an increase in $T_p$. Peak temperature ($T_p$) of 5-FTENC was similar to neat system at low heating rates but higher at 20°C/min. This increase might be due to hindrance in curing caused by particles agglomeration or surface interaction of diamine with particles.

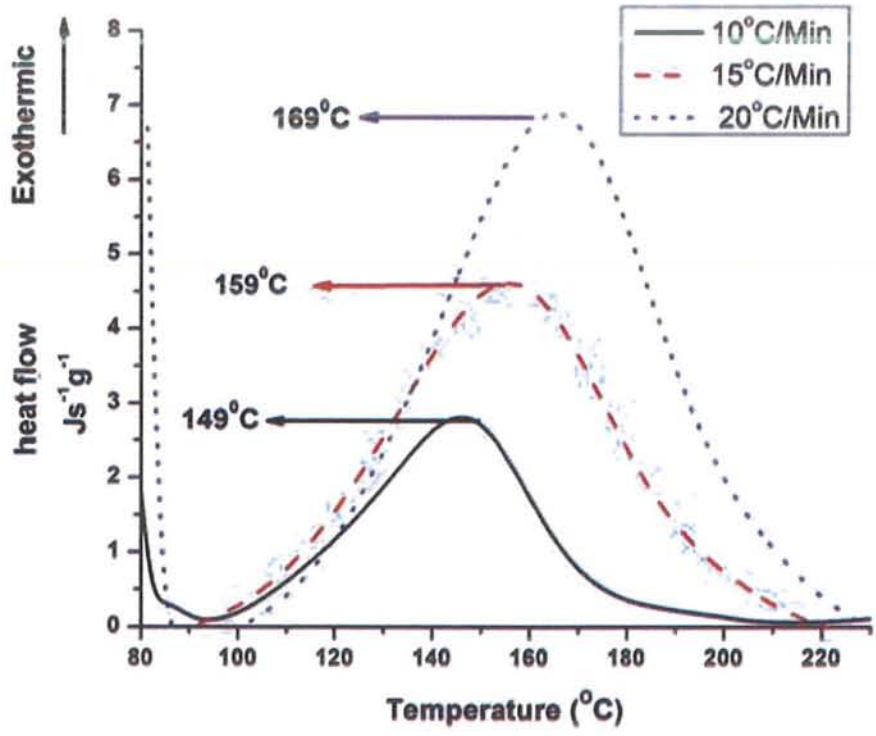


**Figure 3.18** DSC thermograms for 5-FTENC

### 3.2.4.2 Curing cycle of 5-FTENC

The curing cycle of 5-FTENC was assessed by extrapolation of straight lines from graph between temperatures versus heating rates. Curing of 5-FTENC system started from 93 °C, maximum reaction occurred at 148 °C and ended at 213 °C as shown in figure 3.19.

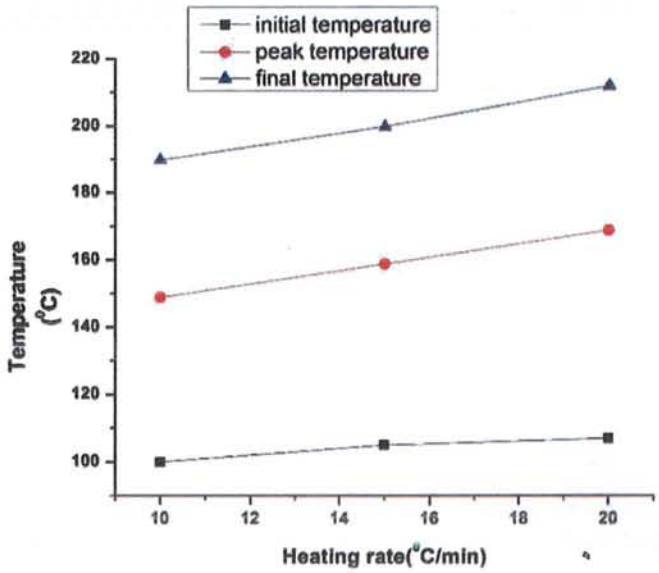


**Figure 3.19** Curing cycle of 5-FTENC

### 3.2.4.3 Curing kinetics of 5-FTENC:

Kissinger and Ozawa methods were used to find the activation energy and the pre-exponential factor. Different parameters, ln ($\beta/T_p^2$), $1/T_p^2$, and ln$\beta$ were calculated from using Kissinger and Ozawa method as shown in table 3.5.

**Table 3.5** Kinetic parameters from Kissinger and Ozawa methods for 5-FTENC

| $\beta$ (°C/min) | $T_p$(°C) | $T_p$ (K) | $T_p^2$ | $1/T_p$ x$10^{-3}$ ($k^{-1}$) | -ln($\beta/Tp^2$) | ln $\beta$ |
|---|---|---|---|---|---|---|
| 5 | 149 | 422 | 178084 | 2.36 | 9.78 | 1 |
| 10 | 159 | 432 | 186624 | 2.31 | 9.42 | 1.17 |
| 15 | 169 | 442 | 195364 | 2.26 | 9.18 | 1.30 |

The activation energy ($E_k$) and Arrhenius constant ($A$) of 5-FTENC were found to be 49.48 KJ/mol and 1.8 $s^{-1}$ as calculated from the slope of linear fit and intercept of Kissinger graph (figure 3.20).

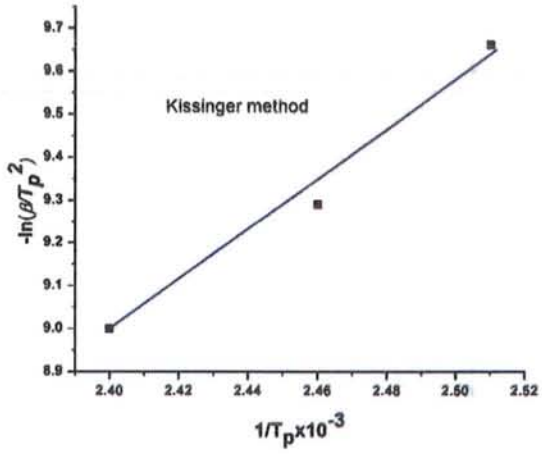


**Figure 3.20** Kissinger linear fit graph for 5-FTENC

Activation energy ($E_o$) from Ozawa method was 50.06 KJ/mol calculated from slope of linear fit graph (figure 3.21). Surface modification of $TiO_2$ nanoparticles retards its catalytic activity which results in activation energy for 5-FTEN almost similar to neat system.

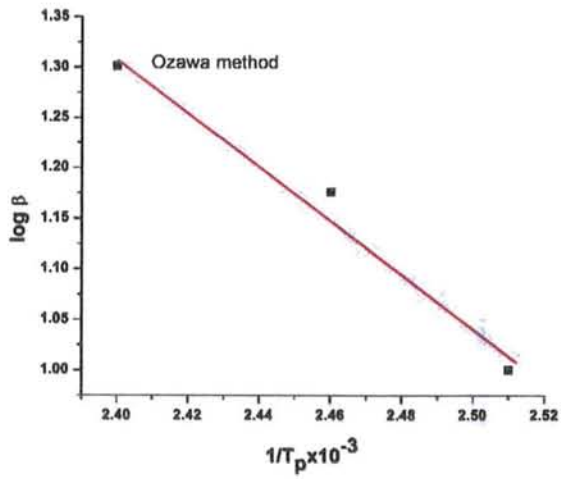


**Figure 3.21** Ozawa linear fit graph for 5-FTENC

### 3.2.5.1 Dynamic differential scanning calorimetry of 7.5-FTENC:

Dynamic DSC for the curing reaction of 7.5-FTENC system was carried out at three different heating rates (figure 3.22). All thermograms show single exothermic peak which corresponded to the curing reaction of oxirane ring and diamine. The thermograms showed that the initial curing temperature ($T_i$), peak curing temperature ($T_p$) and the final curing temperature ($T_f$) increased with increase in heating rate. The reason behind this is that the sample did not have enough time to cure at low temperature. Peak temperature of 7.5-FTENC are higher than that of 7.5TENC because when the surface of titania particles are modified hydroxyl group that are responsible for catalytic activity are consumed and result in an increase in activation energy. Activation energy of 7.5-TENC are almost similar to that of neat which showed that surface modification retard the catalytic activity of titania particles.

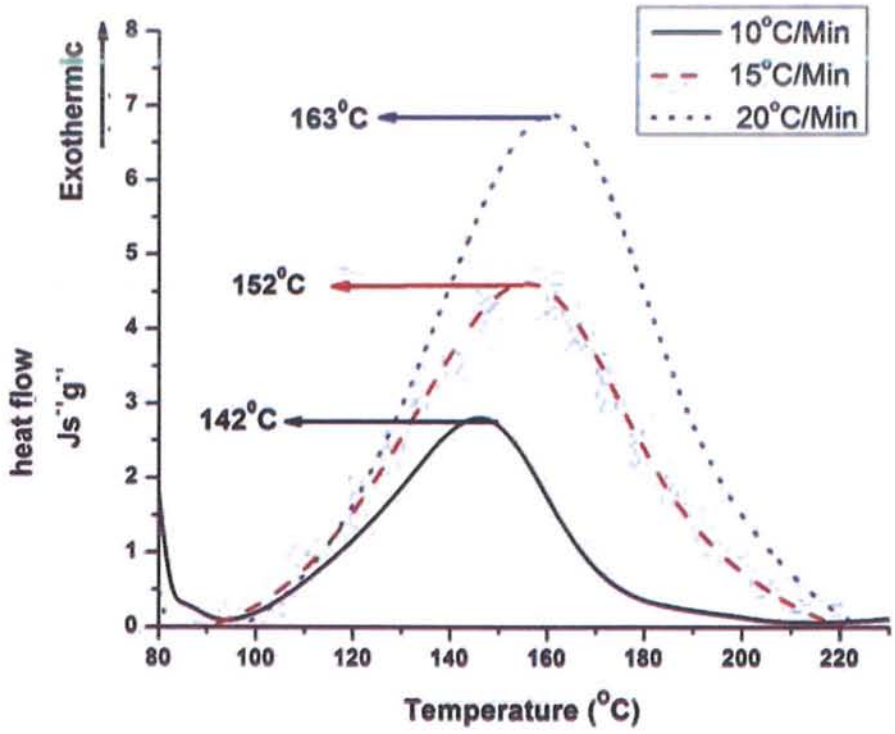


**Figure 3.22** DSC thermograms for 7.5-FTENC

### 3.2.5.2 Curing cycle of 7.5-FTENC:

The curing cycle of 7.5-FTENC was assessed by extrapolation of straight lines from graph between temperatures versus heating rates. Curing of 7.5-FTENC system started from 96.3 °C, maximum reaction occurred place at 152 °C and ended at 211 °C as shown in figure 3.23.

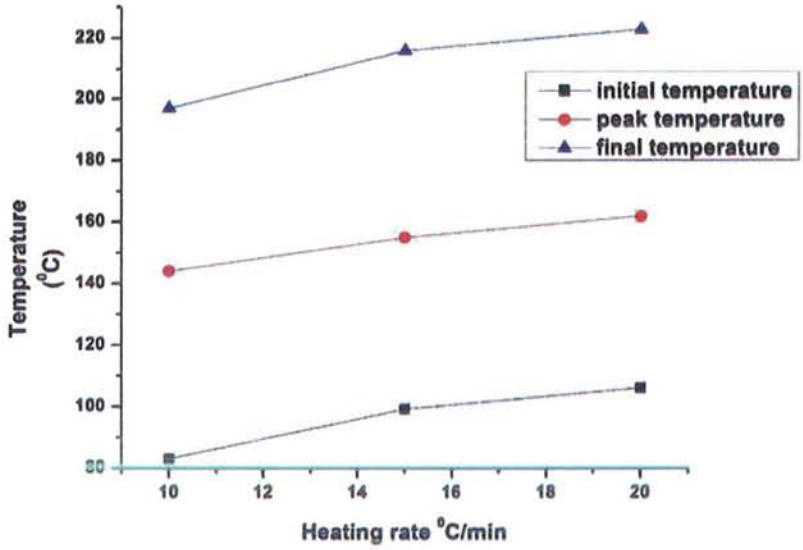


**Figure 3.23** Curing cycle of 7.5-FTENC

### 3.2.5.3 Curing kinetics of 7.5-FTENC:

Kissinger and Ozawa methods were used to find the activation energy and the pre-exponential factor. Different parameters, ln ($\beta/T_p^2$), $1/T_p^2$, and ln$\beta$ were calculated from the DSC thermograms by using Kissinger and Ozawa method table 3.6.

**Table 3.6** Kinetic parameters from Kissinger and Ozawa methods for 7.5-FTENC

| $\beta$ (°C/min) | $T_p$(°C) | $T_p$ (K) | $T_p^2$ | $1/T_p$ x$10^{-3}$( $k^{-1}$ ) | -ln( $\beta/Tp^2$) | ln $\beta$ |
|---|---|---|---|---|---|---|
| 5 | 144 | 417 | 173889 | 2.39 | 9.76 | 1 |
| 10 | 152 | 425 | 180625 | 2.35 | 9.39 | 1.17 |
| 15 | 163 | 436 | 190096 | 2.29 | 9.15 | 1.30 |

The activation energy ($E_k$) and Arrhenius constant ($A$) of 7.5-FTENC were found to be 49.5 KJ/mol and 1.745 $s^{-1}$ calculated from the slope of linear fit and intercept of Kissinger graph (figure 3.24).

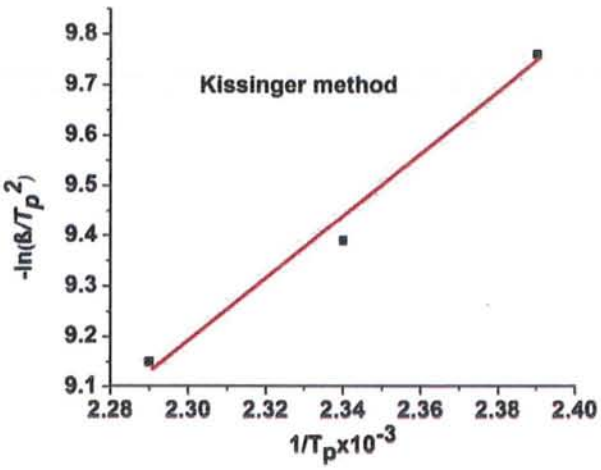


**Figure 3.24** Kissinger linear fit graph for 7.5-FTENC

Activation energy ($E_o$) from Ozawa method was 52.44 KJ/mol calculated from slope of linear fit graph (figure 3.25). Activation energy similar to neat system indicate that surface modification of titania particles retard the catalytic activity of titania.

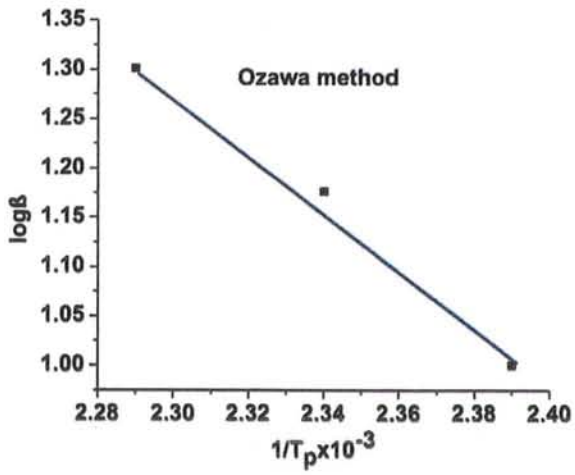


**Figure 3.25** Ozawa linear fit graph for 7.5-FTENC

**Table 3.7** Kinetic parameters for different epoxy –titania systems

| Sr# | Codes | $E_k$ (Kissinger activation energy) KJ/mol | $E_o$ (Ozawa activation energy) KJ/mol | Arrhenius factor $s^{-1}$ |
|---|---|---|---|---|
| 1 | Neat | 49.8 | 49 | 1.8 |
| 2 | 5-TENC | 37.61 | 40.01 | 1.3 |
| 3 | 7.5-TENC | 34.91 | 34.46 | 1 |
| 4 | 5-FTENC | 49.56 | 50.06 | 1.8 |
| 5 | 7.5-FTENC | 49.5 | 52.44 | 1.745 |

From table 3.7 it is observed that activation energies calculated from Kissinger and Ozawa methods for 5-TENC and 7.5-TENC was less than that of neat system, 5-FTENC and 7.5-FTENC. This decrease in activation energy is due to the catalytic effect of $TiO_2$ nanoparticles on curing reaction. Activation energy for 7.5-TENC was less than 5-TENC due to increase in wt% of $TiO_2$ nanoparticles. The activation energies for 5-FTENC and 7.5-TENC were similar to neat system. Because when the surface of $TiO_2$ nanoparticles modified, the surface hydroxyl group that are responsible for catalytic activity of $TiO_2$ form ester linkage with the capping agent (perfluoroheptanoic acid). From this it is concluded that in epoxy titania system $TiO_2$ nanoparticles have catalytic activity on curing of epoxy amine (5-TENC, 7.5-TENC) matrix while in surface modified titania epoxy system (5-FTENC, 7.5-TENC) surface modification of $TiO_2$ nanoparticles retards its catalytic activity.

## 3.3 Characterization of titania epoxy-amine composites:

$TiO_2$ is a versatile semi-conducting material which shows high thermal stability, chemical stability, and heat resistance. Two types of $TiO_2$ based composites were synthesized;

Unmodified titania based composites (using TNP and MT)

Modified titania based composites (using FTNP and FMT)

and characterized using XRD, TGA, DSC and FTIR.

### 3.3.1 Fourier transform infrared spectroscopy (FTIR):

FTIR spectrum of three dimensional network of epoxy-amine is shown in figure 3.26. Neat system consisted of two constituents, diamine (MACM) and epoxy (DGEBA). The amino ($NH_2$) functionality of diamine acted as nucleophile and opened the oxirane ring of epoxy, to give C-N functionality, which appeared at 1245 $cm^{-1}$ and strong absorption band at 3448 $cm^{-1}$ due to stretching mode of hydroxyl group which formed after opening of oxirane ring. The characteristics stretching vibration of O-Ti bond was detected in the region of 462-510 $cm^{-1}$ which indicated the presence of titania network in composite, this peak was not shown in case of reference epoxy amine system (Neat). While the appearance of carbonyl peak at 1746 $cm^{-1}$ showed the surface modified titania particles in epoxy amine matrix (5-FTENC).

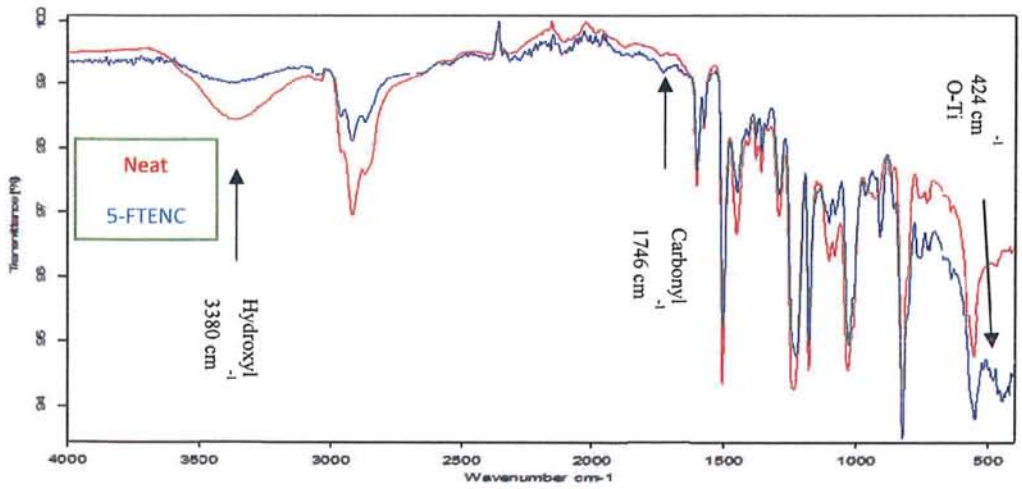


**Figure 3.26** FTIR spectra of reference Neat and 5-TENC

**Table 3.8** IR data of neat system and composites

| | | Wavenumber ($\bar{\nu}\ cm^{-1}$) | | | | | | |
|---|---|---|---|---|---|---|---|---|
| Sr# | Codes | OH | $C_{sp3}$-H Stretching | Carbonyl | C-N | C=C (Ar) | Ph-O | Ti-O-Ti |
| 1 | Neat | 3448 | 2918<br>2850 | - | 1245 | 1605<br>1507 | 1179 | - |
| 2 | 5-TENC | 3363 | 2918<br>2868 | - | 1294 | 1606<br>1507 | 1180 | 462-560 |
| 3 | 7.5-TENC | 3380 | 2918<br>2850 | - | 1293 | 1606<br>1507 | 1180 | 462-560 |
| 4 | 5-FTENC | 3363 | 2918<br>2850 | 1746 | 1294 | 1606<br>1507 | 1180 | 462-560 |
| 5 | 7.5-FTENC | 3350 | 2918<br>2850 | 1746 | 1294 | 1606<br>1507 | 1180 | 462-560 |
| 6 | 5-MTEC | 3363 | 2918<br>2850 | - | 1295 | 1606<br>1507 | 1180 | 462-560 |
| 7 | 7.5-MTEC | 3386 | 2918<br>2850 | - | 1294 | 1606<br>1507 | 1180 | 462-560 |
| 8 | 5-FMTEC | 3350 | 2918<br>1850 | 1746 | 1293 | 1606<br>1507 | 1180 | 462-560 |
| 9 | 7.5-FMTEC | | 2918<br>2850 | 1746 | 1294 | 1606<br>1507 | 1180 | 462-560 |

### 3.3.2 X-ray diffraction analysis (XRD):

Incorporation of Titania particles into polymer matrix was confirmed by the appearance of sharp peaks corresponding to $TiO_2$ particles as shown in figure 3.27(a). In neat system these sharp peaks were not present and only amorphous structure was observed. The appearance of sharp peak showed the successful dispersion of $TiO_2$ particles in epoxy amine matrix as shown in figure 3.27(b).

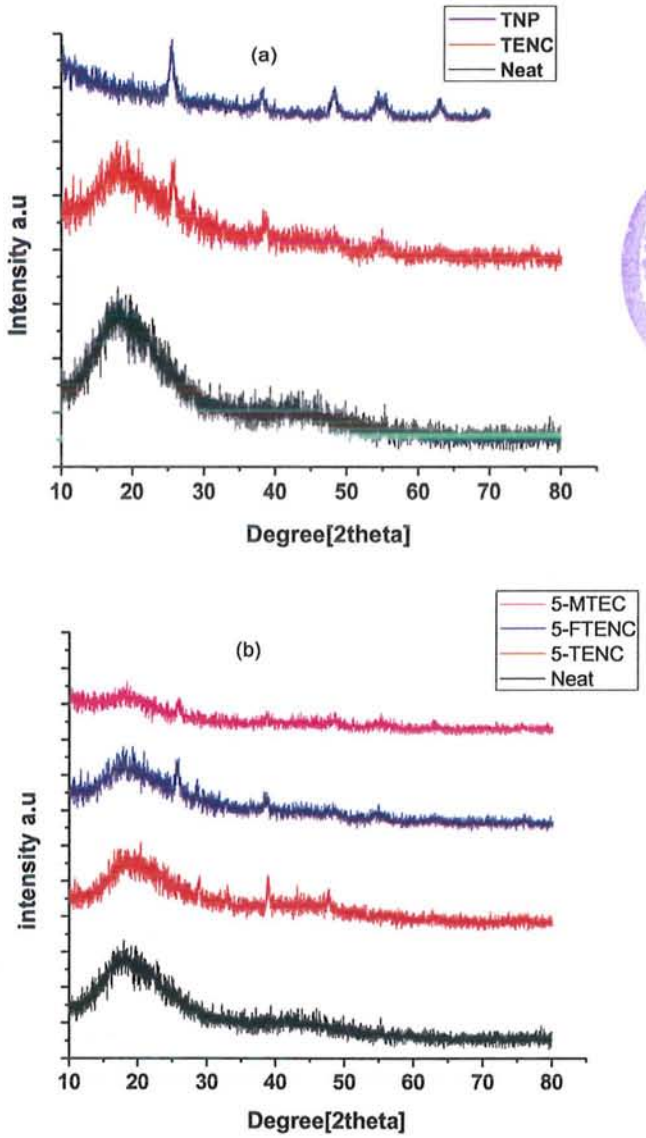


**Figure 3.27** XRD pattern (a) comparison between particles and composites (b)composites

### 3.3.3 Thermal analysis

To investigate the thermal stability of the polymeric materials DSC and TGA were carried out. DSC was used to measure the glass transition temperature ($T_g$) of polymer. The cured sample in sealed aluminum pan is heated under nitrogen at rate of 10°C/min from 50-300°C.

Thermal behaviors of titania composites were investigated to see the effect of titania particles on thermal properties of polymeric material.

#### 3.3.3.1 Differential scanning calorimetry (DSC) of $TiO_2$ composites:

DSC results for both surface modified and unmodified titania based composites are presented below in figure 3.28. Tables 3.9 and 3.10 show that glass transition temperature of titania based composites are higher than that of neat system. The increase in $T_g$ is due to strong interfacial interaction between $TiO_2$ particles and polymeric material.

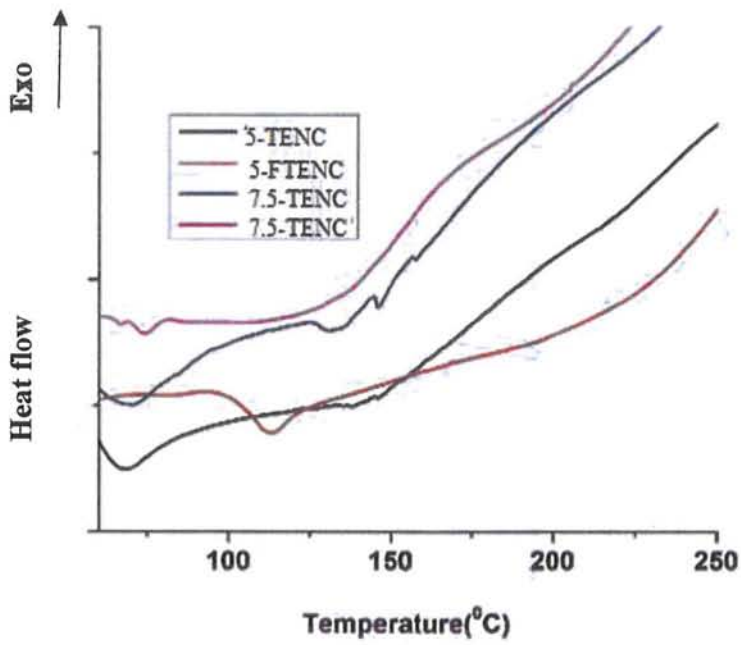


**Figure 3.28** DSC scan of composites

In case of functionalized $TiO_2$ composites, the glass transition temperature are lower than that of functionalized $TiO_2$ composites. This decrease is due to presence of fluoro moiety that were introduced on the surface of particles in the form of perfluoroheptanoic acid which provide more free volume. Although the transition temperatures are still greater than that of neat epoxy amine system.

**Table 3.9** Glass transition temperature for unmodified titania based composites

| Sr.no | % of $TiO_2$ particles | Samples codes | $T_g$(°C) |
|---|---|---|---|
| 1 | 0 | Neat | 67 |
| 2 | 5 | 5-TENC | 130 |
| 3 | 7.5 | 7.5TENC | 126 |
| 4 | 5 | 5-MTEC | 116 |
| 5 | 7.5 | 7.5-MTEC | 120 |

**Table 3.10** Glass transition temperature for surface modified titania based composites

| Sr.no | % of $TiO_2$ particles | Samples codes | $T_g$ (°C) |
|---|---|---|---|
| 1 | 0 | Neat | 67 |
| 2 | 5 | 5-FTENC | 101 |
| 3 | 7.5 | 7.5-FTENC | 70 |
| 4 | 5 | 5-FMTEC | 96 |
| 5 | 7.5 | 7.5-FMTEC | 89 |

### 3.3.3.2 Thermogravimetric analysis (TGA) of $TiO_2$ composites:

Figure 3.29 shows thermogravimetric (TG) curves of titania epoxy composites recorded under nitrogen atmosphere at 10 °C/min. For both surface modified and unmodified titania based composites no weight loss was observed before 300 °C. Thermal decomposition temperatures such as initial decomposition temperature (IDT), temperature at 10 % weight loss ($T_{d10}$), temperature at 50 % weight loss ($T_{d50}$) , and temperature at maximum weight loss ($T_{max}$) of titania-epoxy composites are shown in table 3.11 along with % char yield.

It can be observed that the thermal stability of composites increased with an increase in $TiO_2$ content. However the thermal stability of unmodified titania based composites (TENC, MTEC) is higher than that of modified titania based composites (FTENC, FMTEC). The surface modified titania particles have organic moieties attached to the surface which are more sensitive to high temperature and degrade into carbonaceous solids, $CO_2$ and $H_2O$.

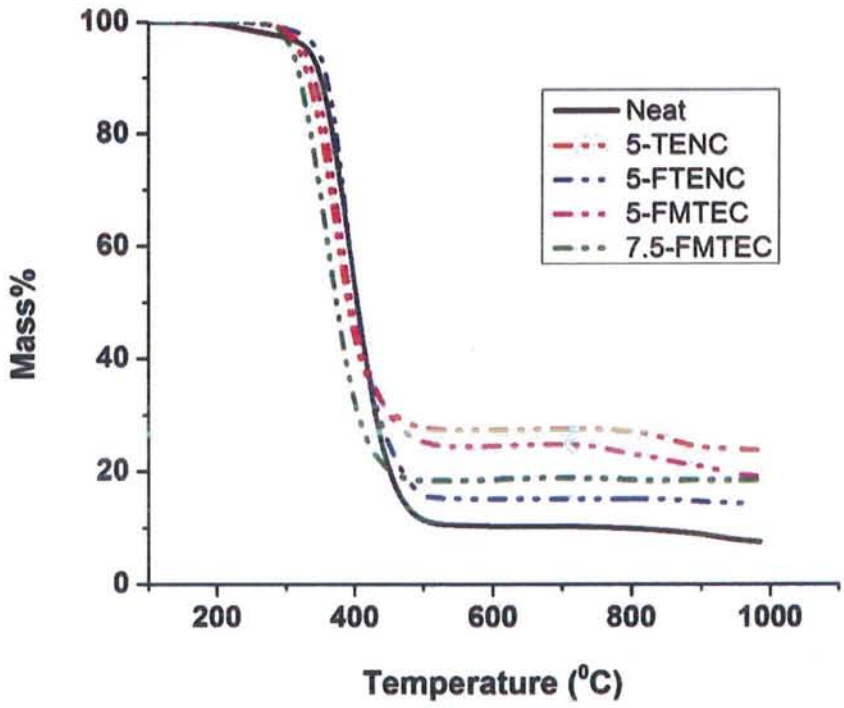


**Figure 3.29** Thermograms of reference epoxy amine (Neat), unmodified titania composites (5TENC) and surface modified titania based composites (5-FTENC, 7.5-MTEC, 5-FMTEC)

After maximum degradation has occurred the composites containing $TiO_2$ particles shows more char yield than neat system. The % char yield for titania composites was higher due to slower release of volatile substances. The surface modified particles based composites also showed high thermal decomposition temperatures as compared to neat system. Thermal decomposition parameters along with % char yield are shown in table 3.11.

**Table 3.11** Thermal decomposition parameters of reference epoxy-amine system and composites

| Samples codes | IDT (°C) | ($T_{d10}$) (°C) | ($T_{d50}$) (°C) | ($T_{max}$) (°C) | Char yield (Wt. %) |
|---|---|---|---|---|---|
| Neat | 271 | 353 | 394 | 984 | 7.5 |
| 5-TENC | 352 | 393 | 433 | 985 | 21.5 |
| 7.5-TENC | 353 | 393 | 437 | 985 | 22 |
| 5-FTENC | 311 | 352 | 393 | 985 | 12 |
| 7.5-FTENC | 317 | 364 | 397 | 985 | 17 |
| 5-MTEC | 352 | 394 | 425 | 984 | 20 |
| 7.5-MTEC | 352 | 390 | 430 | 984 | 21 |
| 5-FMTEC | 302 | 353 | 394 | 983 | 15.42 |
| 7.5-FMTEC | 300 | 312 | 394 | 984 | 16.62 |

### 3.3.4 Wettability and contact angle:

Contact angle measurements were carried out to analyze the surface wettability of composites. Figure 3.30 shows that contact angle for the surface modified particles based composites (FTENC, FMTEC) is greater than that of unmodified particles based composites (FTENC, FMTEC). The increase in contact angle is due to incorporation of fluorinated alkyl chain as perfluoroheptanoic acid on the surface of particles. Fluorinated compounds have low surface energy due to small size and low polarizability of C-F bond. Which results in low dense interactions on the surface and an increase in hydrophobic character[159].

(a)

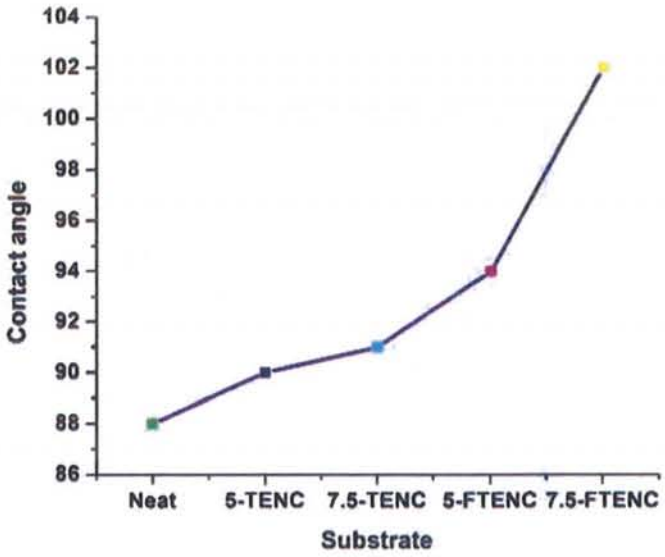


(b)

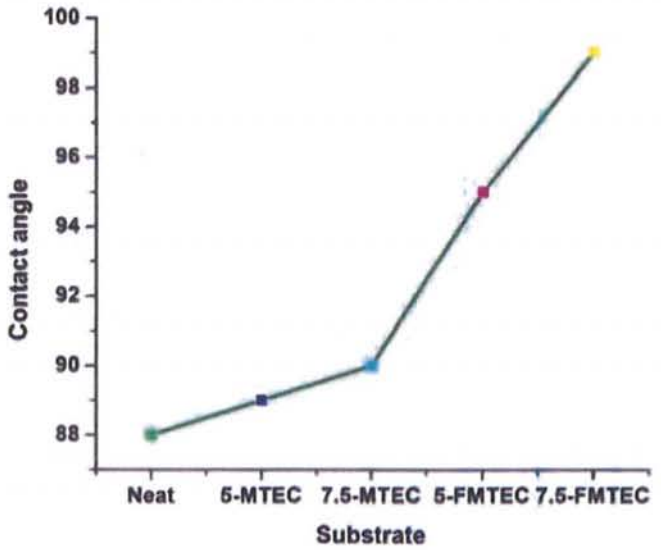


**Figure 3.30** Contact angle results for (a) titania nanoparticles based composites and (b) mesoporous titania based composites

**Table 3.12** Contact angle of epoxy-titania composites

| Sr# | Codes | Contact angle ($\theta$) |
|---|---|---|
| 1 | Neat | 88 |
| 2 | 5-TENC | 90 |
| 3 | 7.5-TENC | 93 |
| 4 | 5-MTEC | 89 |
| 5 | 7.5-MTEC | 90 |
| 6 | 5-FTENC | 94 |
| 7 | 7.5-FTENC | 102 |
| 8 | 5-FMTEC | 95 |
| 9 | 7.5-FMTEC | 99 |

# Conclusions

The present work has led to following conclusions

- Titania nanoparticles and mesoporous titania were successfully synthesized by sol gel method.
- Surface of particles was modified using perflouroheptanoic acid.
- The synthesized nanostructures were characterized by FTIR, XRD, SEM, and TGA.
- From SEM image it was observed that mesoporous titania particles have round sponge like morphology while titania nanoparticles have sintered powdered morphology.
- XRD pattern showed the presence of anatase phase of titania.
- Curing kinetics of epoxy titania composites were carried out to study the effect of titania particles on activation energy. Activation energy ($E_k$, $E_o$) for epoxy titania composites (5-TENC, 7.5-TENC) was lower than neat and surface modified titania epoxy composites (5-FTENC, 7.5-FTENC) due to catalytic effect of titania on curing reaction. While activation energy ($E_k$, $E_o$) for 7.5-TENC was lower than 5-TENC, due to increase in wt % of particles its catalytic activity increase. For 5-FTENC & 7.5-FTENC activation energy was almost similar to neat system because surface modification of titania particles retards its catalytic activity.
- Contact angle measurement was carried out to examine the hydrophobic character of composites. Contact angle for unmodified titania based composites (TENC, MTEC) was greater than that of neat system due to surface roughness. While contact angle for surface modified titania based composites (FTENC, FMTEC) was higher than that of neat system and surface unmodified titania composites (TENC, MTEC). The increased in contact angle was due to incorporation of fluoro moiety in epoxy amine matrix in the form of capping agent for titania particles.
- Thermal stability of composites increased with an increase in $TiO_2$ content due to crystalline nature of particles. Epoxy-titania systems showed onset of thermal degradation above 300°C while for neat system onset degradation temperature was 271°C.

# Conclusions

- The glass transition temperatures ($T_g$) of composites were greater than that of neat system due to reinforcement. In case of functionalized titania-epoxy systems the glass transition temperature ($T_g$) was lower than that of non-functionalized titania-epoxy system due to fluoro moiety which provide more free volume.

# Future plans

The future plans include:

- Curing kinetics of mesoporous titania-epoxy systems.
- Synthesis of epoxy titania composites with higher filler loadings like 8%, 9%, and 10%.
- Conductivity of epoxy-titania composites.

# References


1. Sahoo, S. K.; Labhasetwar, V., Nanotech approaches to drug delivery and imaging. *Drug Discovery Today,* **2003,** *8* (24), 1112-1120.

2. Emerich, D. F.; Thanos, C. G., Targeted nanoparticle-based drug delivery and diagnosis. *Journal of Drug Targeting,* **2007,** *15* (3), 163-183.

3. Whitesides, G. M., The right size in nanobiotechnology. *Nature Biotechnology,* **2003,** *21* (10), 1161-1165.

4. Li, Shanghua., Engineering nanomaterials with enhanced functionality. *Royal Institute of Technology*, **2006**, 15-54.

5. Nagarajan an, Ramathan., Nanoparticles: building blocks for nanotechnology. *American Chemical Society,* **2008,** 277.

6. Rozenberg, B.; Tenne, R., Polymer-assisted fabrication of nanoparticles and nanocomposites. *Progress in Polymer Science,* **2008,** *33* (1), 40-112.

7. Rasmussen, J. W.; Martinez, E.; Louka, P.; Wingett, D. G., Zinc oxide nanoparticles for selective destruction of tumor cells and potential for drug delivery applications. *Expert Opinion on Drug Delivery,* **2010,** *7* (9), 1063-1077.

8. Gupta, A. K.; Gupta, M., Synthesis and surface engineering of iron oxide nanoparticles for biomedical applications. *Biomaterials,* **2005,** *26* (18), 3995-4021.

9. Page, K.; Palgrave, R. G.; Parkin, I. P.; Wilson, M.; Savin, S. L.; Chadwick, A. V., Titania and silver–titania composite films on glass potent antimicrobial coatings. *Journal of Materials Chemistry,* **2007,** *17* (1), 95-104.

10. Rawat, J.; Rana, S.; Srivastava, R.; Misra, R. D. K., Antimicrobial activity of composite nanoparticles consisting of titania photocatalytic shell and nickel ferrite magnetic core. *Materials Science and Engineering,* **2007,** *27* (3), 540-545.

11. Daoud, W. A.; Xin, J. H.; Zhang, Y. H., Surface functionalization of cellulose fibers with titanium dioxide nanoparticles and their combined bactericidal activities. *Surface Science,* **2005,** *599* (1), 69-75.

12. Senthilkumar, K.; Senthilkumar, O.; Yamauchi, K.; Sato, M.; Morito, S.; Ohba, T.; Nakamura, M.; Fujita, Y., Preparation of ZnO nanoparticles for bio-imaging applications. *Physica Status Solidi,* **2009,** *246* (4), 885-888.

13. Aslan, B.; Ozpolat, B.; Sood, A. K.; Lopez-Berestein, G., Nanotechnology in cancer therapy. *Journal of Drug Targeting,* **2013,** *21* (10), 904-913.

14. Shi, J.; Votruba, A. R.; Farokhzad, O. C.; Langer, R., Nanotechnology in drug delivery and tissue engineering: from discovery to applications. *Nano Letters,* **2010,** *10* (9), 3223.

15. Sato, M.; Webster, T. J., Nanobiotechnology: implications for the future of nanotechnology in orthopedic applications. *Expert Review of Medical Devices,* **2004,** *1* (1), 105-114.

16. Khare, A.; Deshmukh, S., Studies toward producing eco-friendly plastics. *Journal of Plastic Film & Sheeting,* **2006,** *22* (3), 193-211.

17. Darder, M.; Aranda, P.; Ruiz-Hitzky, E., Bionanocomposites: a new concept of ecological, bioinspired, and functional hybrid materials. *Advanced Materials,* **2007,** *19* (10), 1309-1319.

18. Alexandre, M.; Beyer, G.; Henrist, C.; Cloots, R.; Rulmont, A.; Jerome, R.; Dubois, P., Preparation and properties of layered silicate nanocomposites based on ethylene vinyl acetate copolymers. *Macromolecular Rapid Communications,* **2001,** *22* (8), 643-646.

19. Bhattacharya, S.; Jang, J.; Yang, L.; Akin, D.; Bashir, R., BioMEMS and nanotechnology based approaches for rapid detection of biological entities. *Journal of Rapid Methods & Automation in Microbiology,* **2007,** *15* (1), 1-32.

20. Wiechers, J. W.; Musee, N., Engineered inorganic nanoparticles and cosmetics: facts, issues, knowledge gaps and challenges. *Journal of Biomedical Nanotechnology,* **2010,** *6* (5), 408-431.

21. Bennat, C.; Muller-Goymann, C., Skin penetration and stabilization of formulations containing microfine titanium dioxide as physical UV filter. *International Journal of Cosmetic Science,* **2000,** *22* (4), 271-284.

22. Katz, Linda M.; Dewan, K.; Bronaugh, R., Nanotechnology in cosmetics. *Food and Chemical Toxicology, **2015**, 85, 127-137.*

23. Schmid, G.; Corain, B., Nanoparticulated gold: synthesis, structures, electronics, and reactivities. *European Journal of Inorganic Chemistry,* **2003,** *2003* (17), 3081-3098.

24. Prasher, R. S.; Hu, X.; Chalopin, Y.; Mingo, N.; Lofgreen, K.; Volz, S.; Cleri, F.; Keblinski, P., Turning carbon nanotubes from exceptional heat conductors into insulators. *Physical Review Letters,* **2009,** *102* (10), 105901.

25. Shankar, K.; Mor, G. K.; Prakasam, H. E.; Yoriya, S.; Paulose, M.; Varghese, O. K.; Grimes, C. A., Highly-ordered $TiO_2$ nanotube arrays up to 220 μm in length: use in water photoelectrolysis and dye-sensitized solar cells. *Nanotechnology,* **2007,** *18* (6), 65707.

26. Law, M.; Greene, L. E.; Johnson, J. C.; Saykally, R.; Yang, P., Nanowire dye-sensitized solar cells. *Nature Materials,* **2005,** *4* (6), 455-459.

27. Srivastava, S.; Tiwari, R. K., Synthesis of epoxy-$TiO_2$ nanocomposites: A study on sliding wear behavior, thermal and mechanical properties. *International Journal of Polymeric Materials,* **2012,** *61* (13), 999-1010.

28. Jeon, I. Y.; Baek, J. B., Nanocomposites derived from polymers and inorganic nanoparticles. *Materials,* **2010,** *3* (6), 3654-3674.

29. Loret, C.; Frith, W. J.; Fryer, P. J., Mechanical and structural properties of maltodextrin/agarose microgels composites. *Applied Rheology,* **2007,** *17* (3), 31412-33136.

30. Arora, A.; Padua, G., Nanocomposites in food packaging. *Nanotechnology Research Methods for Food and Bioproducts,* **2014,** *41-54.*

31. Cheng, Z.; Lin, J., Layered organic–inorganic hybrid perovskites: structure, optical properties, film preparation, patterning and templating engineering. *Crystengcomm,* **2010,** *12* (10), 2646-2662.

32. Fu, S. Y.; Feng, X. Q.; Lauke, B.; Mai, Y. W., Effects of particle size, particle/matrix interface adhesion and particle loading on mechanical properties of particulate polymer composites. *Composites Part B: Engineering,* **2008,** *39* (6), 933-961.

33. Bocek, J.; Matejka, L.; Mentlik, V.; Trnka, P.; Slouf, M., Electrical and thermomechanical properties of epoxy-POSS nanocomposites. *European Polymer Journal,* **2011,** *47* (5), 861-872.

34. Wang, L.; Wang, K.; Chen, L.; Zhang, Y.; He, C., Preparation, morphology and thermal/mechanical properties of epoxy/nanoclay composite. *Composites Part A: Applied Science and Manufacturing,* **2006,** *37* (11), 1890-1896.

35. Moisala, A.; Li, Q.; Kinloch, I.; Windle, A., Thermal and electrical conductivity of single and multiwalled carbon nanotube-epoxy composites. *Composites Science and Technology,* **2006,** *66* (10), 1285-1288.

36. Guadagno, L.; Raimondo, M.; Vittoria, V.; Vertuccio, L.; Naddeo, C.; Russo, S.; De Vivo, B.; Lamberti, P.; Spinelli, G.; Tucci, V., Development of epoxy mixtures for application in aeronautics and aerospace. *Royal Society of Chemistry Advances,* **2014,** *4* (30), 15474-15488.

37. Wan, Y.J.; Gong, L.X.; Tang, L.C.; Wu, L.B.; Jiang, J.X., Mechanical properties of epoxy composites filled with silane-functionalized graphene oxide. *Composites part A: Applied Science and Manufacturing,* **2014,** *64*, 79-89.

38. May, C., Epoxy resins: chemistry and technology. *Journal of Controlled Release Society,* **1987**,1247.

39. Ratna, D., Handbook of thermoset resins. *Ismithers Shawbury,* **2009**, 409.

40. Schaubroeck, D.; De Baets, J.; Desmet, T.; Van Vlierberghe, S.; Schacht, E.; Van Calster, A., Introduction of amino groups on the surface of thin photo definable epoxy resin layers via chemical modification. *Applied Surface Science,* **2009,** *255* (21), 8780-8787.

41. Toldy, A.; Szolnoki, B.; Marosi, G., Flame retardancy of fibre-reinforced epoxy resin composites for aerospace applications. *Polymer Degradation and Stability,* **2011**, *96* (3), 371-376.

42. Park, S.J.; Jin, F.L., Thermal stabilities and dynamic mechanical properties of sulfone containing epoxy resin cured with anhydride. *Polymer Degradation and Stability,* **2004,** *86* (3), 515-520.

43. Mustata, F.; Cascaval, C. N., Rheological and thermal behaviour of an epoxy resin modified with reactive diluents. *Journal of Polymer Engineering,* **1997,** *17* (6), 491-506.

44. Lee, A.; Lichtenhan, J. D., Thermal and viscoelastic property of epoxy/clay and hybrid inorganic/organic epoxy nanocomposites. *Journal of Applied Polymer Science,* **1999,** *73* (10), 1993-2001.

45. Berahim, H.; Sirait, K.; Soesianto, F. In a new performance of RTV epoxy resin insulation material in tropical climate, Properties and applications of dielectric materials, 2003. Proceedings of the 7th International Conference on, *Institute of Electrical and Electronics Engineers,* **2003**, 607-610.

46. Brydson, J. A., Plastics materials. *Butterworth Heinemann*, **1999**, 898.

47. Hackam, R., Outdoor HV composite polymer insulators. *Institute of Electrical and Electronic Engineers*, **1999**, 557-585.

48. Syakur, A.; Berahim, H., Hydrophobic contact angle and surface degradation of epoxy resin compound with silicon rubber and silica. *Electrical and Electronic Engineering,* **2012,** *2* (5), 284-291.

49. Hall, J. F., History and bibliography of polymeric insulators for outdoor applications. *Institute of Electrical and Electronic Engineers Transactions on Power Delivery,* **1993,** *8* (1), 376-385.

50. Kumagai, S.; Yoshimura, N., Tracking and erosion of HTV silicone rubber and suppression mechanism of ATH. *Institute of Electronic and Electrical Engineers Transactions on Dielectrics and Electrical Insulation,* **2001,** *8* (2), 203-211.

51. Arora, J. S.; Cremaldi, J. C.; Holleran, M. K.; Ponnusamy, T.; He, J.; Pesika, N. S.; John, V. T., Hydrogel inverse replicas of breath figures exhibit superhydrophobicity due to patterned surface roughness. *Langmuir,* **2016,** *32* (4), 1009-1017.

52. Xue, C.H.; Jia, S.T.; Zhang, J.; Tian, L.Q.; Chen, H.Z.; Wang, M., Preparation of superhydrophobic surfaces on cotton textiles. *Science and Technology of Advanced Materials,* **2008,** *9* (3), 035008.

53. Guo, Z.; Chen, X.; Li, J.; Liu, J.H.; Huang, X.J., ZnO/CuO hetero-hierarchical nanotrees array: hydrothermal preparation and self-cleaning properties. *Langmuir,* **2011,** *27* (10), 6193-6200.

54. Zenerino, A.; Darmanin, T.; Taffin de Givenchy, E.; Amigoni, S.; Guittard, F. d.r., Connector ability to design superhydrophobic and oleophobic surfaces from conducting polymers. *Langmuir,* **2010,** *26* (16), 13545-13549.

55. JEKLU, N., Mechanical and wetting properties of nanosilica/epoxy-coated stainless steel. *Materiali in Tehnologije,* **2015,** *49* (4), 613-618.

56. Akutsu, F.; Inoki, M.; Daicho, N.; Kasashima, Y.; Shiraishi, N.; Marushima, K., Curing behavior and properties of epoxy resins cured with the diamine having the quinoxaline or triazine structure. *Journal of Applied Polymer Science,* **1998,** *69* (9), 1737-1741.

57. Zhang, X.; Xu, W.; Xia, X.; Zhang, Z.; Yu, R., Toughening of cycloaliphatic epoxy resin by nanosize silicon dioxide. *Materials Letters,* **2006,** *60* (28), 3319-3323.

58. Wong, C., Polymers for electronic & photonic application. Elsevier, **2013,** 633.

59. Armelin, E.; Pla, R.; Liesa, F.; Ramis, X.; Iribarren, J. I.; Aleman, C., Corrosion protection with polyaniline and polypyrrole as anticorrosive additives for epoxy paint. *Corrosion Science,* **2008,** *50* (3), 721-728.

60. Sandler, J.; Shaffer, M.; Prasse, T.; Bauhofer, W.; Schulte, K.; Windle, A., Development of a dispersion process for carbon nanotubes in an epoxy matrix and the resulting electrical properties. *Polymer,* **1999,** *40* (21), 5967-5971.

61. Jahromi, S.; Kuipers, W.; Norder, B.; Mijs, W., Liquid crystalline epoxide thermosets. Dynamic mechanical and thermal properties. *Macromolecules,* **1995,** *28* (7), 2201-2211.

62. Curing of epoxy resins. *U.S.Pattent 2,868,767, issued january 13*,**1959**.

63. Kornmann, X.; Lindberg, H.; Berglund, L. A., Synthesis of epoxy/clay nanocomposites. Influence of the nature of the curing agent on structure. *Polymer,* **2001,** *42* (10), 4493-4499.

64. Ashcroft, W., Curing agents for epoxy resins. *In Chemistry and Technology of Epoxy resins*, **1993**,37-71.

65. Gooch, J. W., Encyclopedic dictionary of polymers. *Springer Science & Business Media,* **2010**, 1.

66. Horie, K.; Hiura, H.; Sawada, M.; Mita, I.; Kambe, H., Calorimetric investigation of polymerization reactions. III. Curing reaction of epoxides with amines. *Journal of Polymer Science Part A-1: Polymer Chemistry,* **1970,** *8* (6), 1357-1372.

67. Riccardi, C. C.; Williams, R. J., A kinetic scheme for an amine/epoxy reaction with simultaneous etherification. *Journal of Applied Polymer Science,* **1986,** *32* (2), 3445-3456.

68. Murayama, T.; Bell, J., Relation between the network structure and dynamic mechanical properties of a typical amine-cured epoxy polymer. *Journal of Polymer Science Part A-2: Polymer Physics,* **1970,** *8* (3), 437-445.

69. Murai, S.; Kakiuchi, F.; Sekine, S.; Tanaka, Y.; Kamatani, A.; Sonoda, M.; Chatani, N., Efficient catalytic addition of aromatic. *Nature,* **1993,** *366*, 9.

70. Foix, D.; Yu, Y.; Serra, A.; Ramis, X.; Salla, J. M., Study on the chemical modification of epoxy/anhydride thermosets using a hydroxyl terminated hyperbranched polymer. *European Polymer Journal,* **2009,** *45* (5), 1454-1466.

71. Vyazovkin, S.; Sbirrazzuoli, N., Mechanism and kinetics of epoxy– amine cure studied by differential scanning calorimetry. *Macromolecules,* **1996,** *29* (6), 1867-1873.

72. Xu, L.; Fu, J.; Schlup, J., *In situ* near-infrared spectroscopic investigation of epoxy resin aromatic amine cure mechanisms. *Journal of American Chemical Society,* **1994,** *116* (7), 2821-2826.

73. Karkanas, P. I.; Partridge, I. K., Cure modeling and monitoring of epoxy/amine resin systems. I. Cure kinetics modeling. *Journal of Applied Polymer Science,* **2000,** *77* (7), 1419-1431.

74. Barton, J., The application of differential scanning calorimetry (DSC) to the study of epoxy resin curing reactions. *Epoxy resins and Composites,* **1985**, 111-154.

75. Prime, R. B., Differential scanning calorimetry of the epoxy cure reaction. *Polymer Engineering & Science,* **1973,** *13* (5), 365-371.

76. Verdonck, E.; Schaap, K.; Thomas, L. C., A discussion of the principles and applications of modulated temperature DSC (MTDSC). *International Journal of Pharmaceutics,* **1999,** *192* (1), 3-20.

77. Xie, H.; Liu, B.; Yuan, Z.; Shen, J.; Cheng, R., Cure kinetics of carbon nanotube/tetrafunctional epoxy nanocomposites by isothermal differential scanning calorimetry. *Journal of Polymer Science Part B: Polymer Physics,* **2004,** *42* (20), 3701-3712.

78. Vyazovkin, S.; Sbirrazzuoli, N., Kinetic methods to study isothermal and nonisothermal epoxy-anhydride cure. *Macromolecular Chemistry and Physics,* **1999,** *200* (10), 2294-2303.

79. Gonzalez-Romero, V.; Casillas, N., Isothermal and temperature programmed kinetic studies of thermosets. *Polymer Engineering & Science,* **1989,** *29* (5), 295-301.

80. Kamal, M.; Sourour, S., Kinetics and thermal characterization of thermoset cure. *Polymer Engineering & Science,* **1973,** *13* (1), 59-64.

81. Malek, J., The kinetic analysis of non-isothermal data. *Thermochimica Acta,* **1992,** *200*, 257-269.

82. Rosu, D.; Cascaval, C.; Mustata, F.; Ciobanu, C., Cure kinetics of epoxy resins studied by non-isothermal DSC data. *Thermochimica Acta,* **2002,** *383* (1), 119-127.

83. Criado, J.; Ortega, A., Non-isothermal transformation kinetics: remarks on the Kissinger method. *Journal of Non-crystalline Solids,* **1986,** *87* (3), 302-311.

84. Popescu, C., Integral method to analyze the kinetics of heterogeneous reactions under non-isothermal conditions a variant on the Ozawa-Flynn-Wall method. *Thermochimica Acta,* **1996,** *285* (2), 309-323.

85. Hardis, R.; Jessop, J. L.; Peters, F. E.; Kessler, M. R., Cure kinetics characterization and monitoring of an epoxy resin using DSC, Raman spectroscopy, and DEA. *Composites Part A: Applied Science and Manufacturing,* **2013,** *49*, 100-108.

86. Sakka, S., Special Issue on "sol-gel Processed $TiO_2$ based materials for solar cells, photocatalysts and other applications". *Journal of Sol-gel Science & Technology,* **2001,** *22* (1), 5.

87. Morris, D.; Egdell, R., Application of V-doped $TiO_2$ as a sensor for detection of $SO_2$. *Journal of Materials Chemistry,* **2001,** *11* (12), 3207-3210.

88. Tsukamoto, D.; Shiraishi, Y.; Sugano, Y.; Ichikawa, S.; Tanaka, S.; Hirai, T., Gold nanoparticles located at the interface of anatase/rutile $TiO_2$ particles as active plasmonic photocatalysts for aerobic oxidation. *Journal of the American Chemical, Society* **2012,** *134* (14), 6309-6315.

89. Ohko, Y.; Tatsuma, T.; Fujii, T.; Naoi, K.; Niwa, C.; Kubota, Y.; Fujishima, A., Multicolour photochromism of $TiO_2$ films loaded with silver nanoparticles. *Nature Materials,* **2003,** *2* (1), 29-31.

90. Miyasaka, T.; Ikegami, M.; Kijitori, Y., Photovoltaic performance of plastic dye-sensitized electrodes prepared by low-temperature binder-free coating of mesoscopic titania. *Journal of the Electrochemical Society,* **2007,** *154* (5), 455-A461.

91. Zarazua, I.; De la Rosa, E.; Lopez-Luke, T.; Reyes-Gomez, J.; Ruiz, S.; Angeles Chavez, C.; Zhang, J. Z., Photovoltaic conversion enhancement of CdSe quantum dot-sensitized $TiO_2$ decorated with Au nanoparticles and $P_3OT$. *Journal of Physical Chemistry,* **2011,** *115* (46), 23209-23220.

92. Wang, Y.; Zhang, L.; Deng, K.; Chen, X.; Zou, Z., Low temperature synthesis and photocatalytic activity of rutile $TiO_2$ nanorod superstructures. *Journal of Physical Chemistry,* **2007,** *111* (6), 2709-2714.

93. Baiju, K.; Shukla, S.; Sandhya, K.; James, J.; Warrier, K., Photocatalytic activity of sol− gel derived nanocrystalline titania. *Journal of Physical Chemistry,* **2007,** *111* (21), 7612-7622.

94. Riyas, S.; Yasir, V. A.; Das, P. N. M., Crystal structure transformation of $TiO_2$ in presence of $Fe_2O_3$ and NiO in air atmosphere. *Bulletin of Materials Science,* **2002,** *25* (4), 267-273.

95. Fujishima, A.; Honda, K., Electrochemical photolysis of water at a semiconductor electrode. *Nature,* **1972,** *238* (5358), 37-38.

96. Hsien, Y. H.; Chang, C. F.; Chen, Y. H.; Cheng, S., Photodegradation of aromatic pollutants in water over $TiO_2$ supported on molecular sieves. *Applied catalysis B: Environmental,* **2001,** *31* (4), 241-249.

97. Fujishima, A.; Rao, T. N.; Tryk, D. A., Titanium dioxide photocatalysis. *Journal of Photochemistry and Photobiology C: Photochemistry Reviews,* **2000,** *1* (1), 1-21.

98. Carp, O.; Huisman, C. L.; Reller, A., Photoinduced reactivity of titanium dioxide. *Progress in Solid State Chemistry,* **2004,** *32* (1), 33-177.

99. Englehart, J. Influence of sunscreen components on the transport and retention of titanium dioxide nanoparticles in water-saturated porous media. *Tufts University,* **2011.**

100. Chen, X.; Mao, S. S., Synthesis of titanium dioxide ($TiO_2$) nanomaterials. *Journal of Nanoscience and Nanotechnology,* **2006,** *6* (4), 906-925.

101. Diebold, U., The surface science of titanium dioxide. *Surface Science Reports,* **2003,** *48* (5), 53-229.

102. Nishimoto, S. i.; Ohtani, B.; Kajiwara, H.; Kagiya, T., Correlation of the crystal structure of titanium dioxide prepared from titaniumtetra-2-propoxide with the photocatalytic activity for redox reactions in aqueous propan-2-ol and silver salt solutions. *Journal of the Chemical Society, Faraday Transactions 1: Physical Chemistry in Condensed Phases,* **1985,** *81* (1), 61-68.

103. Zhang, Q.; Gao, L.; Guo, J., Effect of hydrolysis conditions on morphology and crystallization of nanosized $TiO_2$ powder. *Journal of the European Ceramic Society,* **2000,** *20* (12), 2153-2158.

104. Hanaor, D. A.; Sorrell, C. C., Review of the anatase to rutile phase transformation. *Journal of Materials Science,* **2011,** *46* (4), 855-874.

105. Hirano, M.; Nakahara, C.; Ota, K.; Tanaike, O.; Inagaki, M., Photoactivity and phase stability of $ZrO_2$-doped anatase-type $TiO_2$ directly formed as nanometer-sized particles by hydrolysis under hydrothermal conditions. *Journal of Solid State Chemistry,* **2003,** *170* (1), 39-47.

106. Chao, H.; Yun, Y.; Xingfang, H.; Larbot, A., Effect of silver doping on the phase transformation and grain growth of sol-gel titania powder. *Journal of the European Ceramic Society,* **2003,** *23* (9), 1457-1464.

107. Vorkapic, D.; Matsoukas, T., Effect of temperature and alcohols in the preparation of titania nanoparticles from alkoxides. *Journal of the American Ceramic Society,* **1998,** *81* (11), 2815-2820.

108. Wang, C. C.; Ying, J. Y., Sol gel synthesis and hydrothermal processing of anatase and rutile titania nanocrystals. *Chemistry of Materials,* **1999,** *11* (11), 3113-3120.

109. Akhtar, M. K.; Xiong, Y.; Pratsinis, S. E., Vapor synthesis of titania powder by titanium tetrachloride oxidation. *American Institue of Chemical Engineers Journal,* **1991,** *37* (10), 1561-1570.

110. Wiesner, M. R.; Lowry, G. V.; Alvarez, P.; Dionysiou, D.; Biswas, P., Assessing the risks of manufactured nanomaterials. *Journal of American Chemical Society*, **2006** 4336-4345.

111. Yang, H. G.; Liu, G.; Qiao, S. Z.; Sun, C. H.; Jin, Y. G.; Smith, S. C.; Zou, J.; Cheng, H. M.; Lu, G. Q., Solvothermal synthesis and photoreactivity of anatase $TiO_2$ nanosheets with dominant facets. *Journal of the American Chemical Society,* **2009,** *131* (11), 4078-4083.

112. O'regan, B.; Grfitzeli, M., A low-cost, high-efficiency solar cell based on dye-sensitized. *Nature,* **1991,** *353* (6346), 737-740.

113. Yang, R.; Zhang, Y.P.; Zhao, R.Y., An improved model for analyzing the performance of photocatalytic oxidation reactors in removing volatile organic compounds and its application. *Journal of the Air & Waste Management Association,* **2004,** *54* (12), 1516-1524.

114. Stone, V. F.; Davis, R. J., Synthesis, characterization, and photocatalytic activity of titania and niobia mesoporous molecular sieves. *Chemistry of Materials,* **1998,** *10* (5), 1468-1474.

115. Antonelli, D., Synthesis of phosphorus-free mesoporous titania via templating with amine surfactants. *Microporous and Mesoporous Materials,* **1999,** *30* (2), 315-319.

116. Yang, P.; Zhao, D.; Margolese, D. I.; Chmelka, B. F.; Stucky, G. D., Generalized syntheses of large-pore mesoporous metal oxides with semicrystalline frameworks. *Nature,* **1998,** *396* (6707), 152-155.

117. Cassiers, K.; Linssen, T.; Mathieu, M.; Bai, Y. Q.; Zhu, H. Y.; Cool, P.; Vansant, E. F., Surfactant-directed synthesis of mesoporous titania with nanocrystalline anatase walls and remarkable thermal stability. *The Journal of Physical Chemistry,* **2004,** *108* (12), 3713-3721.

118. Wakefield, G.; Green, M.; Lipscomb, S.; Flutter, B., Modified titania nanomaterials for sunscreen applications reducing free radical generation and DNA damage. *Materials Science and Technology,* **2004,** *20* (8), 985-988.

119. Quagliarini, E.; Bondioli, F.; Goffredo, G. B.; Cordoni, C.; Munafo, P., Self-cleaning and de-polluting stone surfaces: $TiO_2$ nanoparticles for limestone. *Construction and Building Materials,* **2012,** *37*, 51-57.

120. Takami, A., Development of titania heated exhaust-gas oxygen sensor. *American Ceramic Society,* **1988,** *67* (12), 1956-1960.

121. Wijewardane, S.; Goswami, D., A review on surface control of thermal radiation by paints and coatings for new energy applications. *Renewable and Sustainable Energy Reviews,* **2012,** *16* (4), 1863-1873.

122. Day, R., The role of titanium dioxide pigments in the degradation and stabilisation of polymers in the plastics industry. *Polymer Degradation and Stability,* **1990,** *29* (1), 73-92.

123. Newman, M. D.; Stotland, M.; Ellis, J. I., The safety of nanosized particles in titanium dioxide and zinc oxide based sunscreens. *Journal of the American Academy of Dermatology,* **2009,** *61* (4), 685-692.

124. Weir, A.; Westerhoff, P.; Fabricius, L.; Hristovski, K.; Von Goetz, N., Titanium dioxide nanoparticles in food and personal care products. *Environmental Science & Technology,* **2012,** *46* (4), 2242-2250.

125. Chen, X.; Mao, S. S., Titanium dioxide nanomaterials: synthesis, properties, modifications, and applications. *Chemical Reviews,* **2007,** *107* (7), 2891-2959.

126. Montazer, M.; Seifollahzadeh, S., Enhanced self-cleaning, antibacterial and UV protection properties of nano $TiO_2$ treated textile through enzymatic pretreatment. *Photochemistry and Photobiology,* **2011,** *87* (4), 877-883.

127. Matos, J.; Laine, J.; Herrmann, J.-M., Effect of the type of activated carbons on the photocatalytic degradation of aqueous organic pollutants by UV-irradiated titania. *Journal of Catalysis,* **2001,** *200* (1), 10-20.

128. Mor, G. K.; Shankar, K.; Paulose, M.; Varghese, O. K.; Grimes, C. A., Use of highly ordered $TiO_2$ nanotube arrays in dye-sensitized solar cells. *Nano Letters,* **2006,** *6* (2), 215-218.

129. Neouze, M.-A.; Schubert, U., Surface modification and functionalization of metal and metal oxide nanoparticles by organic ligands. *Monatshefte furChemie/Chemical Monthly,* **2008,** *139* (3), 183-195.

130. Cozzoli, P. D.; Kornowski, A.; Weller, H., Low temperature synthesis of soluble and processable organic-capped anatase TiO2 nanorods. *Journal of the American Chemical Society,* **2003,** *125* (47), 14539-14548.

131. Qu, Q.; Geng, H.; Peng, R.; Cui, Q.; Gu, X.; Li, F.; Wang, M., Chemically binding carboxylic acids onto $TiO_2$ nanoparticles with adjustable coverage by solvothermal strategy. *Langmuir,* **2010,** *26* (12), 9539-9546.

132. Duffy, N. W.; Dobson, K. D.; Gordon, K. C.; Robinson, B. H.; McQuillan, A. J., *In situ* infrared spectroscopic analysis of the adsorption of ruthenium (II) bipyridyl dicarboxylic acid photosensitisers to $TiO_2$ in aqueous solutions. *Chemical Physics Letters,* **1997,** *266* (5-6), 451-455.

133. Manzione, L.; Gillham, J.; McPherson, C., Rubber modified epoxies. Transitions and morphology. *Journal of Applied Polymer Science,* **1981,** *26* (3), 889-905.

134. Ratna, D.; Simon, G., Thermomechanical properties and morphology of blends of a hydroxy functionalized hyperbranched polymer and epoxy resin. *Polymer,* **2001,** *42* (21), 8833-8839.

135. Chen, H. J.; Wang, L.; Chiu, W. Y., Synthesis and characterization of MEH-PPV/nanosized titania hybrids prepared via in situ sol–gel reaction. *Materials Chemistry and Physics,* **2008,** *112* (2), 551-556.

136. Kickelbick, G., Concepts for the incorporation of inorganic building blocks into organic polymers on a nanoscale. *Progress in Polymer Science,* **2003,** *28* (1), 83-114.

137. Chen, H. J.; Wang, L.; Chiu, W. Y., Chelation and solvent effect on the preparation of titania colloids. *Materials Chemistry and Physics,* **2007,** *101* (1), 12-19.

138. Tsai, M. H.; Liu, S. J.; Chiang, P. C., Synthesis and characteristics of polyimide/titania nano hybrid films. *Thin Solid Films,* **2006,** *515* (3), 1126-1131.

139. Mazzocchetti, L.; Scandola, M.; Pollicino, A., Study of the organic–inorganic phase interactions in polyester titania hybrids. *Polymer,* **2008,** *49* (24), 5215-5224.

140. Lu, S.; Zhang, H.; Zhao, C.; Wang, X., New epoxy/silica-titania hybrid materials prepared by the sol–gel process. *Journal of Applied Polymer Science,* **2006,** *101* (2), 1075-1081.

141. Siegel, R. W. In Mechanical properties of nanophase materials. *Materials Science Forum, Trans Tech,* **1997**, 851-860.

142. Ng, C.; Schadler, L.; Siegel, R., Synthesis and mechanical properties of $TiO_2$-epoxy nanocomposites. *Nanostructured Materials,* **1999,** *12* (1-4), 507-510.

143. Yu, J. C.; Ho, W.; Lin, J.; Yip, H.; Wong, P. K., Photocatalytic activity, antibacterial effect, and photoinduced hydrophilicity of $TiO_2$ films coated on a stainless steel substrate. *Environmental Science & Technology,* **2003,** *37* (10), 2296-2301.

144. Parameswaranpillai, J.; George, A.; Pionteck, J.; Thomas, S., Investigation of cure reaction, rheology, volume shrinkage and thermomechanical properties of nano-$TiO_2$ filled epoxy/DDS composites. *Journal of Polymers,* **2013.**

145. Carballeira, P.; Haupert, F., Toughening effects of titanium dioxide nanoparticles on $TiO_2$/epoxy resin nanocomposites. *Polymer Composites,* **2010,** *31* (7), 1241-1246.

146. Singha, S.; Thomas, M. J., Dielectric properties of epoxy nanocomposites. *Institute of Electrical and Electronic Engineers Transactions on Dielectrics and Electrical Insulation,* **2008**, *15* (1), 12-23.

147. Morselli, D.; Bondioli, F.; Sangermano, M.; Messori, M., Photo-cured epoxy networks reinforced with $TiO_2$ *in-situ* generated by means of non-hydrolytic sol–gel process. *Polymer,* **2012,** *53* (2), 283-290.

148. Rubab, Z.; Afzal, A.; Siddiqi, H. M.; Saeed, S., Augmenting thermal and mechanical properties of epoxy thermosets: the role of thermally-treated versus surface-modified $TiO_2$ nanoparticles. *Materials Express,* **2014,** *4* (1), 54-64.

149. Lu, S.; Chun, W.; Yu, J.; Yang, X., Preparation and characterization of the mesoporous $SiO_2$–$TiO_2$/epoxy resin hybrid materials. *Journal of Applied Polymer Science,* **2008,** *109* (4), 2095-2102.

150. Chatterjee, A.; Islam, M. S., Fabrication and characterization of $TiO_2$–epoxy nanocomposite. *Materials Science and Engineering,* **2008,** *487* (1), 574-585.

151. Bondioli, F.; Darecchio, M. E.; Luyt, A. S.; Messori, M., Epoxy resin modified with in situ generated metal oxides by means of sol–gel process. *Journal of Applied Polymer Science,* **2011,** *122* (3), 1792-1799.

152. Sumfleth, J.; de Almeida Prado, L. A.; Sriyai, M.; Schulte, K., Titania-doped multi-walled carbon nanotubes epoxy composites: Enhanced dispersion and synergistic effects in multiphase nanocomposites. *Polymer,* **2008,** *49* (23), 5105-5112.

153. Omrani, A.; Afsar, S.; Safarpour, M. A., Thermoset nanocomposites using hybrid nano $TiO_2$–$SiO_2$. *Materials Chemistry and Physics,* **2010,** *122* (2), 343-349.

154. Yasmin, A.; Abot, J. L.; Daniel, I. M., Processing of clay/epoxy nanocomposites by shear mixing. *Scripta Materialia,* **2003,** *49* (1), 81-86.

155. Zhang, H.; Zhang, Z.; Friedrich, K.; Eger, C., Property improvements of in situ epoxy nanocomposites with reduced interparticle distance at high nanosilica content. *Acta Materialia,* **2006,** *54* (7), 1833-1842.

156. Jun, Y.; Zarrin, H.; Fowler, M.; Chen, Z., Functionalized titania nanotube composite membranes for high temperature proton exchange membrane fuel cells. *International Journal of Hydrogen Energy,* **2011,** *36* (10), 6073-6081.

157. Abazari, R.; Mahjoub, A. R.; Sanati, S., A facile and efficient preparation of anatase titania nanoparticles in micelle nanoreactors: morphology, structure, and their high photocatalytic activity under UV light illumination. *Royal Society of Chemistry Advances,* **2014,** *4* (99), 56406-56414.

158. Pazokifard, S.; Farrokhpay, S.; Mirabedini, M.; Esfandeh, M., Comparative study on sol-gel treatment of $TiO_2$ nanoparticles using different fluorosilane-based compounds. *Chemeca Challenging Tomorrow,* **2013**, 26.

159. Dalvi, V. H.; Rossky, P. J., Molecular origins of fluorocarbon hydrophobicity. *Proceedings of the National Academy of Sciences,* **2010,** *107* (31), 13603-13607.

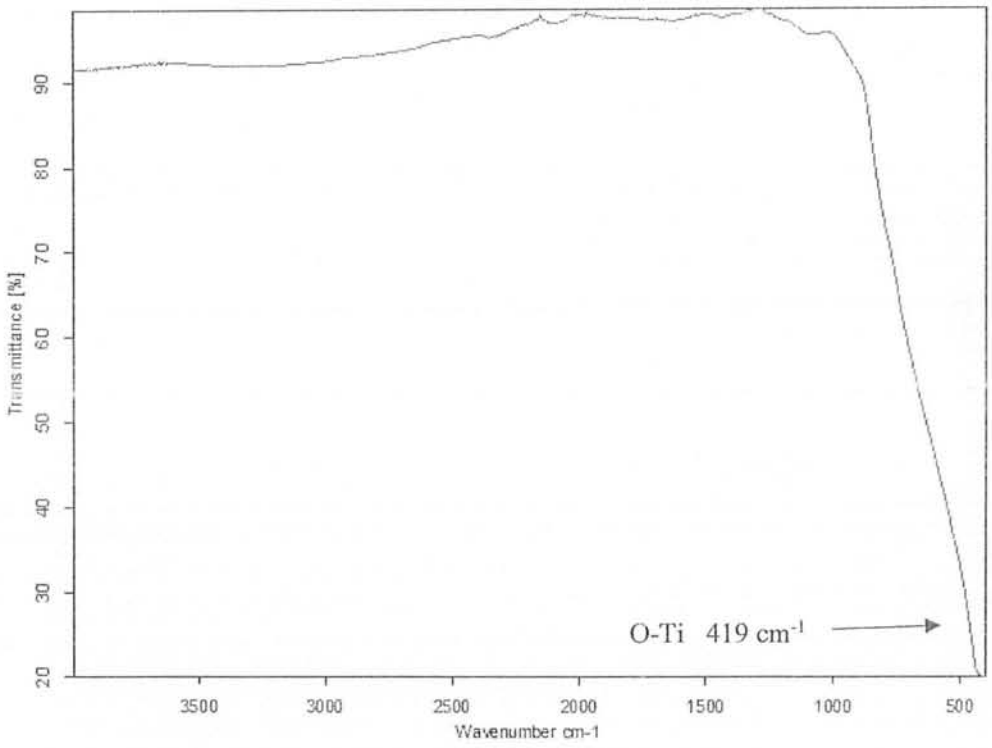


**Annex I** : FTIR of TNP

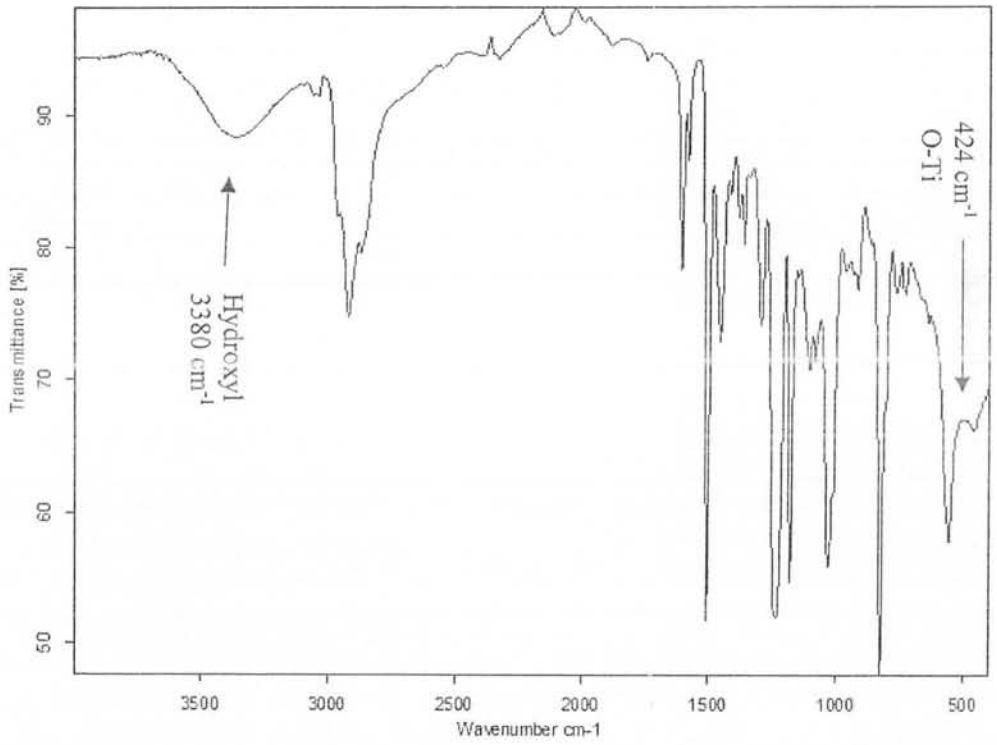


**Annex II:** FTIR of 5-TENC

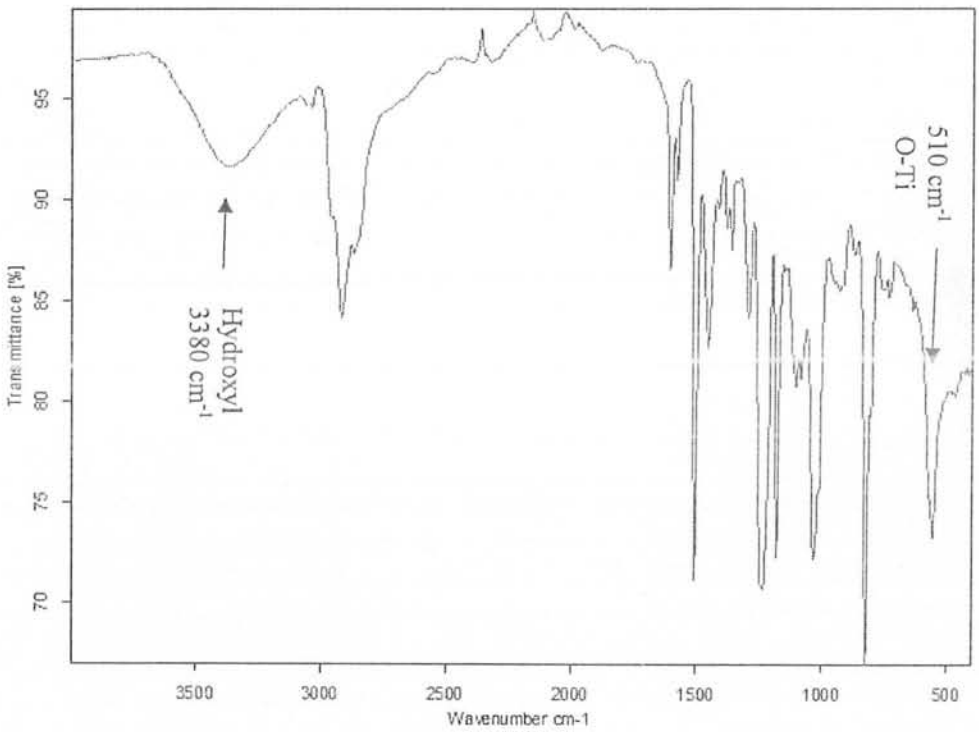


**Annex III:** FTIR OF 7.5-TENC

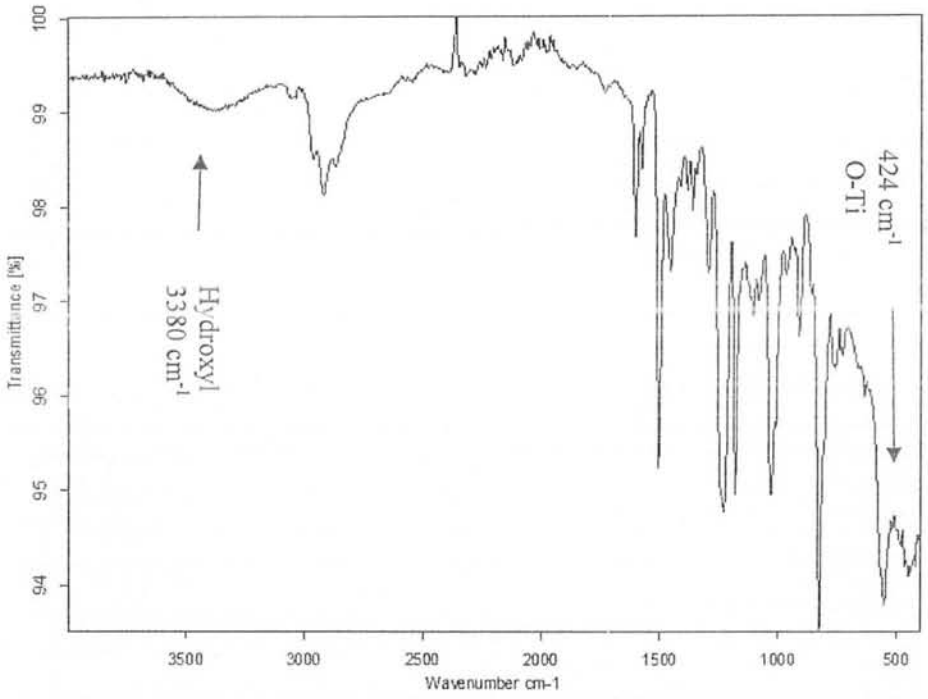


**Annex IV:** FTIR OF 5-MTEC

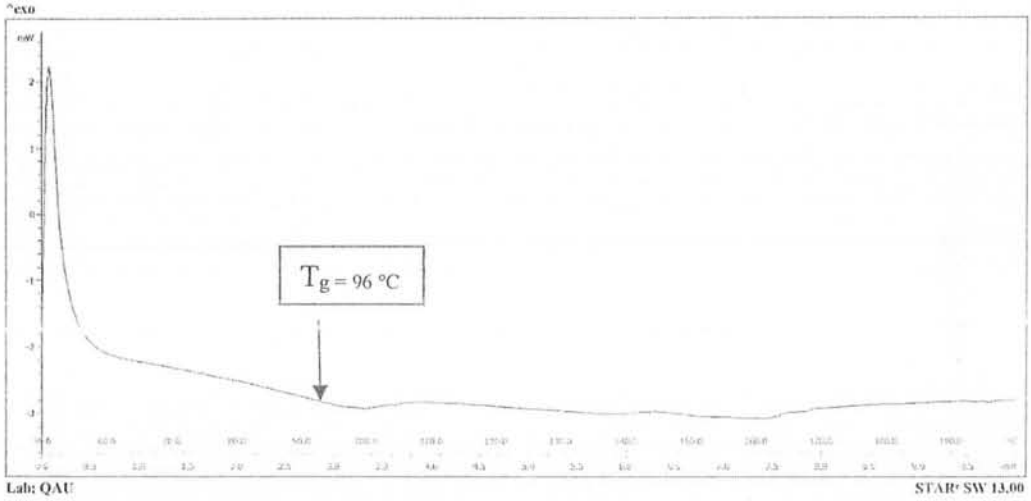


**Annex V:** DSC scan for 5-FMTEC

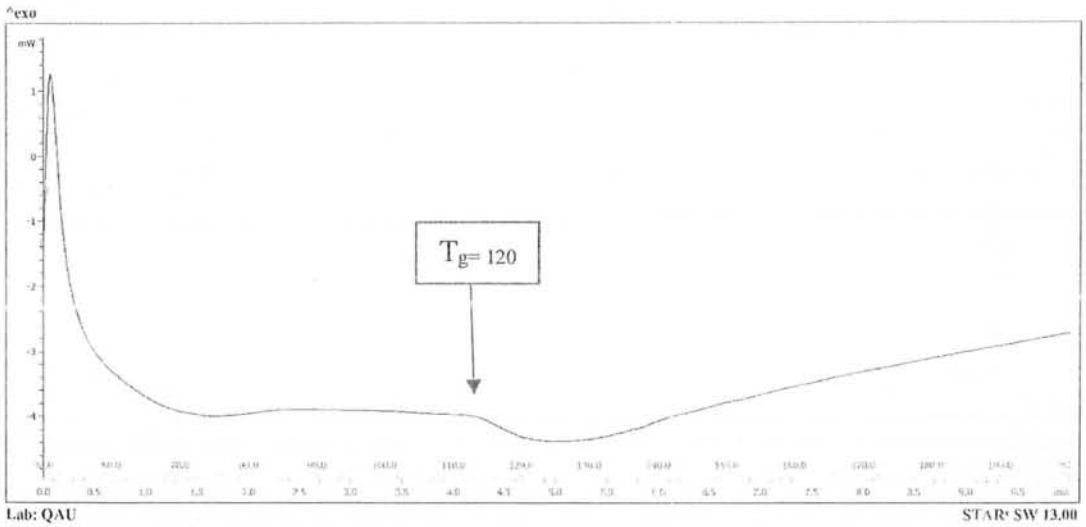


**Annex VI:** DSC scan for 7.5-MTEC